Electronic Supplementary Material (ESI) for ChemComm.

Supporting information

Biguanides, anion receptors and sensors

Mariia Pushina, Pavel Anzenbacher,Jr.*

Department of Chemistry, Bowling Green State University Bowling Green, OH 43403, USA E-mail: pavel@bgsu.edu

Table of Contents

1 General

Materials and Methods. All chemicals were analytical grade and they were used without purification.
NMR. Proton NMR (^{1}H-NMR) and carbon-13 NMR (^{13}C-NMR) spectra were recorded on Bruker Avance III spectrometer at 500 MHz at 348 K. Proton and carbon NMR chemical shifts (δ) are reported in parts per million (ppm) relative to residual solvent signals in DMSO-d_6 (δ = 2.50, 39.52). Coupling constants (J) are reported in hertz (Hz) and refer to apparent multiplicities. The following abbreviations are used for the multiplicities: s (singlet), d (doublet), t (triplet), q (quartet), p (pentet), m (multiplet), br (broad).
High-Resolution Mass Spectra. High-resolution mass spectra (HRMS) were obtained on Shimadzu AXIMA Performance MALDI TOF mass spectrometer in reflectron mode using Dithranol (CAS 1143-38-0) as a matrix.
Absorbance. The absorption spectra were recorded between 250 nm and 550 nm for **S1**, 250 nm and 500 nm for **S2**, 250 nm and 450 nm for **S3**, 250 nm and 500 nm for **S4**, 250 nm and 500 nm for **S5**, and 250 nm and 500 nm for **S6**, respectively. The absorbance from probes was scanned in 2 nm step. Scans were taken under laboratory temperature. The titrations were performed in mixture dimethyl sulfoxide (DMSO):$CHCl_3$ (3:7) with addition of Triton X-100 at laboratory temperature. Titration isotherms were constructed from changes in the absorbance maximum at 420 nm for **S1**, 317 nm for **S2**, 280 nm for **S3**, 400 nm for **S4**, 315 nm for **S5**, and 280 nm for **S6**, respectively.
Fluorescence. The emission spectra were recorded between 420 nm and 620 nm for **S1**, 320 nm and 500 nm for **S2**, 320 nm and 500 nm for **S3**, 400 nm and 650 nm for **S4**, and 320 nm and 500 nm for **S6**, respectively. The emission from probes was scanned in 2 nm step with appropriate excitation and emission monochromators band pass settings with dwell time 0.20 sec. Scans were taken under laboratory temperature. Fluorescence guest and competitive titrations were performed in mixture DMSO:$CHCl_3$ (3:7) with addition of Triton X-100 at laboratory temperature. Titration isotherms were constructed from changes in the fluorescence maximum at 451 nm for **S1**, 358 nm for **S2**, 352 nm for **S3**, 448 nm for **S4**, and 351 nm for **S6**, respectively. Data analysis and curve fitting were performed according to previously published methods[1].

2 Sensors Synthesis

Synthesis Schemes

Scheme S1. Synthesis of intermediate **1**: butanol, reflux, 18 h, 82%.

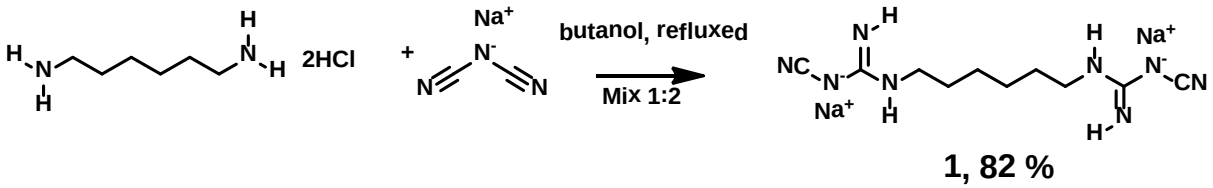

1, 82 %

Scheme S2. Synthesis of sensor **S1**: 1) 2-ethoxyethanol, reflux, 5 h, 43%; 2) H_2O, r.t., 34%.

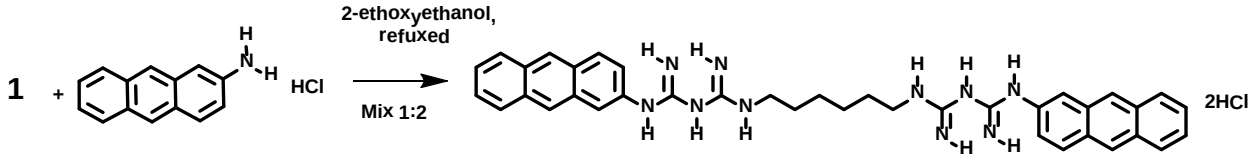

2, 44 %

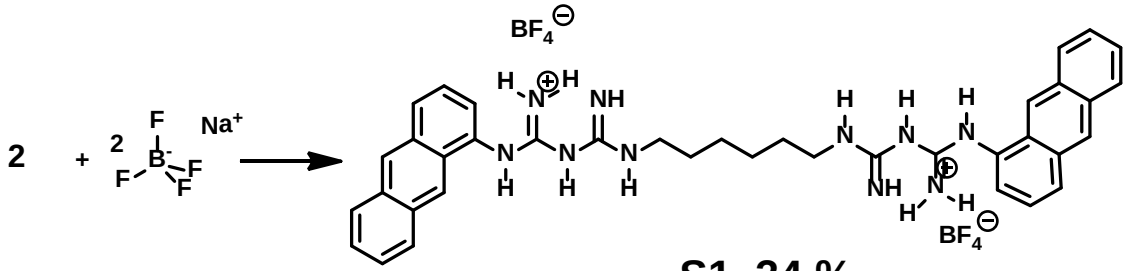

S1, 34 %

Scheme S3. Synthesis of sensor **S2**: 1) 2-ethoxyethanol, reflux, 5 h, 44%; 2) H_2O, r.t., 80%.

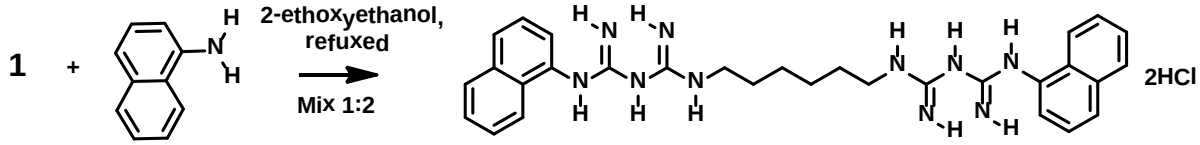

3, 44 %

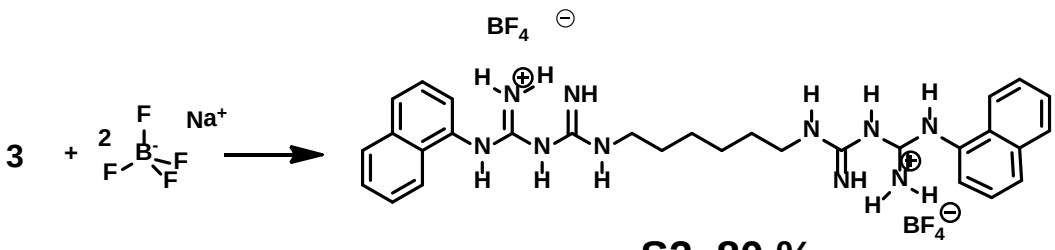

S2, 80 %

Scheme S4. Synthesis of sensor **S3**: 1) 2-ethoxyethanol, reflux, 5 h, 43%; 2) H_2O, r.t., 66%.

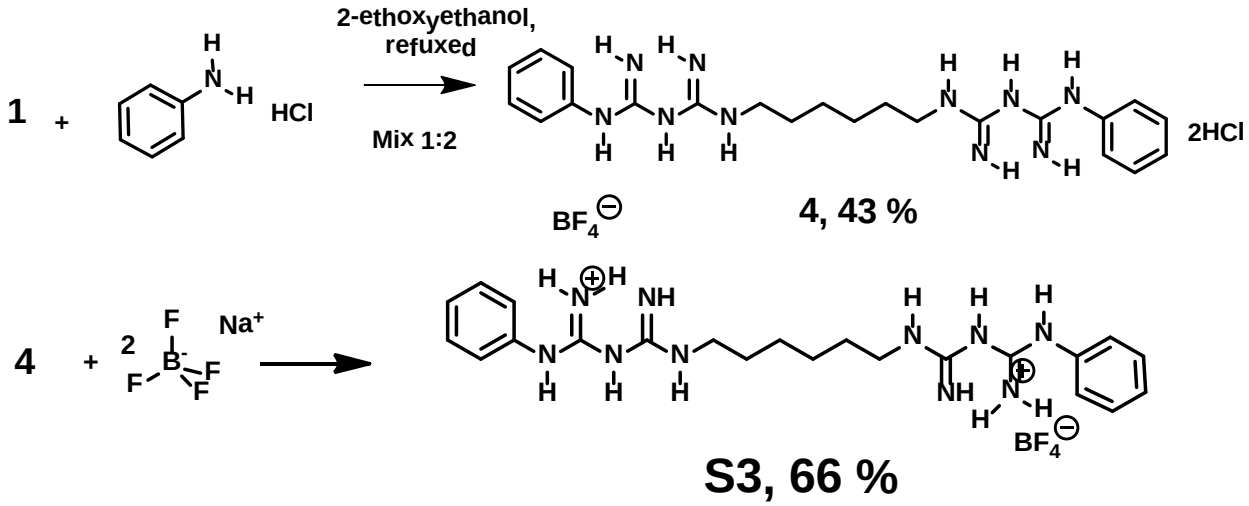

Scheme S5. Synthesis of intermediate **5**: butanol, reflux, 18 h, 62%.

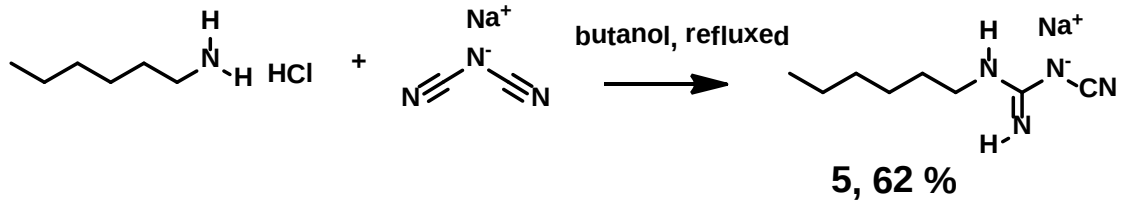

Scheme S6. Synthesis of sensor **S4**: 1) 2-ethoxyethanol, reflux, 5 h, 37%; 2) H_2O, r.t., 63%.

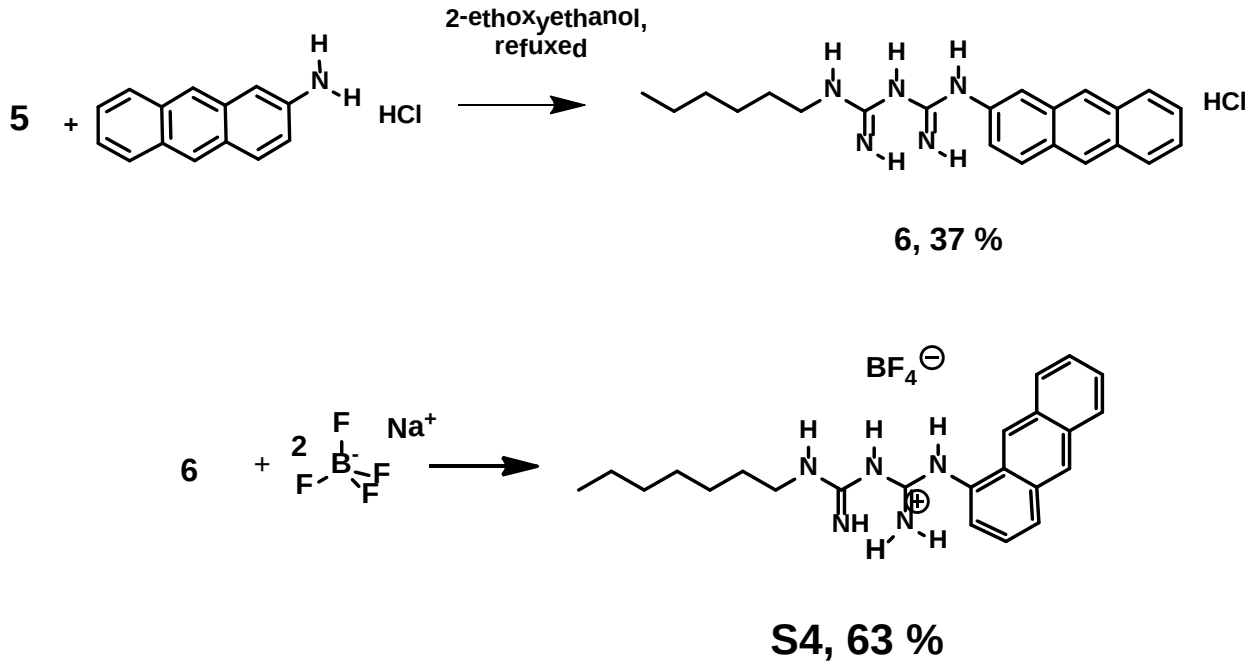

Scheme S7. Synthesis of sensor **S5**: 1) 2-ethoxyethanol, reflux, 3 h, 24%; 2) H_2O, r.t., 31%.

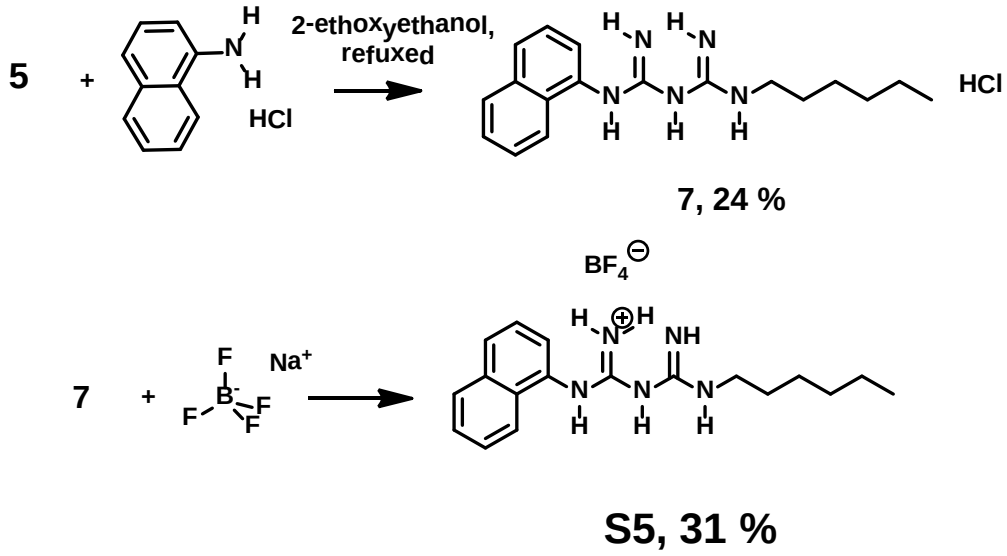

S5, 31 %

Scheme S8. Synthesis of sensor **S6**: 1) 2-ethoxyethanol, reflux, 3 h, 29%; 2) H_2O, r.t., 32%.

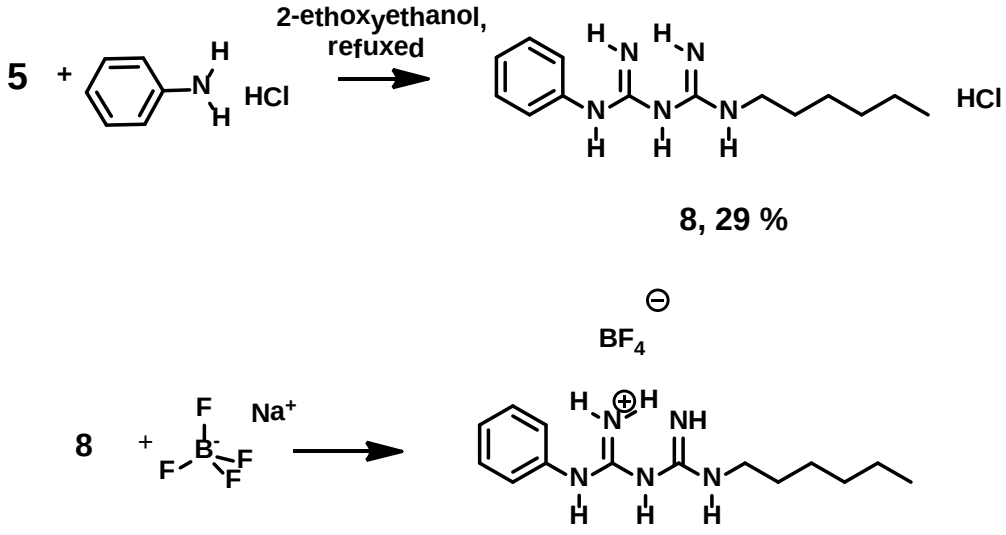

S6, 32 %

Procedures

The synthesis of all sensors was based on general method of preparation of biscyanoguanidines.[2]

6-Di-(N^3-cyano-N^1-guanidino)hexane (1). Commercially available Hexane-1,6-diamine dihydrochloride (2.00 g, 10.6 mmol) and sodium dicyanimide (1.88 g, 21.2 mmol) were powdered together and refluxed in butanol (50 mL) for 18 h. The solvent was removed under reduced pressure and obtained white powder was recrystallized from water.

1,14-Bis(anthracen-1-ylamino)-3,12-diimino-2,4,11,13-tetraazatetradecane-1,14-diiminium tetrafluoroborate (S1). Compound **1** (0.25 g, 1 mmol) was mixed with 2-aminoanthracene hydrochloride (0.46 g, 2 mmol). The mixture was refluxed in 2-ethoxyethanol (5 mL) for 5 h. The solvent was then evaporated on a rotary evaporator. The powder was recrystallized from water. The obtained compound was dissolved in water:DMSO (8:2) and added into saturated solution of $NaBF_4$ in water. The pale yellow precipitate was filtered and dried in vacuum. Spectral data for **S1**: ^{1}H-NMR (DMSO-d_6, 500 MHz): δ = 9.20 (s, 2H), 8.48 (s, 2H), 8.38 (s, 2H), 8.08 – 7.96 (m, 8H), 7.71 – 7.42 (m, 8H), 7.29 (s, 2H), 6.78 (s, 2H), 2.54 (s, 4H), 1.48 (m, 4H), 1.29 (m, 4H). ^{13}C-CPD (DMSO-d_6, 125 MHz): δ = 159.52, 154.44, 135.12, 131.42, 131.22, 130.31, 128.37, 127.73, 127.26, 125.54, 125.45, 125.36, 124.68, 124.46, 233.31, 115.84, 41.14, 28.24, 25.68 ppm. HRMS (MALDI) *m/z* found 637.3444 $[M+H]^+$; calc 637.3499 for $C_{38}H_{41}N_{10}^+$. ^{1}H-NMR spectrum in DMSO-d_6 at 500 MHz (**Figure S1**), and ^{13}C-CPD-NMR spectrum in DMSO-d_6 at 125 MHz (**Figure S2**) for **S1** are shown below.

3,12-Diimino-1,14-bis(naphthalen-1-ylamino)-2,4,11,13-tetraazatetradecane-1,14-diiminium tetrafluoroborate (S2). Compound **1** (1.00 g, 4 mmol) was mixed with naphthylamine hydrochloride (1.44 g, 8 mmol). The mixture was refluxed in 2-ethoxyethanol (20 mL) for 5 h. The solvent was then evaporated on a rotary evaporator. The powder was recrystallized from water and 3,12-diimino-1,14-bis(naphthalen-1-ylamino)-2,4,11,13-tetraazatetradecane-1,14-diiminium dihydrochloride was obtained. The compound was dissolved in water and added into saturated solution of $NaBF_4$ in water. The light purple precipitate was filtered and dried in vacuum. Spectral data for **S2**: ^{1}H-NMR (DMSO-d_6, 500 MHz): δ = 9.05 (s, 2H), 8.07 (d, J = 8.0 Hz, 2H), 7.98 – 7.89 (m, 2H), 7.79 (d, J = 8.1 Hz, 2H), 7.62 – 7.48 (m, 8H), 7.33 (s, 2H), 7.04 (s, 3H), 6.84 (s, 3H), 2.98 (d, J = 6.0 Hz, 4H), 1.33 (s, 4H), 1.14 (s, 4H). ^{13}C-CPD (DMSO-d_6, 125 MHz): δ = 159.11, 156.26, 133.58, 133.03, 128.44, 127.85, 125.82, 125.79, 125.59, 125.18, 122.63, 122.12, 40.97, 28.12, 25.54 ppm. HRMS (MALDI) *m/z* found 537.3292 $[M+H]^+$; calc 537.3188 for $C_{30}H_{37}N_{10}^+$. ^{1}H-NMR spectrum in DMSO-d_6 at 500 MHz (**Figure S3**), and ^{13}C-CPD-NMR spectrum in DMSO-d_6 at 125 MHz (**Figure S4**) for **S2** are shown below.

3,12-Diimino-1,14-bis(phenylamino)-2,4,11,13-tetraazatetradecane-1,14-diiminium tetrafluoroborate (S3). Compound **1** (1.00 g, 4 mmol) was mixed with aniline hydrochloride (1.04 g, 8 mmol). The mixture was refluxed in 2-ethoxyethanol (5 mL) for 5 h. The solvent was then evaporated on a rotary evaporator. The powder was recrystallized from water. The obtained compound was dissolved in water and added into saturated solution of $NaBF_4$ in water. The precipitate was filtered and dried in vacuum. Spectral data for **S3**: ^{1}H-NMR (DMSO-d_6, 500 MHz): δ = 9.26 (s, 2H), 7.65 (s, 2H), 7.39 – 7.35 (m, 4H), 7.32 – 7.27 (m, 4H), 7.21 (s, 3H), 7.06 (t, J = 7.3 Hz, 3H), 6.76 (s, 3H), 3.08 (s, 4H), 1.51 – 1.44 (m, 4H), 1.30 (m, 4H). ^{13}C-CPD (DMSO-d_6, 125 MHz): δ = 159.52, 154.55, 138.22, 128.28, 123.12, 120.74, 41.03, 28.25, 25.60 ppm. HRMS (MALDI) *m/z* found 437.2706 $[M+H]^+$; calcd 437.2877 for $C_{22}H_{33}N_{10}^+$. ^{1}H-NMR spectrum in DMSO-d_6 at 500 MHz (**Figure S5**), and ^{13}C-CPD-NMR spectrum in DMSO-d_6 at 125 MHz (**Figure S6**) for **S3** are shown below.

N^3-cyano-N^1-guanidinohexane (5). Hexylamine hydrochloride (the hexylamine hydrochloride was prepared by bubbling gaseous hydrogen chloride through a dichloromethane solution of hexylamine) (3.14 g, 22.4 mmol) and sodium dicyanimide (2.00 g, 24.4 mmol) were powdered together and refluxed in butanol (60 mL) for 18 h. The solvent was removed under reduced pressure and obtained white powder was recrystallized from water.

(3-(Anthracen-2-yl)guanidino)(hexylamino)methaniminium hydrochloride (S4). Compound **5** (0.22 g, 1.3 mmol) was mixed with 2-aminoanthracene hydrochloride (0.30 g, 1.3 mmol). The mixture was refluxed in 2-ethoxyethanol (4 mL) for 5 h. The solvent was then evaporated on a rotary evaporator. The pale green powder was recrystallized from water. Spectral data for **S4**: ^{1}H-NMR (DMSO-d_6, 500 MHz): δ = 9.18 (s, 1H), 8.50 (s, 1H), 8.41 (s, 1H), 8.08 – 8.00 (m, 4H), 7.68 – 7.24 (m, 5H), 6.76 (s, 2H), 3.10 (m, 2H) 1.54 – 1.46 (m, 2H), 1.29 (m, 2H), 1.25 (m, 4H), 0.83 (m, 3H). ^{13}C-CPD (DMSO-d_6, 125 MHz): δ = 159.31, 154.22, 135.08, 131.15, 130.90, 130.06, 128.09, 127.49, 127.45, 126.99, 125.26, 125.08, 124.41, 124.23, 121.91, 115.58, 40.95, 30.22, 27.90, 25.27, 21.27, 13.09 ppm. HRMS (MALDI) *m/z* found 362.2452 $[M+H]^+$; calcd 362.2335 for $C_{22}H_{28}N_5^+$. ^{1}H-NMR spectrum in DMSO-d_6 at 500 MHz (**Figure S7**), and ^{13}C-CPD-NMR spectrum in DMSO-d_6 at 125 MHz (**Figure S8**) for **S4** are shown below.

(3-Hexylguanidino)(naphthalen-1-ylamino)methaniminium tetrafluoroborate (S5). Compound **5** (1.00 g, 5.96 mmol) was mixed with naphthylamine hydrochloride (1.07 g, 5.96 mmol). The mixture was refluxed in 2-ethoxyethanol (5 mL) for 3 h. The solvent was then evaporated on a rotary evaporator. The powder was recrystallized from water. The obtained compound was dissolved in water and added into saturated solution of $NaBF_4$ in water. The light purple precipitate was filtered and dried in vacuum. Spectral data for **S5**: ^{1}H-NMR (DMSO-d_6, 500 MHz): δ = 9.04 (s, 1H), 8.06 (d, J = 8.0 Hz, 1H), 8.00 – 7.92 (m, 1H), 7.79 (d, J = 8.1 Hz, 1H), 7.68 – 7.44 (m, 4H), 7.34 (s, 1H), 7.04 (s, 1H), 6.83 (s, 2H), 2.99 (dd, J = 13.1, 6.7 Hz, 2H), 1.48 – 1.06 (m, 8H), 0.85 (t, J = 7.0 Hz, 3H). ^{13}C-CPD (DMSO-d_6, 125 MHz): δ = 159.16, 156.24, 133.61, 133.07, 128.46, 127.88, 125.83, 125.79, 125.60, 125.21, 122.64, 122.15, 41.04, 30.50, 28.17, 25.50, 21.58, 13.43 ppm. HRMS (MALDI) *m/z* found 312.2279 $[M+H]^+$; calcd 312.2179 for $C_{18}H_{26}N_5^+$. ^{1}H-NMR spectrum in DMSO-d_6 at 500 MHz (**Figure S9**), and ^{13}C-CPD-NMR spectrum in DMSO-d_6 at 125 MHz (**Figure S10**) for **S5** are shown below.

(3-Hexylguanidino)(phenylamino)methaniminium tetrafluoroborate (S6). Compound **5** (1.50 g, 8.9 mmol) was mixed with aniline hydrochloride (1.15 g, 8.9 mmol). The mixture was refluxed in 2-ethoxyethanol (10 mL) for 5 h. The solvent was then evaporated on a rotary evaporator. The powder was recrystallized from water. The obtained compound was dissolved in water and added into saturated solution of $NaBF_4$ in water. The precipitate was filtered and dried in vacuum. Spectral data for **S6**: ^{1}H-NMR (DMSO-d_6, 500 MHz): δ = 8.94 (s, 1H), 7.60 – 7.05 (m, 7H), 6.64 (s, 1H), 3.09 (dd, J = 7.1, 5.8 Hz, 2H), 1.47 (dd, J = 14.0, 7.0 Hz, 2H), 1.38 – 1.22 (m, 6H), 0.87 (m, 3H). ^{13}C-CPD (DMSO-d_6, 125 MHz): δ = 159.52, 154.41, 138.18, 128.38, 123.32, 121.01, 41.17, 30.53, 28.22, 25.55, 21.60, 13.44 ppm. HRMS (MALDI) *m/z* found 262.2077 $[M+H]^+$; calcd 262.2024 for $C_{14}H_{24}N_5^+$. ^{1}H-NMR spectrum in DMSO-d_6 at 500 MHz (**Figure S11**), and ^{13}C-CPD-NMR spectrum in DMSO-d_6 at 125 MHz (**Figure S12**) for **S6** are shown below.

Figure S1. Spectral data for **S1**: ^{1}H-NMR (DMSO-d_6, 500 MHz, 348 K).

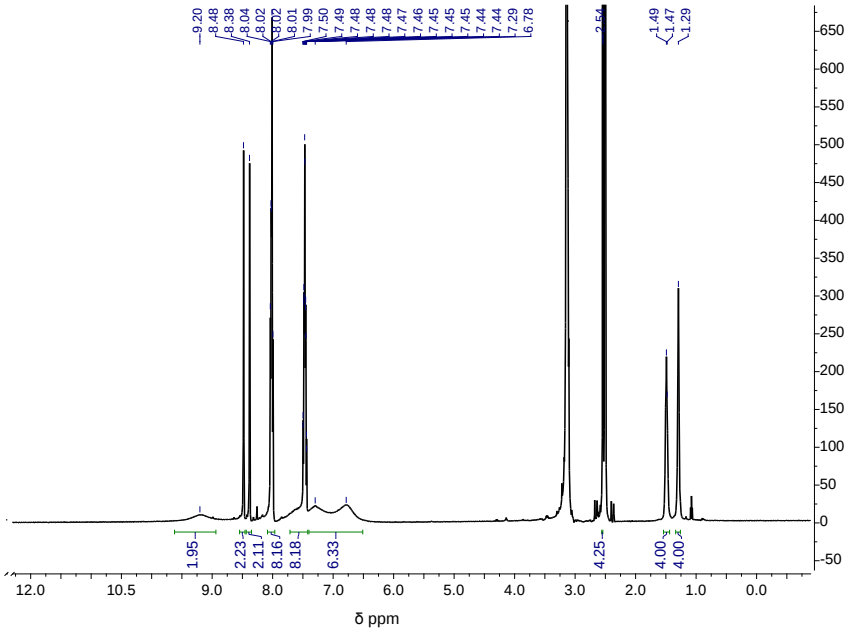

Figure S2. Spectral data for **S1**: ^{13}C-NMR (DMSO-d_6, 125 MHz, 348 K).

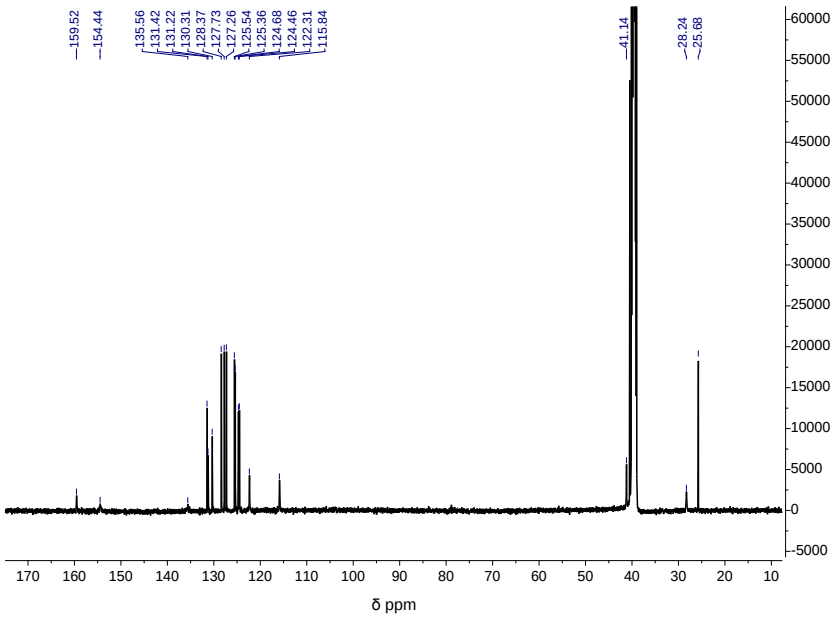

Figure S3. Spectral data for **S2**: ^{1}H-NMR (DMSO-d_6, 500 MHz, 348 K).

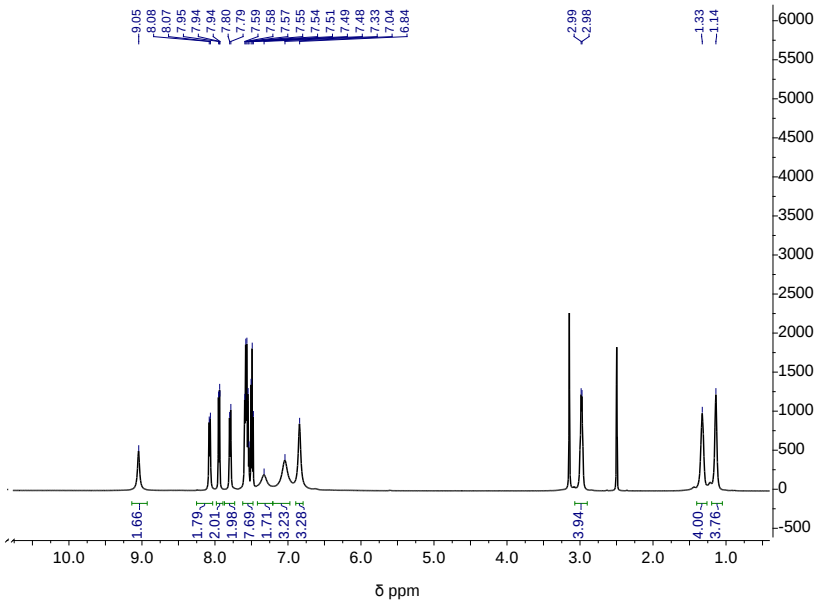

Figure S4. Spectral data for **S2**: ^{13}C-NMR (DMSO-d_6, 125 MHz, 348 K).

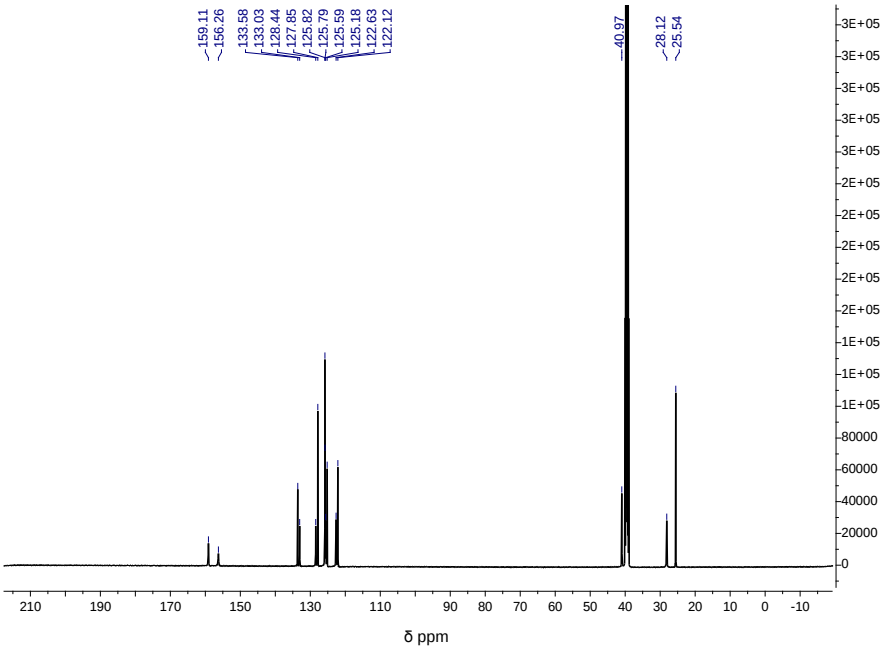

Figure S5. Spectral data for **S3**: ^{1}H-NMR (DMSO-d_6, 500 MHz, 348 K).

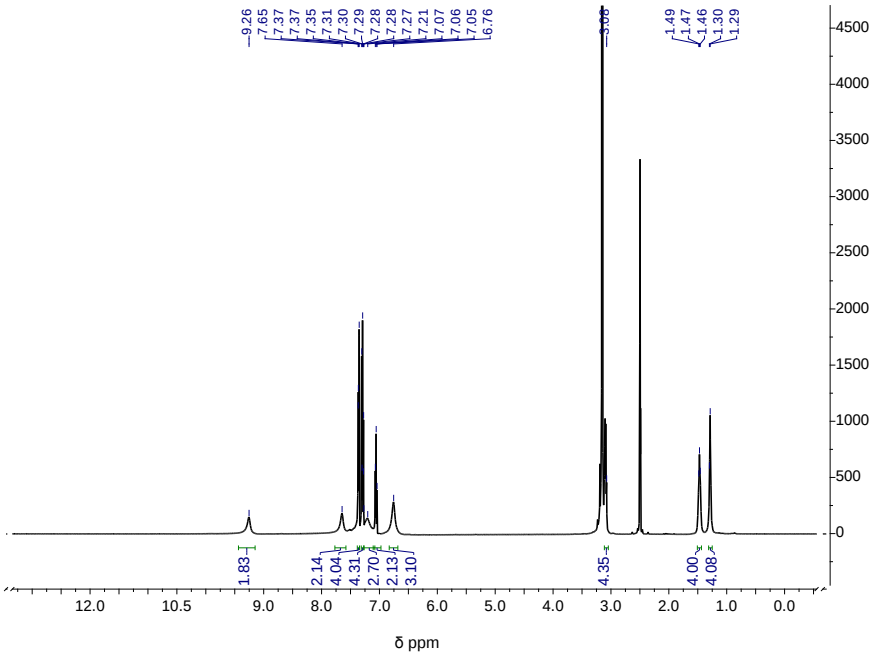

Figure S6. Spectral data for **S3**: ^{13}C-NMR (DMSO-d_6, 125 MHz, 348 K).

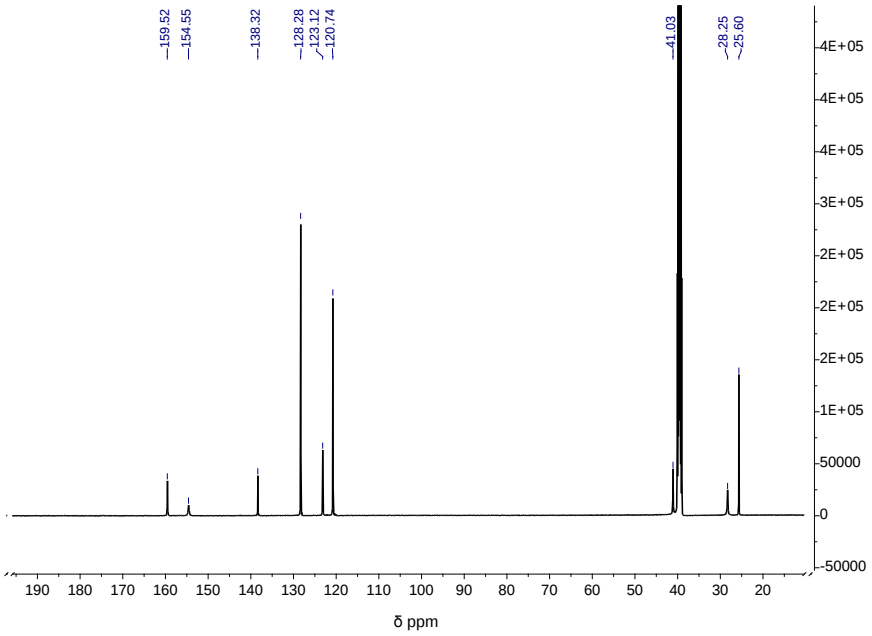

Figure S7. Spectral data for **S4**: ^{1}H-NMR (DMSO-d_6, 500 MHz, 348 K).

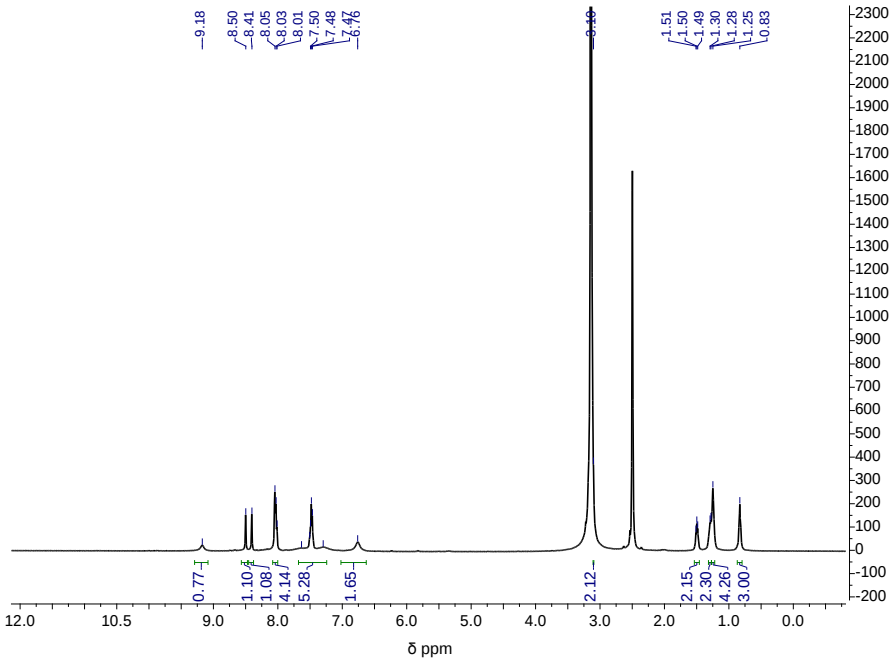

Figure S8. Spectral data for **S4**: ^{13}C-NMR (DMSO-d_6, 125 MHz, 348 K).

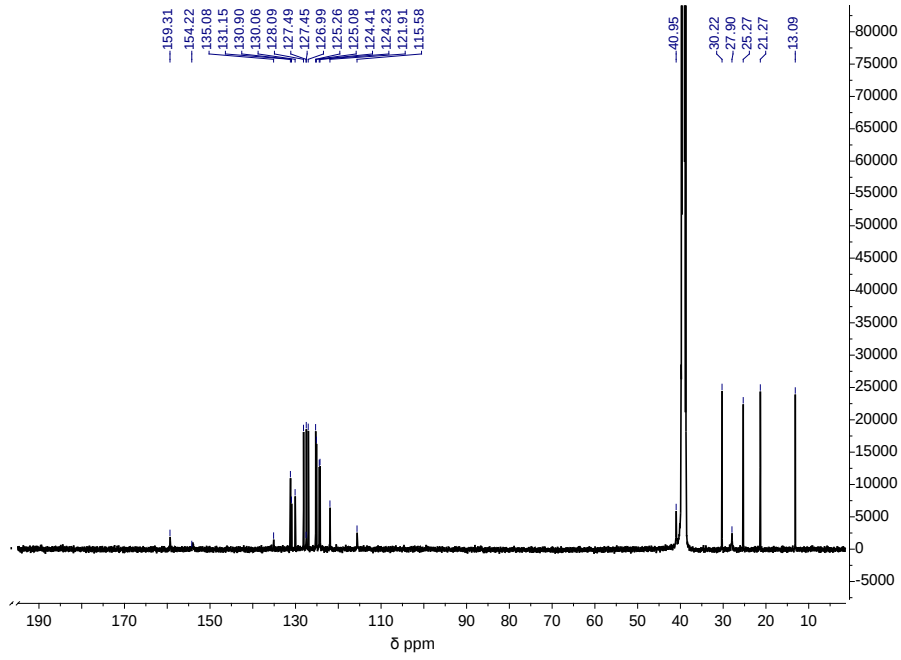

Figure S9. Spectral data for **S5:** ^{1}H-NMR (DMSO-d6, 500 MHz, 348 K).

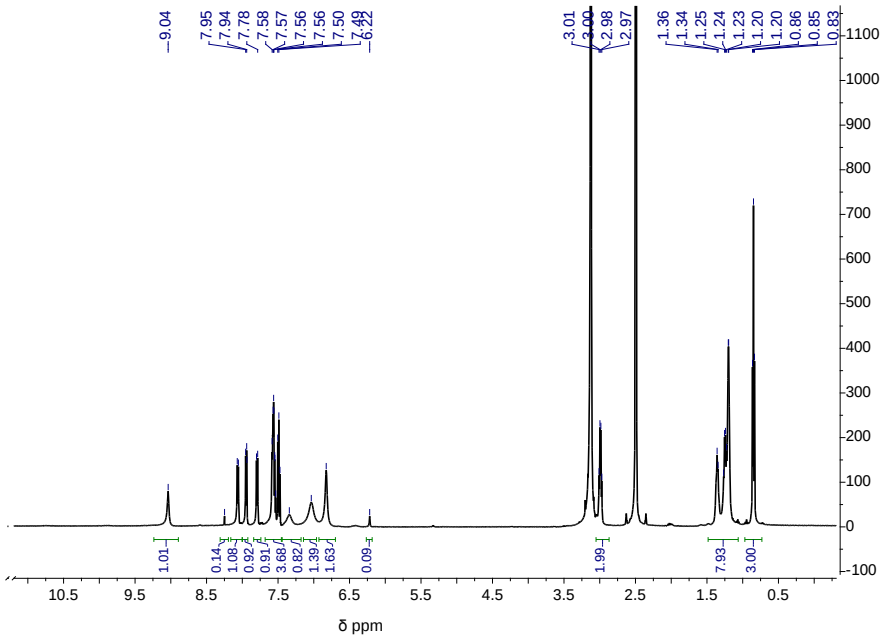

Figure S10. Spectral data for **S5**: ^{13}C-NMR (DMSO-d_6, 125 MHz, 348 K).

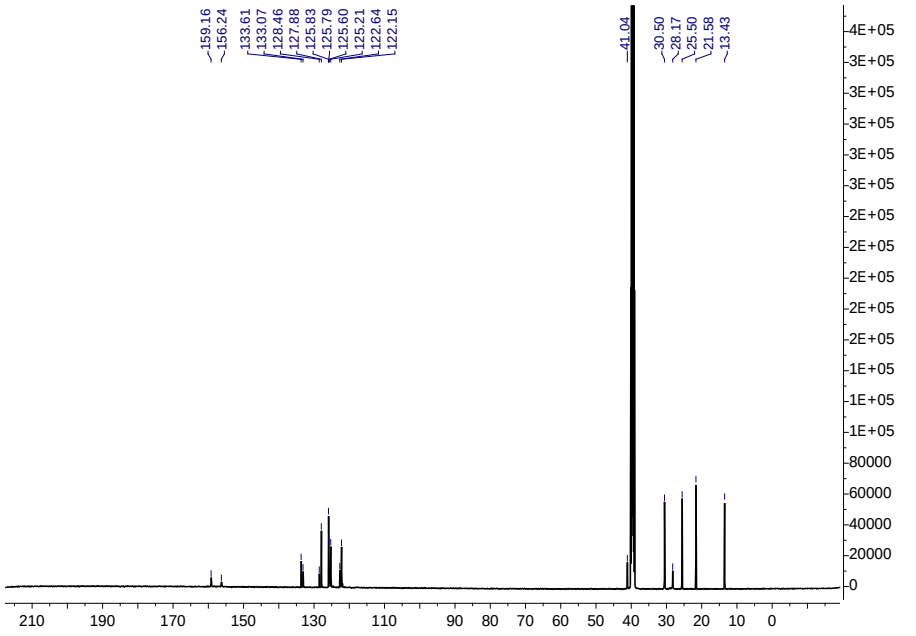

Figure S11. Spectral data for **S6:** ^{1}H-NMR (DMSO-d6, 500 MHz, 348 K).

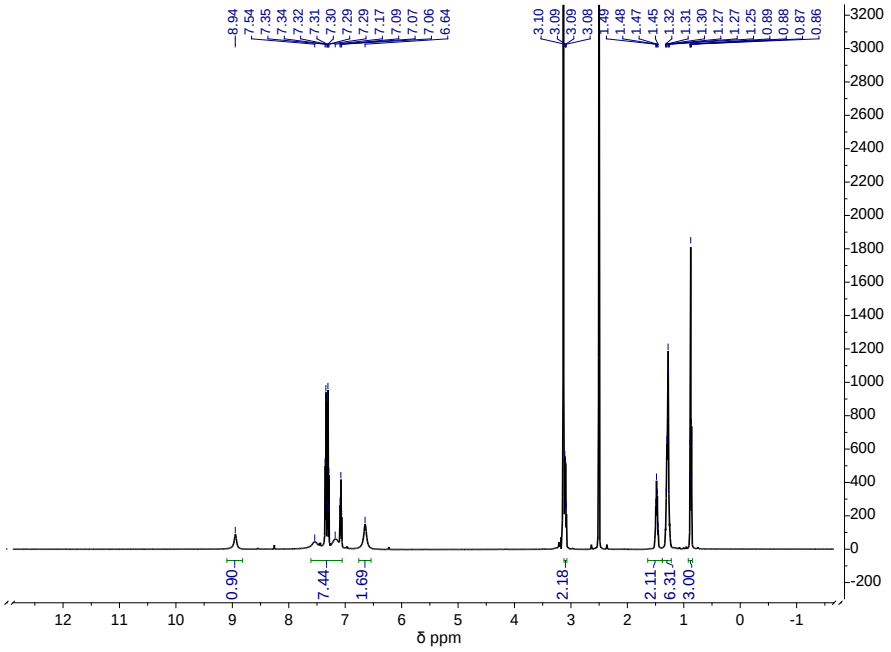

Figure S12. Spectral data for **S6**: ^{13}C-NMR (DMSO-d_6, 125 MHz, 348 K).

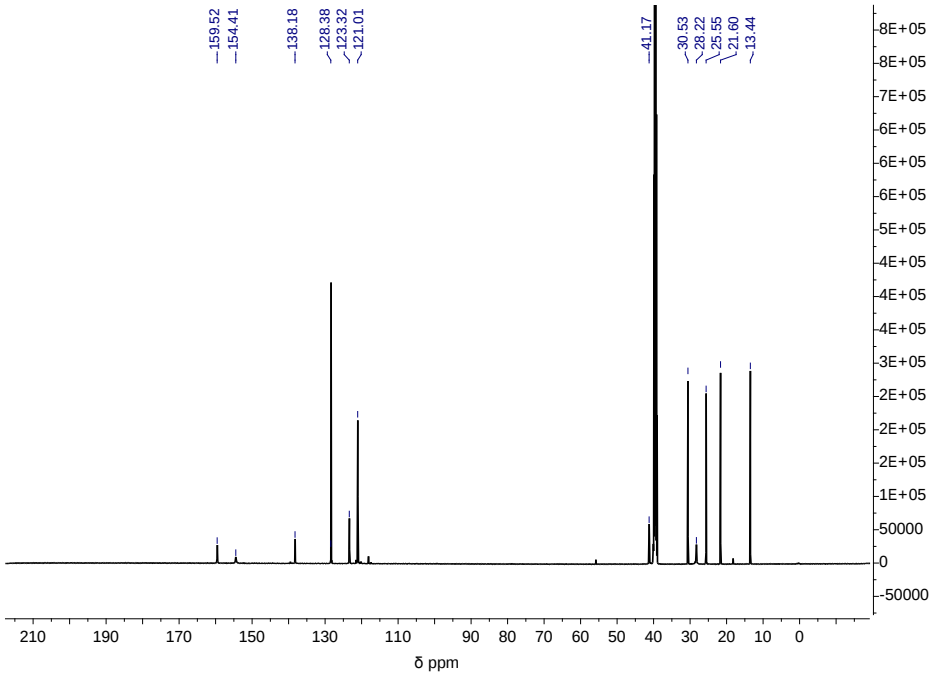

3 Photophysical Properties

The photophysical properties of sensors **S1**-**S6** (*Table S1*) were measured in mixture DMSO:$CHCl_3$ at room temperature. Absorption spectra were obtained using Hitachi U-3010 double beam UV-visible spectrophotometer (Tokyo, Japan). Fluorescence spectra were acquired at laboratory temperature using a quartz cuvette with 1 cm path length at right angle detection. Emission spectra and fluorescence lifetime measurements were carried out with Edinburgh FLS920-stm combined steady state and lifetime spectrofluorimeter (Edinburgh Instruments Ltd., Livingston, UK). Laser radiation (λ = 355 nm) was used as an excitation source for fluorescence lifetime determination experiments. Absolute quantum yields were obtained upon excitation at absorption maxima using Hamamatsu Quantaurus-QY C11347-11 Absolute PLQY Spectrometer equipped with 150 W xenon lamp and multichannel detector/CCD sensor (Hamamatsu, Japan).

Table S1. Photophysical properties of sensors **S1**-**S6**. Absorption and emission maxima ($\lambda_{ABS,max}$, $\lambda_{EM,max}$, repectively), absolute fluorescence quantum yields Φ_{FL}, fluorescence lifetimes τ_{FL}, and molar extinction coefficients ε_M were acquired in DMSO:$CHCl_3$ (3:7 v/v).

Sensor	$\lambda_{ABS,max}$[a]	$\lambda_{EM,max}$[b]	Φ_{FL} (λ_{EXC})[c]	τ_{FL}	τ_{FL} with addition of Triton X-100 (0.1 mM)
	[nm]	[nm]	[%]	[ns]	[ns]
S1	397	441	47.03 (395 nm)	5.00 (42.90 %) 10.38 (57.10 %)	4.59 (20.65 %) 9.42 (79.35 %)
S2	295	350	37.54 (296 nm)	2.11 (68.24 %) 11.05 (31.76 %)	2.32 (80.14 %) 11.27 (19.86 %)
S3	275	344	1.11 (300 nm)	3.75 (85.42 %) 20.08 (14.58 %)	2.77 (88.93 %) 20.57 (11.07 %)
S4	397	442	41.06 (395 nm)	8.33 (45.15 %) 13.08 (54.85 %)	6.94 (29.71 %) 12.16 (70.29 %)
S5	295	352	6.54 (296 nm)	2.66 (70.40 %) 11.03 (29.60 %)	2.84 (73.75 %) 11.20 (26.25 %)
S6	275	348	1.01 (300 nm)	3.10 (83.10 %) 19.24 (16.90 %)	2.50 (87.16 %) 20.52 (12.84 %)

[a] Only the lowest energy maxima are listed.
[b] Only the highest energy maxima are listed.
[c] Absolute quantum yields were determined upon excitation at wavelength indicated for solutions with optical density A = 0.2 (all errors < 4%).

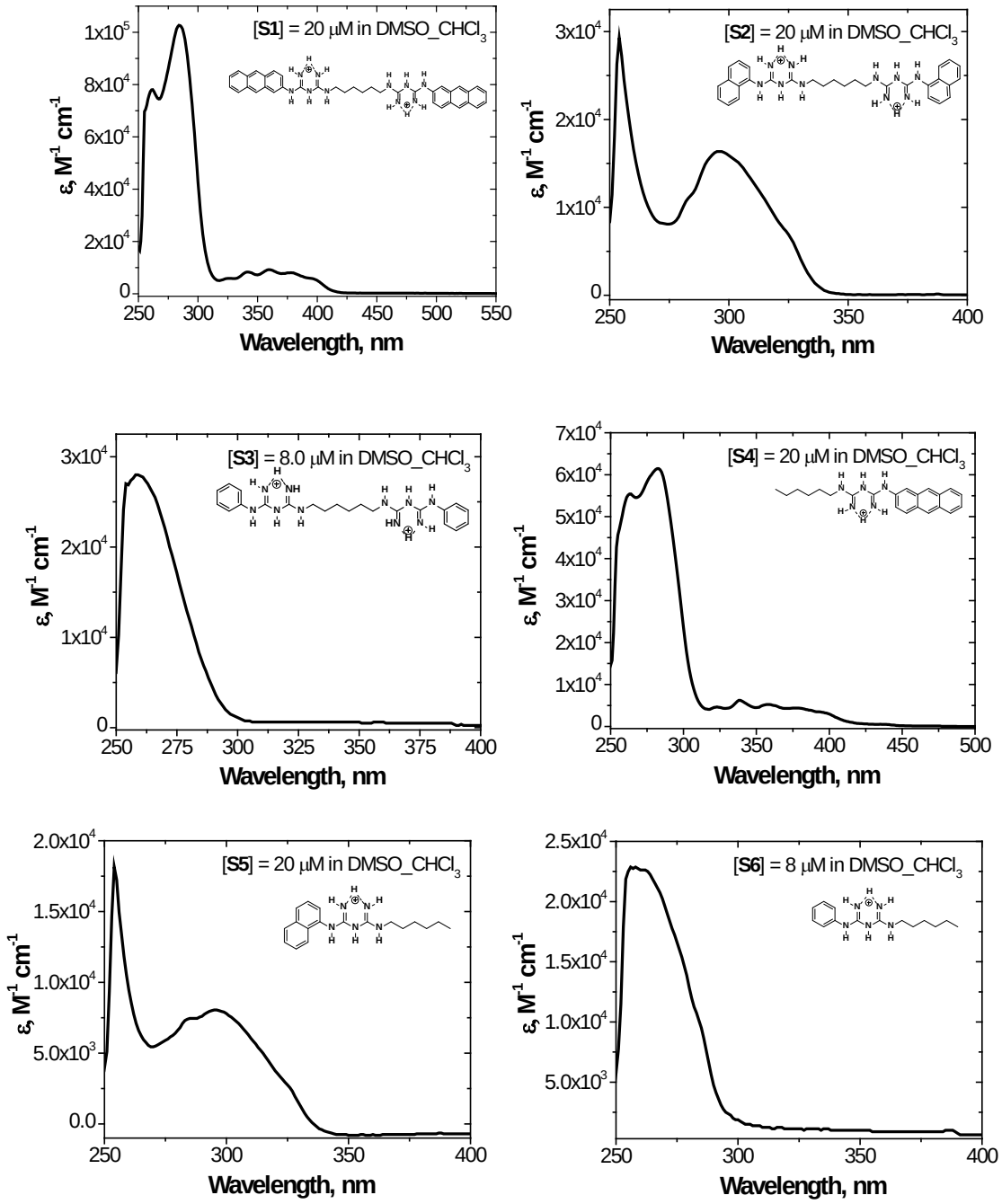

Figure S13. UV-vis absorption spectra of **S1**-**S6** in DMSO:$CHCl_3$ (3:7) with addition of Triton X-100.

4 UV-vis absorption Titrations

All UV-vis absorbtion titrations were measured in DMSO:$CHCl_3$ (3:7 v/v) with addition of Triton X-100 (0.36 mM) at room temperature. The absorbance spectra were recorded using a Hitachi U-3010 spectrophotometer. The bathochromic shifts of spectra of sensors **S1-S6** upon the titration with anions were used to calculate the binding constants. Titration isotherms were obtained by plotting the change in optical density at a certain wavelength, usually in their absorption maximum against the concentration of the anion.

Table S2. Binding affinities K_a (M^{-2}) for sensors **S1**-**S6** to various anions obtained from UV-vis absorption titration in DMSO:$CHCl_3$ (3:7 v/v) at room temperature. NR – no response. ND – Binding constants could not be determined due to more complex equilibria.

Analyte	Affinity constant (*K*a, $M^{-2} \times 10^4$)					
	S1	**S2**	**S3**	**S4**	**S5**	**S6**
Fluoride	2.90	1.70	0.99	1.90	1.40	0.83
Chloride	NR	NR	NR	NR	NR	NR
Acetate	37.0	5.80	1.80	12.0	5.20	1.20
Oxalate	49.0	6.80	1.60	19.0	6.70	1.40
Malonate	5.60	2.90	1.10	5.60	2.00	2.90
Glutamate	0.51	0.39	0.27	0.44	0.29	0.54
Benzoate	4.90	0.92	ND	4.30	ND	ND
Phthalate	0.10	0.74	ND	0.86	ND	ND
H_2Phosphate	15.0	NR	1.20	8.80	NR	NR

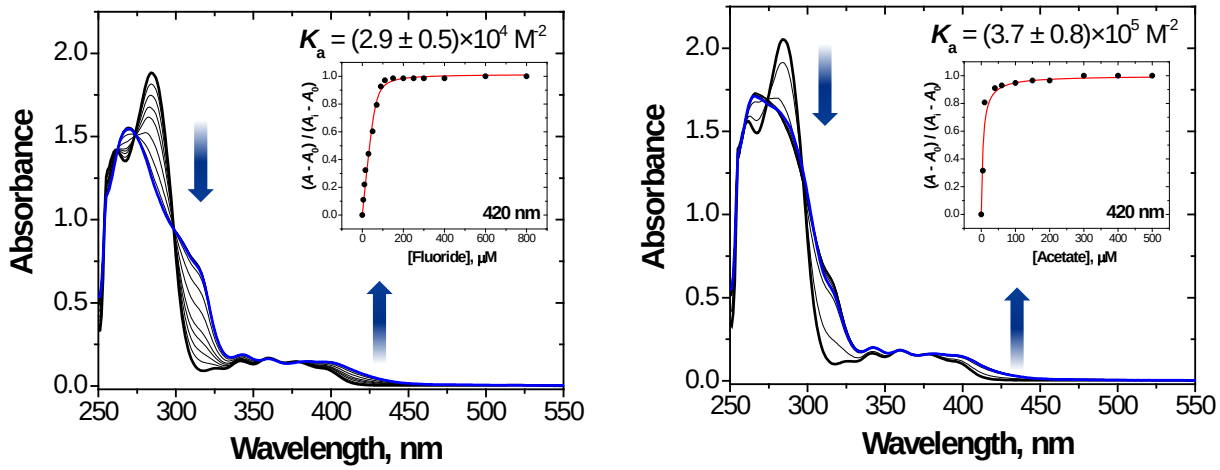

Figure S14. Left: Absorption titration spectra and isotherm of **S1** (20μM) upon addition of Fluoride anion in DMSO:$CHCl_3$ (3:7, v/v) with Triton X-100 (0.36mM). **Right:** Absorption titration spectra and isotherm of **S1** (20μM) upon addition of Acetate anion in DMSO:$CHCl_3$ (3:7, v/v) with Triton X-100 (0.36mM).

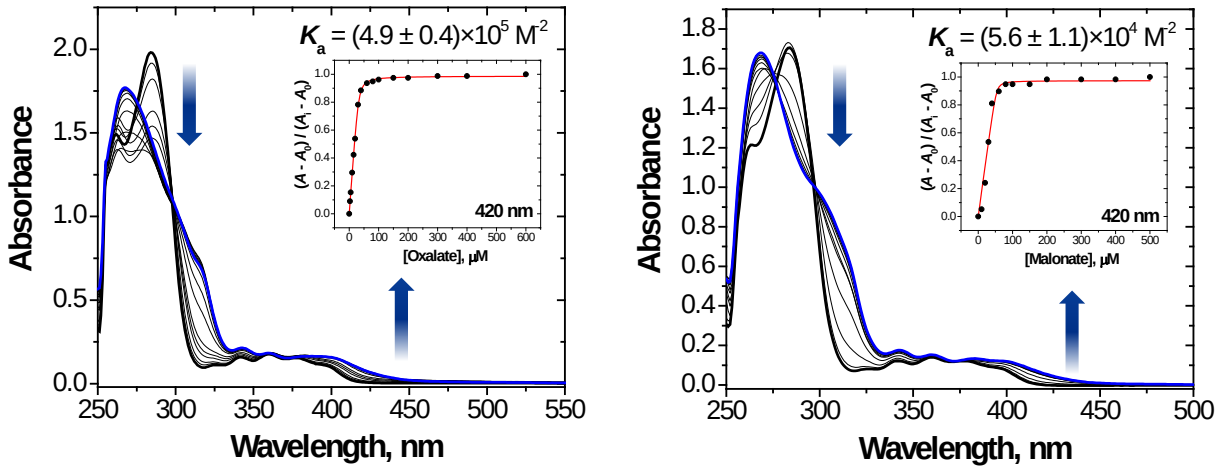

Figure S15. Left: Absorption titration spectra and isotherm of **S1** (20μM) upon addition of Oxalate anion in DMSO:$CHCl_3$ (3:7, v/v) with Triton X-100 (0.36mM). **Right:** Absorption titration spectra and isotherm of **S1** (20μM) upon addition of Malonate anion in DMSO:$CHCl_3$ (3:7, v/v) with Triton X-100 (0.36mM).

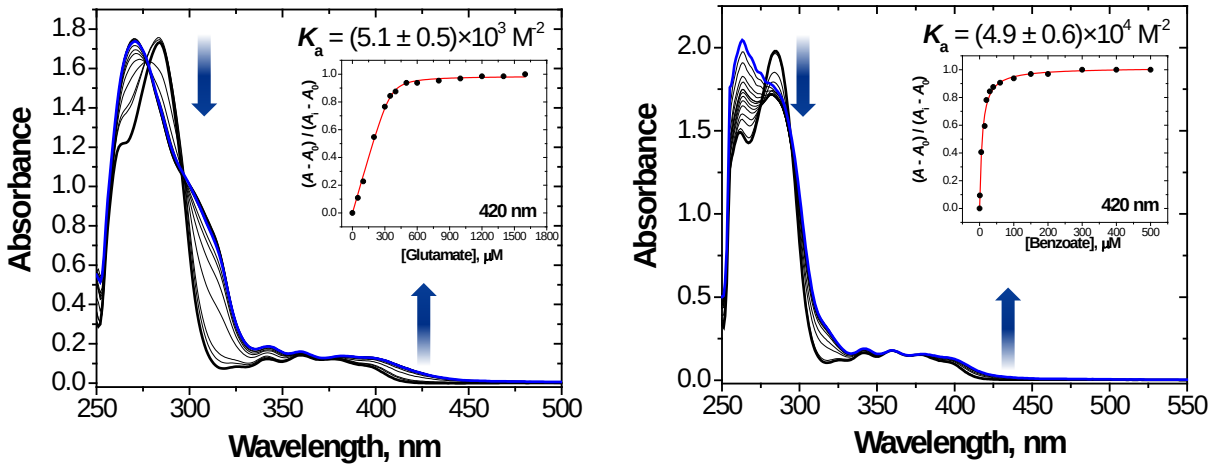

Figure S16. Left: Absorption titration spectra and isotherm of **S1** (20μM) upon addition of Glutamate anion in DMSO:$CHCl_3$ (3:7, v/v) with Triton X-100 (0.36mM). **Right:** Absorption titration spectra and isotherm of **S1** (20μM) upon addition of Benzoate anion in DMSO:$CHCl_3$ (3:7, v/v) with Triton X-100 (0.36mM).

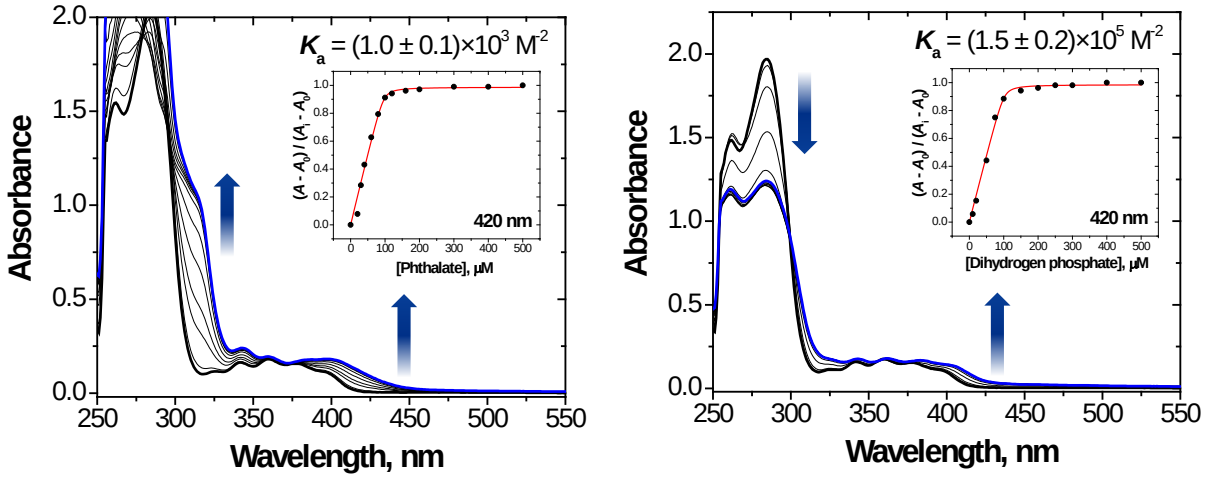

Figure S17. Left: Absorption titration spectra and isotherm of **S1** (20μM) upon addition of Phthalate anion in DMSO:$CHCl_3$ (3:7, v/v) with Triton X-100 (0.36mM). **Right:** Absorption titration spectra and isotherm of **S1** (20μM) upon addition of Dihydrogen phosphate anion in DMSO:$CHCl_3$ (3:7, v/v) with Triton X-100 (0.36mM).

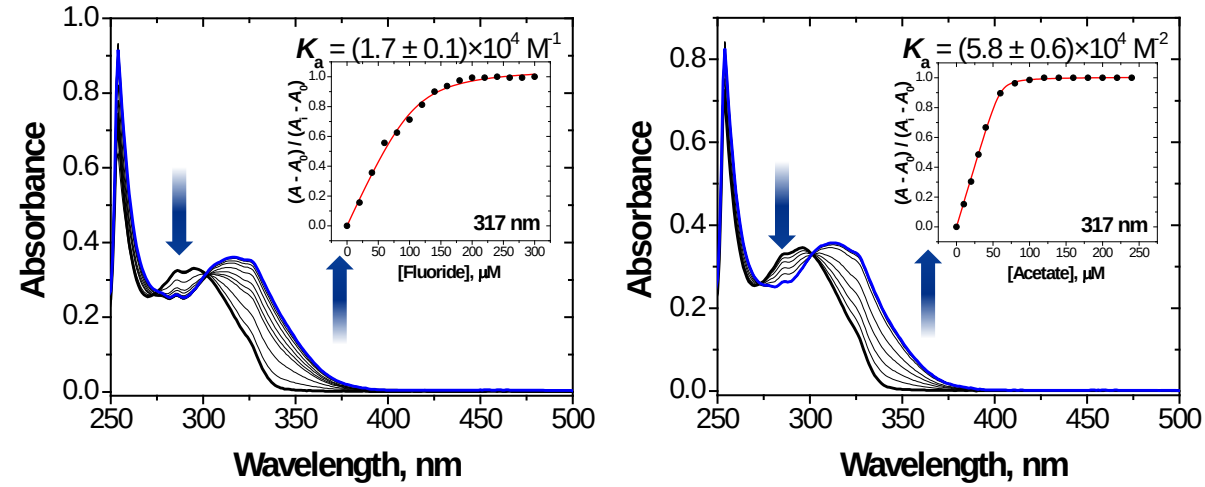

Figure S18. Left: Absorption titration spectra and isotherm of **S1** (20μM) upon addition of Fluoride anion in DMSO:$CHCl_3$ (3:7, v/v) with Triton X-100 (0.36mM). **Right:** Absorption titration spectra and isotherm of **S1** (20μM) upon addition of Acetate anion in DMSO:$CHCl_3$ (3:7, v/v) with Triton X-100 (0.36mM).

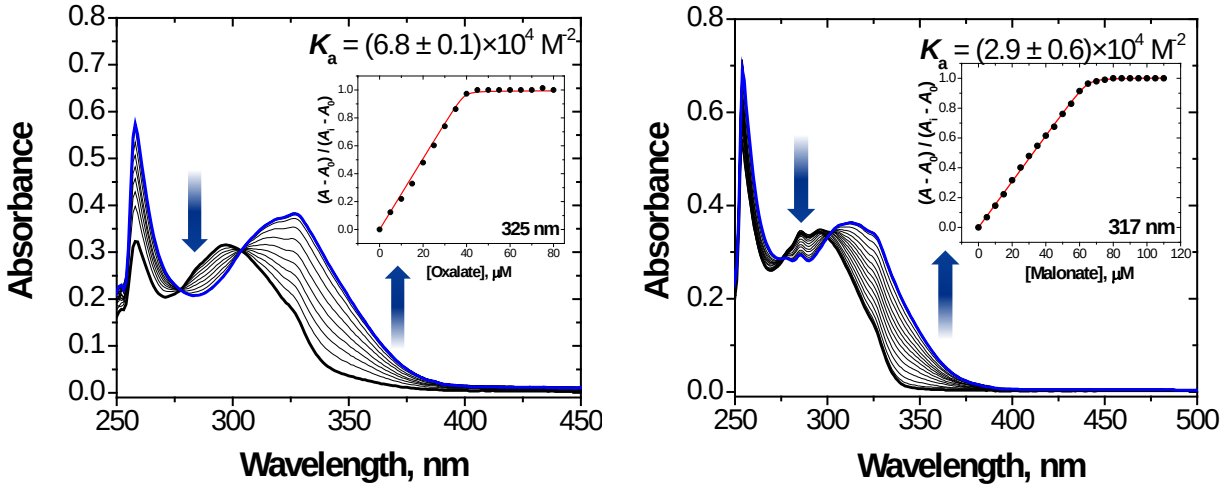

Figure S19. Left: Absorption titration spectra and isotherm of **S2** (20μM) upon addition of Oxalate anion in DMSO:$CHCl_3$ (3:7, v/v) with Triton X-100 (0.36mM). **Right:** Absorption titration spectra and isotherm of **S2** (20μM) upon addition of Malonate anion in DMSO:$CHCl_3$ (3:7, v/v) with Triton X-100 (0.36mM).

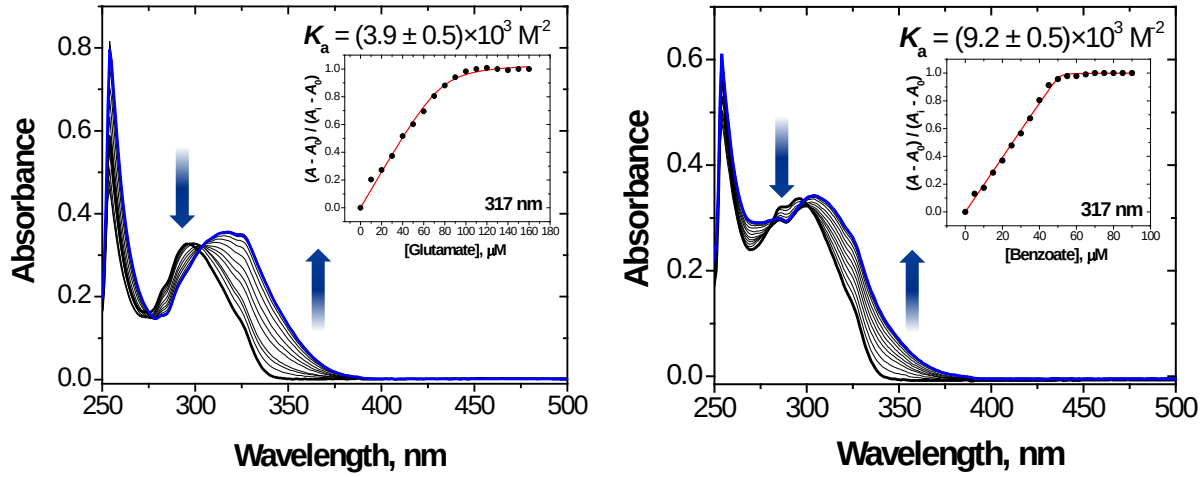

Figure S20. Left: Absorption titration spectra and isotherm of **S2** (20μM) upon addition of Glutamate anion in DMSO:$CHCl_3$ (3:7, v/v) with Triton X-100 (0.36mM). **Right:** Absorption titration spectra and isotherm of **S2** (20μM) upon addition of Benzoate anion in DMSO:$CHCl_3$ (3:7, v/v) with Triton X-100 (0.36mM).

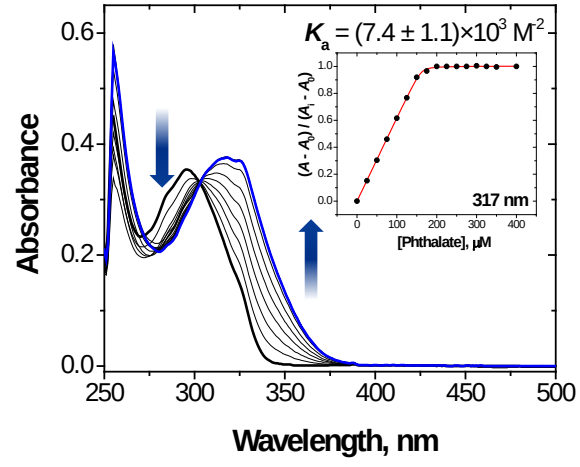

Figure S21. Absorption titration spectra and isotherm of **S2** (20μM) upon addition of Phthalate anion in DMSO:$CHCl_3$ (3:7, v/v) with Triton X-100 (0.36mM).

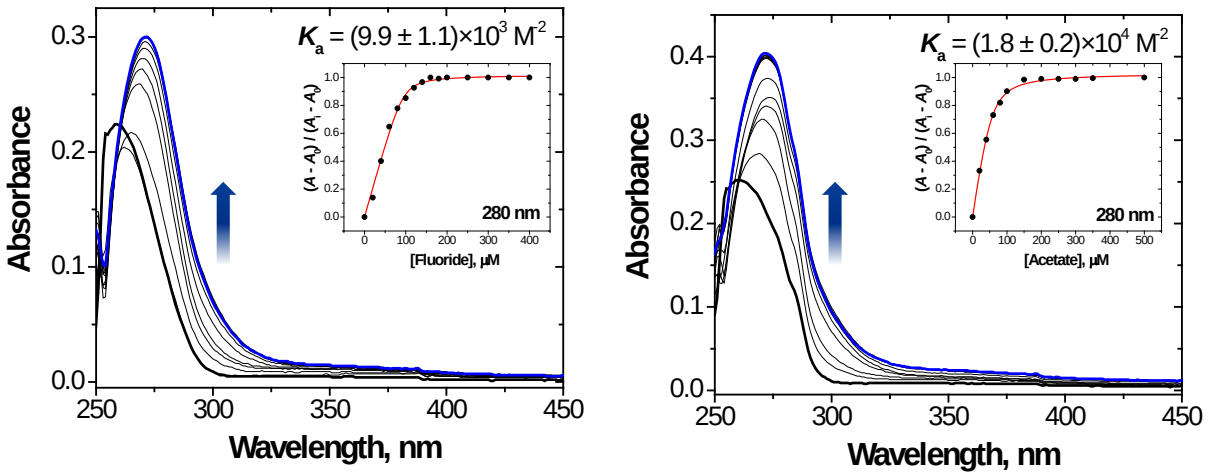

Figure S22. Left: Absorption titration spectra and isotherm of **S3** (8μM) upon addition of Fluoride anion in DMSO:$CHCl_3$ (3:7, v/v) with Triton X-100 (0.36mM). **Right:** Absorption titration spectra and isotherm of **S3** (8μM) upon addition of Acetate anion in DMSO:$CHCl_3$ (3:7, v/v) with Triton X-100 (0.36mM).

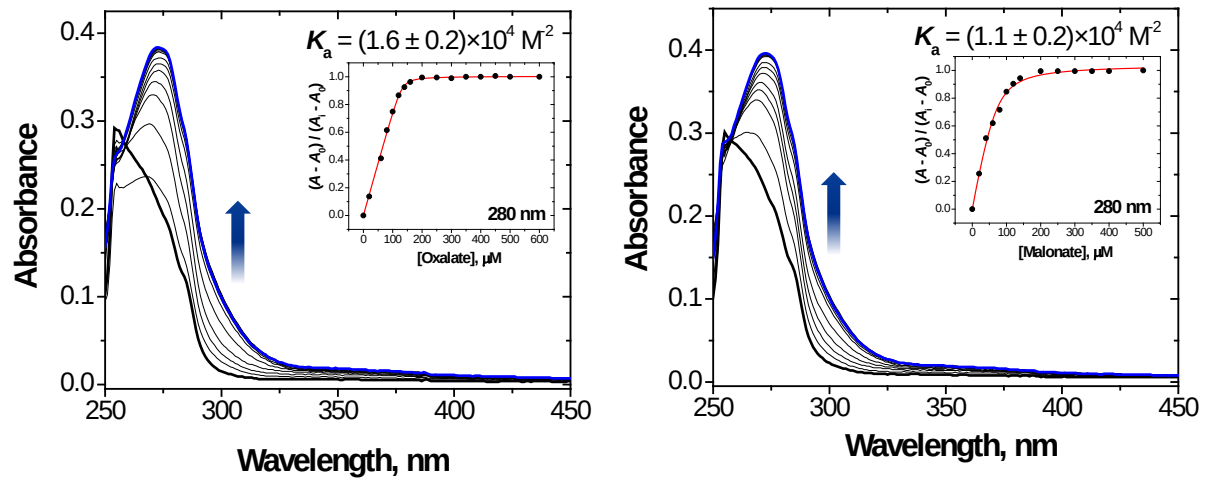

Figure S23. Left: Absorption titration spectra and isotherm of **S3** (8μM) upon addition of Oxalate anion in DMSO:$CHCl_3$ (3:7, v/v) with Triton X-100 (0.36mM). **Right:** Absorption titration spectra and isotherm of **S3** (8μM) upon addition of Malonate anion in DMSO:$CHCl_3$ (3:7, v/v) with Triton X-100 (0.36mM).

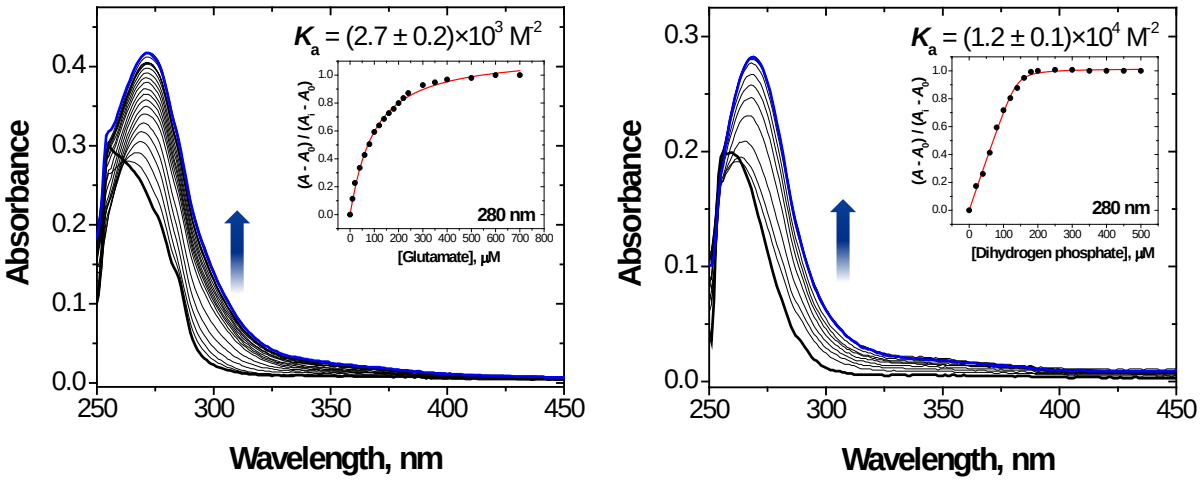

Figure S24. Left: Absorption titration spectra and isotherm of **S3** (8μM) upon addition of Glutamate anion in DMSO:$CHCl_3$ (3:7, v/v) with Triton X-100 (0.36mM). **Right:** Absorption titration spectra and isotherm of **S3** (8μM) upon addition of Dihydrogen phosphate anion in DMSO:$CHCl_3$ (3:7, v/v) with Triton X-100 (0.36mM).

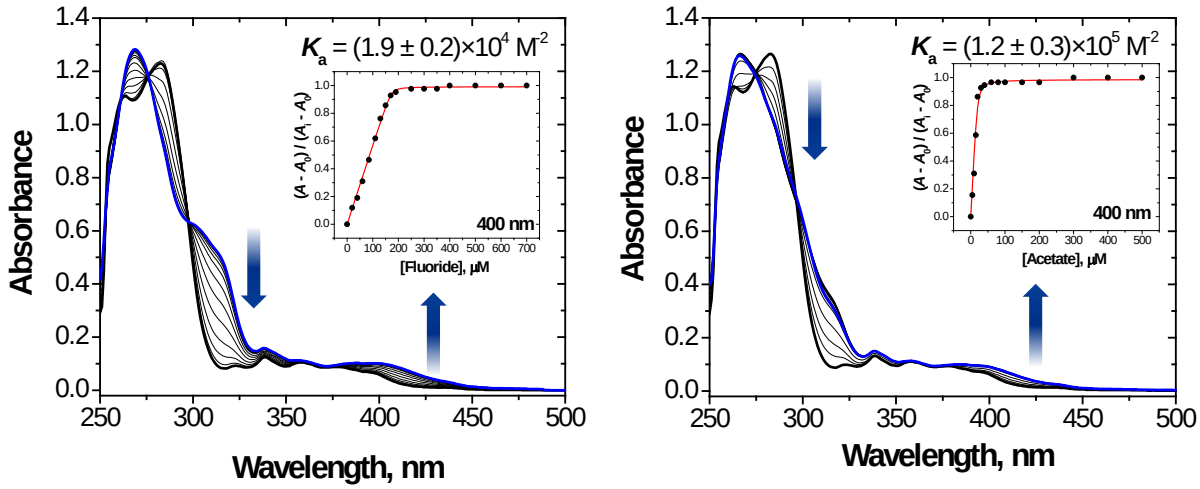

Figure S25. Left: Absorption titration spectra and isotherm of **S4** (20μM) upon addition of Fluoride anion in DMSO:$CHCl_3$ (3:7, v/v) with Triton X-100 (0.36mM). **Right:** Absorption titration spectra and isotherm of **S4** (20μM) upon addition of Acetate anion in DMSO:$CHCl_3$ (3:7, v/v) with Triton X-100 (0.36mM).

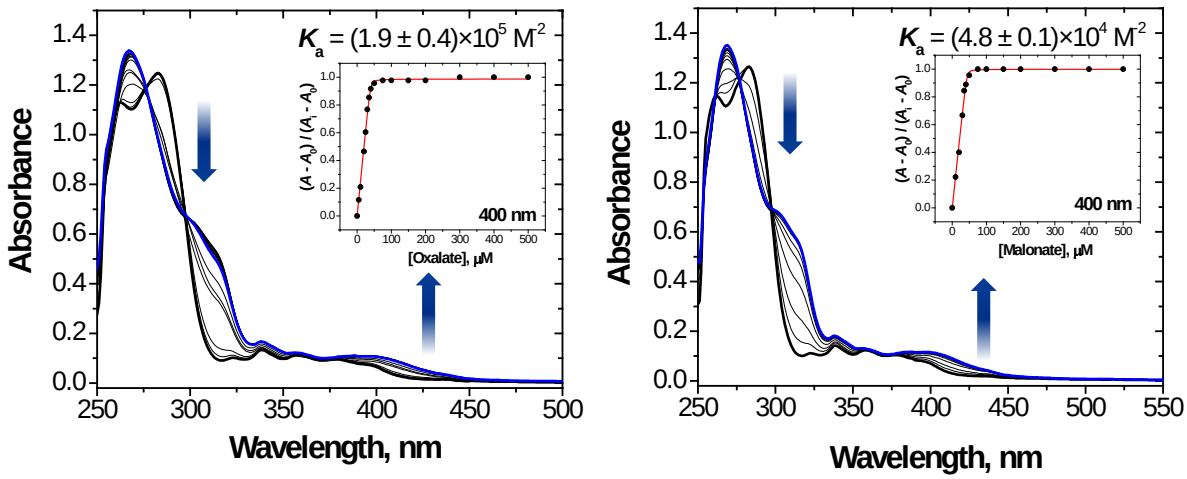

Figure S26. Left: Absorption titration spectra and isotherm of **S4** (20μM) upon addition of Oxalate anion in DMSO:$CHCl_3$ (3:7, v/v) with Triton X-100 (0.36mM). **Right:** Absorption titration spectra and isotherm of **S4** (20μM) upon addition of Malonate anion in DMSO:$CHCl_3$ (3:7, v/v) with Triton X-100 (0.36mM).

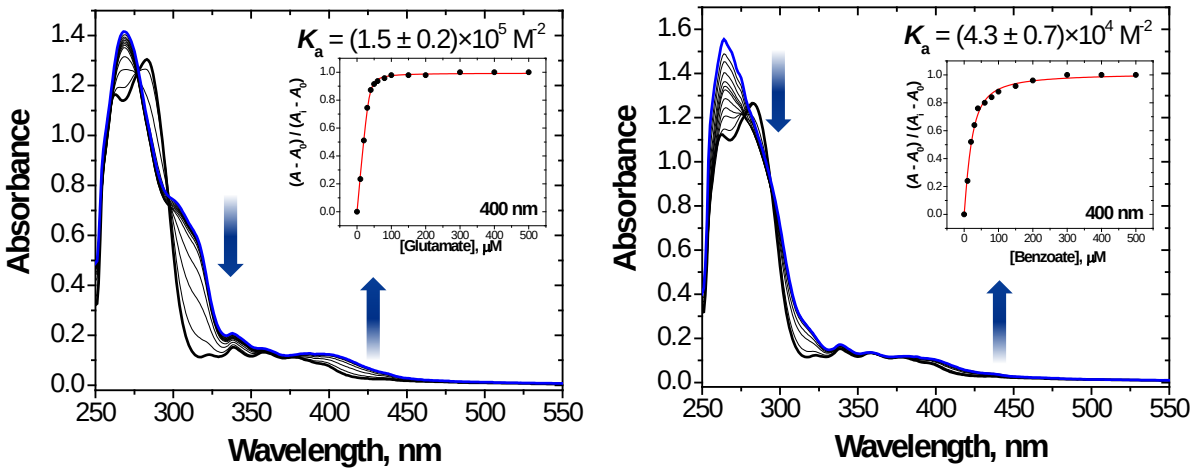

Figure S27. Left: Absorption titration spectra and isotherm of **S4** (20μM) upon addition of Glutamate anion in DMSO:$CHCl_3$ (3:7, v/v) with Triton X-100 (0.36mM). **Right:** Absorption titration spectra and isotherm of **S4** (20μM) upon addition of Benzoate anion in DMSO:$CHCl_3$ (3:7, v/v) with Triton X-100 (0.36mM).

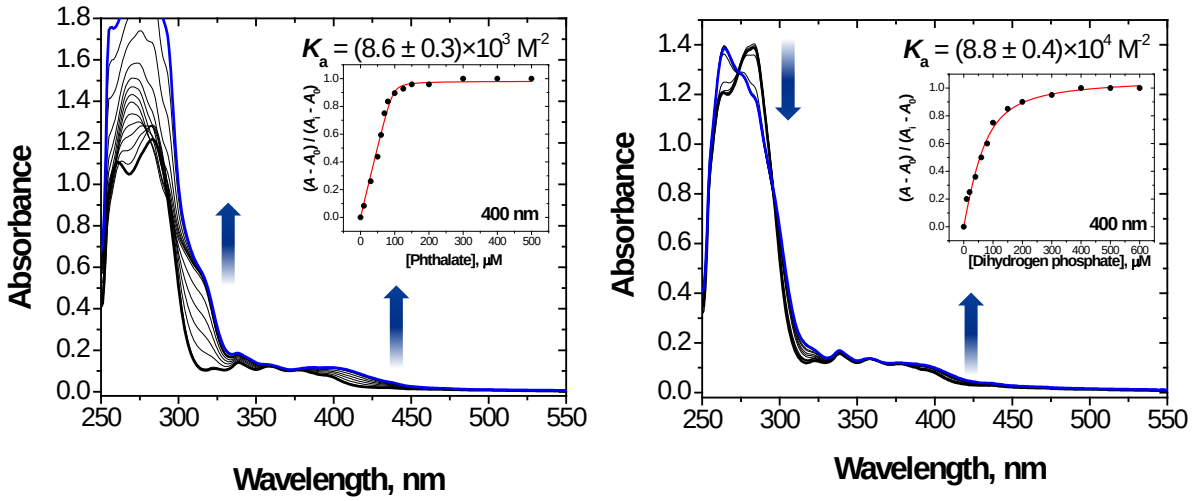

Figure S28. Left: Absorption titration spectra and isotherm of **S4** (20μM) upon addition of Phthalate anion in DMSO:$CHCl_3$ (3:7, v/v) with Triton X-100 (0.36mM). **Right:** Absorption titration spectra and isotherm of **S4** (20μM) upon addition of Dihydrogen phosphate anion in DMSO:$CHCl_3$ (3:7, v/v) with Triton X-100 (0.36mM).

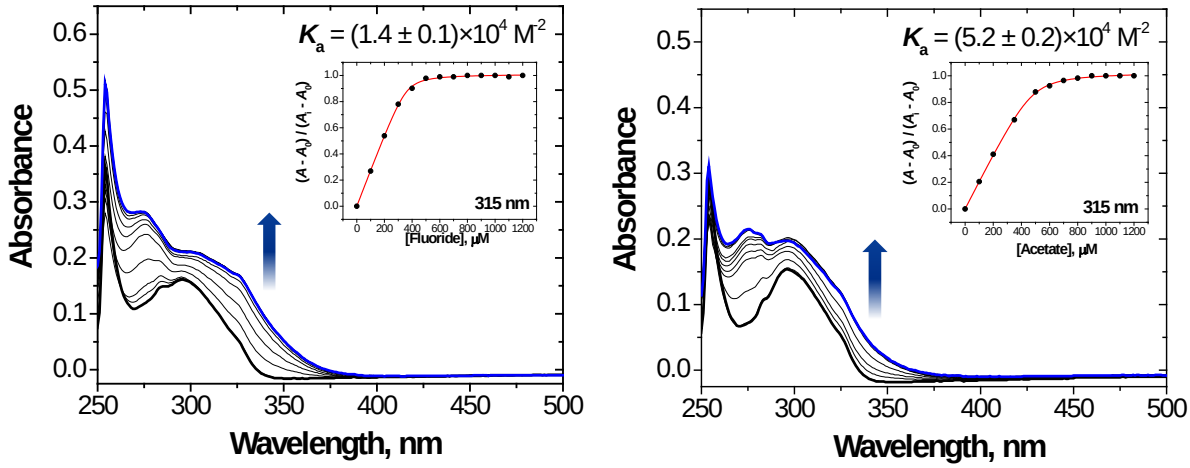

Figure S29. Left: Absorption titration spectra and isotherm of **S5** (20μM) upon addition of Fluoride anion in DMSO:$CHCl_3$ (3:7, v/v) with Triton X-100 (0.36mM). **Right:** Absorption titration spectra and isotherm of **S5** (20μM) upon addition of Acetate anion in DMSO:$CHCl_3$ (3:7, v/v) with Triton X-100 (0.36mM).

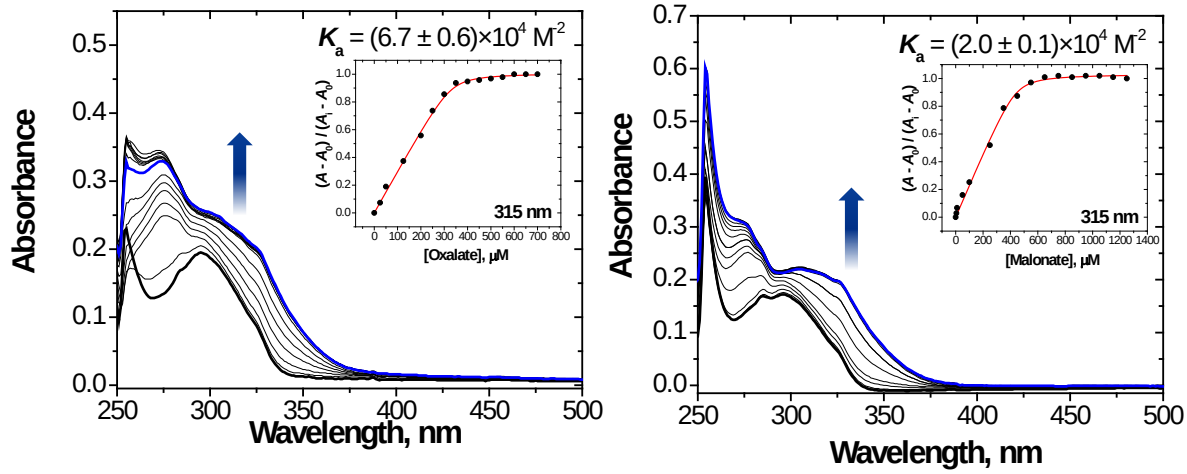

Figure S30. Left: Absorption titration spectra and isotherm of **S5** (20μM) upon addition of Oxalate anion in DMSO:$CHCl_3$ (3:7, v/v) with Triton X-100 (0.36mM). **Right:** Absorption titration spectra and isotherm of **S5** (20μM) upon addition of Malonate anion in DMSO:$CHCl_3$ (3:7, v/v) with Triton X-100 (0.36mM).

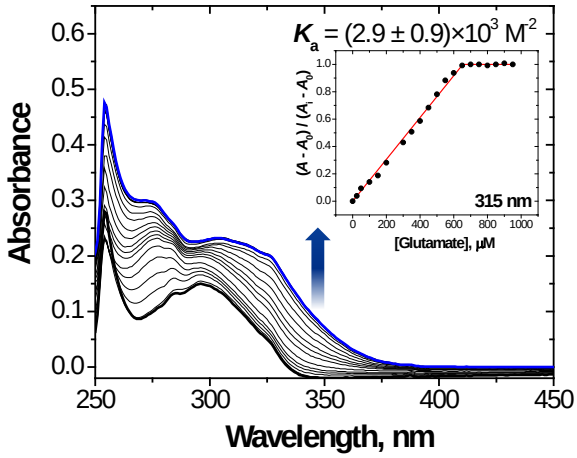

Figure S31. Absorption titration spectra and isotherm of **S5** (20μM) upon addition of Glutamate anion in DMSO:$CHCl_3$ (3:7, v/v) with Triton X-100 (0.36mM).

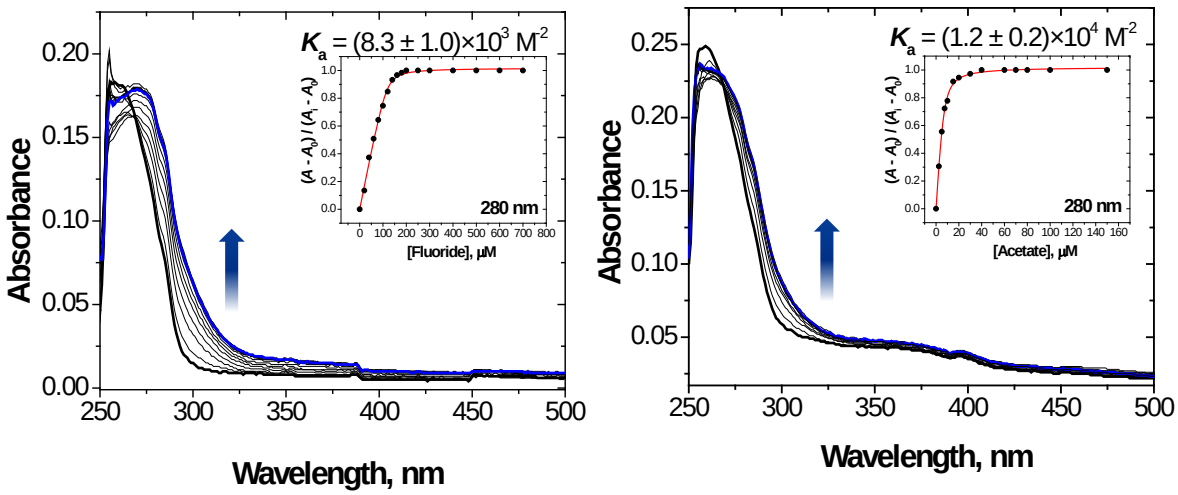

Figure S32. Left: Absorption titration spectra and isotherm of **S6** (8μM) upon addition of Fluoride anion in DMSO:$CHCl_3$ (3:7, v/v) with Triton X-100 (0.36mM). **Right:** Absorption titration spectra and isotherm of **S6** (8μM) upon addition of Acetate anion in DMSO:$CHCl_3$ (3:7, v/v) with Triton X-100 (0.36mM).

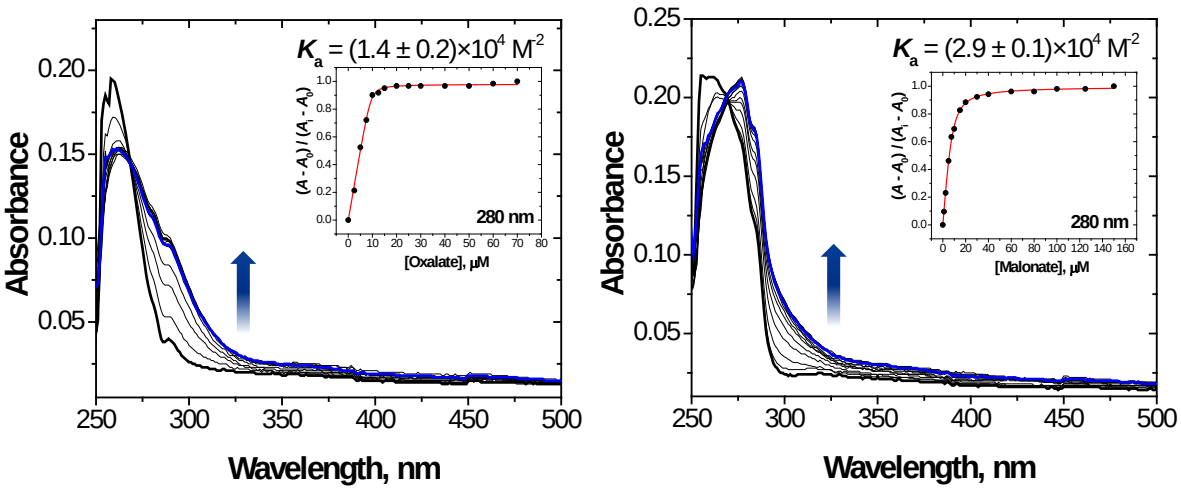

Figure S33. Left: Absorption titration spectra and isotherm of **S6** (8μM) upon addition of Oxalate anion in DMSO:$CHCl_3$ (3:7, v/v) with Triton X-100 (0.36mM). **Right:** Absorption titration spectra and isotherm of **S6** (8μM) upon addition of Malonate anion in DMSO:$CHCl_3$ (3:7, v/v) with Triton X-100 (0.36mM)

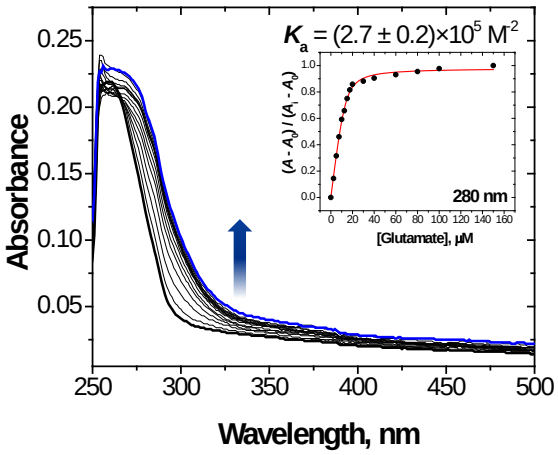

Figure S34. Absorption titration spectra and isotherm of **S6** (8μM) upon addition of Glutamate anion in DMSO:$CHCl_3$ (3:7, v/v) with Triton X-100 (0.36mM).

5 Fluorescence Titrations

All fluorescence titrations were measured in DMSO:$CHCl_3$ (3:7 v/v) with addition of Triton X-100 (0.36 mM) at room temperature using a quartz fluorescence cuvette (Starna Cells) with 1 cm path length at right angle detection on Edinburgh FLS920-stm steady state spectrofluorimeter (Edinburgh Instruments Ltd., Livingston, UK). The titrations were carried as follows. The sensor solutions (2.5 mL) in DMSO:$CHCl_3$ (3:7 v/v) with Triton X-100 (0.36 mM) in cuvette were titrated with stock solution of various anions (62.5 mM in DMSO:$CHCl_3$ (3:7 v/v)) and the change in fluorescence intensity was recorded.

Table S3. Binding affinities K_a (M^{-2}) for sensors **S1**-**S6** to various anions obtained from fluorescence titration in DMSO:$CHCl_3$ (3:7 v/v) with addition of Triton X-100 (0.36 mM) at room temperature.

Analyte	Affinity constant (*K*a, $M^{-2} \times 10^4$)					
	S1	**S2**	**S3**	**S4**	**S5**	**S6**
Fluoride	10.0	6.90	1.40	6.30	ND	1.00
Chloride	5.80	0.12	NR	NR	NR	NR
Acetate	51.0	11.0	3.30	12.0	ND	3.30
Oxalate	41.0	12.0	4.10	19.0	ND	1.70
Malonate	14.0	5.50	2.60	4.80	ND	3.00
Glutamate	1.30	0.87	0.57	4.40	ND	0.28
Benzoate	7.80	5.00	0.66	4.30	ND	3.10
Phthalate	0.48	3.80	0.30	0.86	ND	1.70
H_2Phosphate	35.0	ND	0.48	8.80	ND	2.20

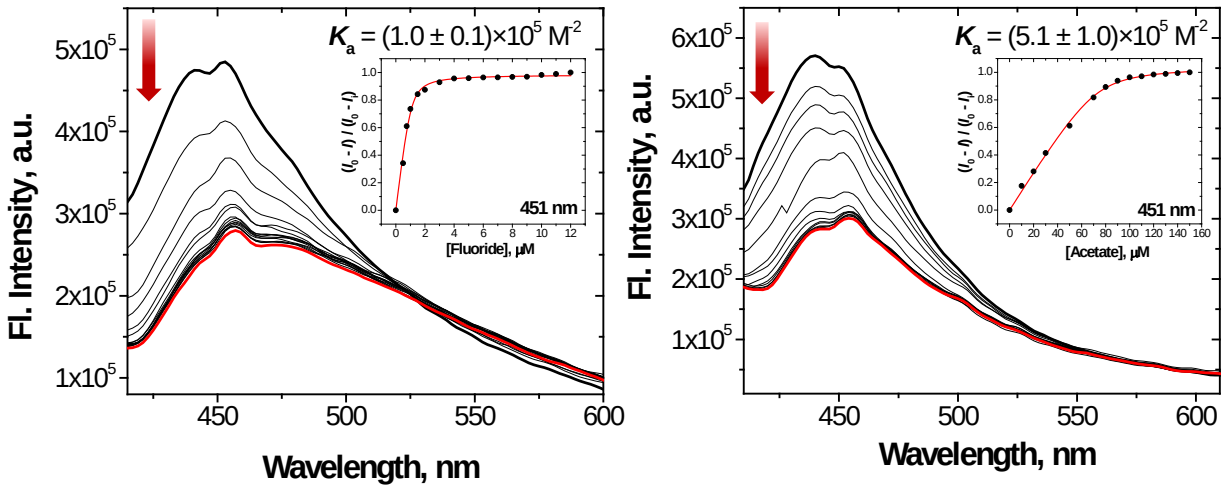

Figure S35. Left: Fluorescence titration spectra (λ_{ex}=375 nm) and isotherm of **S1** (0.2 µM) upon addition of Fluoride anion in DMSO:$CHCl_3$ (3:7, v/v) with Triton X-100 (0.36mM). **Right:** Fluorescence titration spectra (λ_{ex}=375 nm) and isotherm of **S1** (0.2 µM) upon addition of Acetate anion in DMSO:$CHCl_3$ (3:7, v/v) with Triton X-100 (0.36mM).

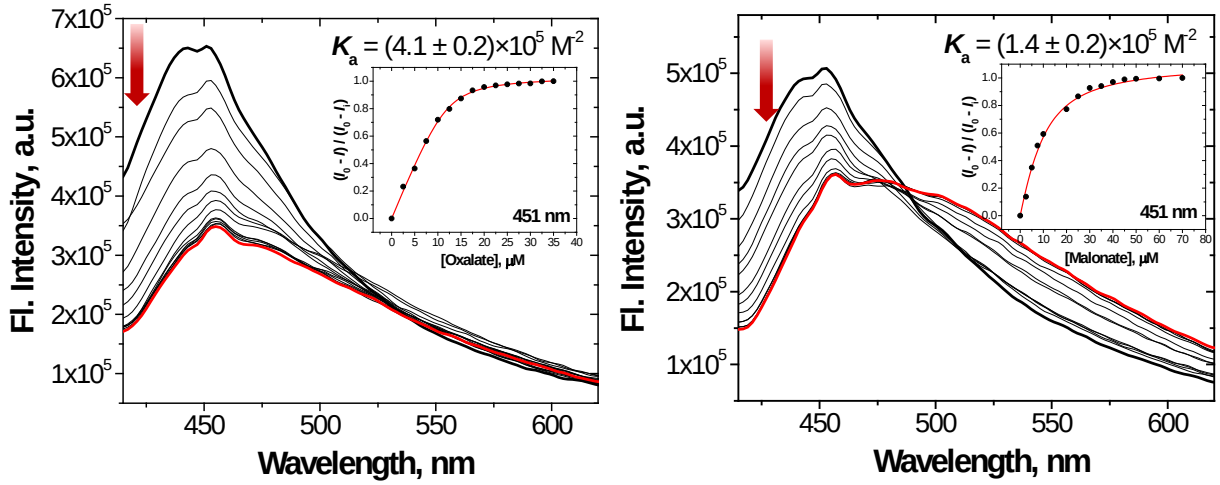

Figure S36. Left: Fluorescence titration spectra (λ_{ex}=375 nm) and isotherm of **S1** (0.2 μM) upon addition of Oxalate anion in DMSO:$CHCl_3$ (3:7, v/v) with Triton X-100 (0.36mM). **Right:** Fluorescence titration spectra (λ_{ex}=375 nm) and isotherm of **S1** (0.2 μM) upon addition of Malonate anion in DMSO:$CHCl_3$ (3:7, v/v) with Triton X-100 (0.36mM).

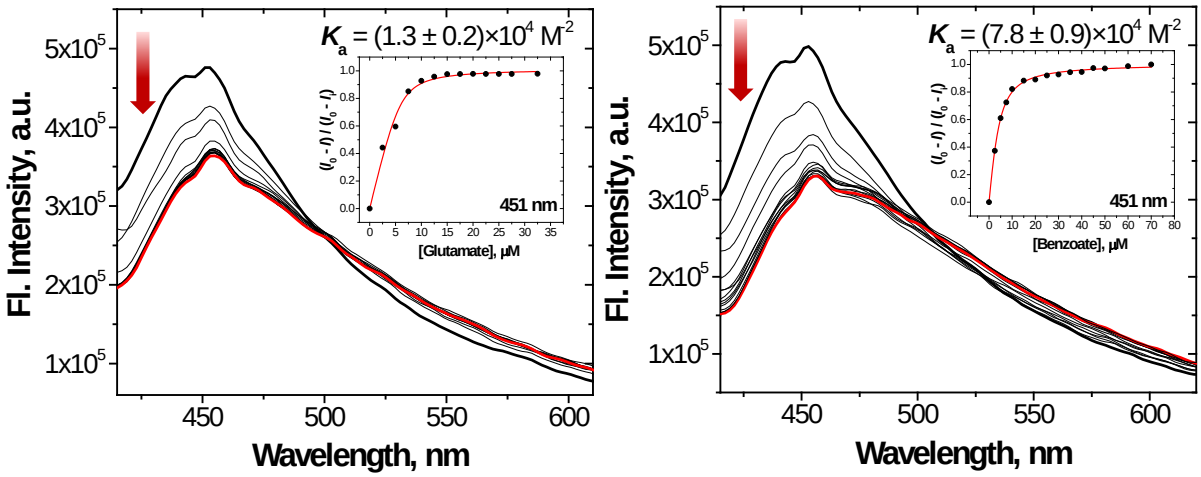

Figure S37. Left: Fluorescence titration spectra (λ_{ex}=375 nm) and isotherm of **S1** (0.2 μM) upon addition of Glutamate anion in DMSO:$CHCl_3$ (3:7, v/v) with Triton X-100 (0.36mM). **Right:** Fluorescence titration spectra (λ_{ex}=375 nm) and isotherm of **S1** (0.2 μM) upon addition of Benzoate anion in DMSO:$CHCl_3$ (3:7, v/v) with Triton X-100 (0.36mM).

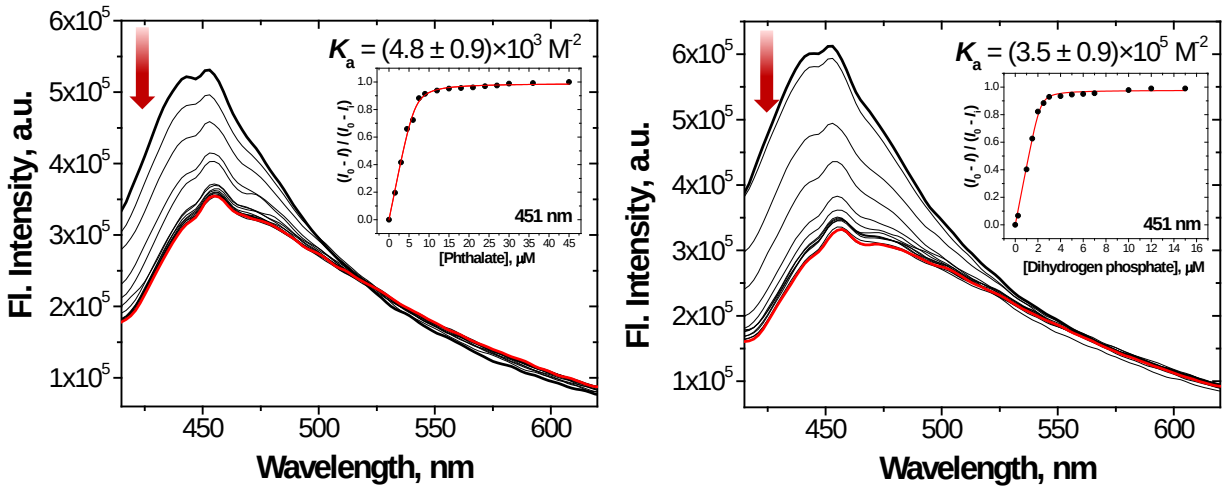

Figure S38. Left: Fluorescence titration spectra (λ_{ex}=375 nm) and isotherm of **S1** (0.2 μM) upon addition of Phthalate anion in DMSO:$CHCl_3$ (3:7, v/v) with Triton X-100 (0.36mM). **Right:** Fluorescence titration spectra (λ_{ex}=375 nm) and isotherm of **S1** (0.2 μM) upon addition of Dihydrogen phosphate anion in DMSO:$CHCl_3$ (3:7, v/v) with Triton X-100 (0.36mM).

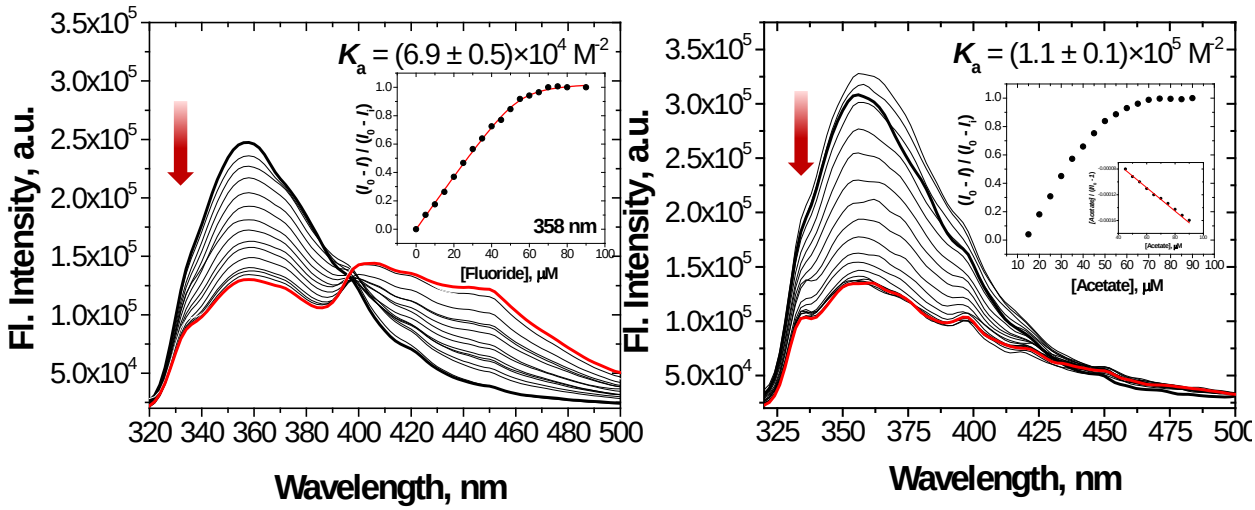

Figure S39. Left: Fluorescence titration spectra (λ_{ex}=305 nm) and isotherm of **S2** (20μM) upon addition of Fluoride anion in DMSO:$CHCl_3$ (3:7, v/v) with Triton X-100 (0.36mM). **Right:** Fluorescence titration spectra (λ_{ex}=305 nm) and isotherm of **S2** (20μM) upon addition of Acetate anion in DMSO:$CHCl_3$ (3:7, v/v) with Triton X-100 (0.36mM).

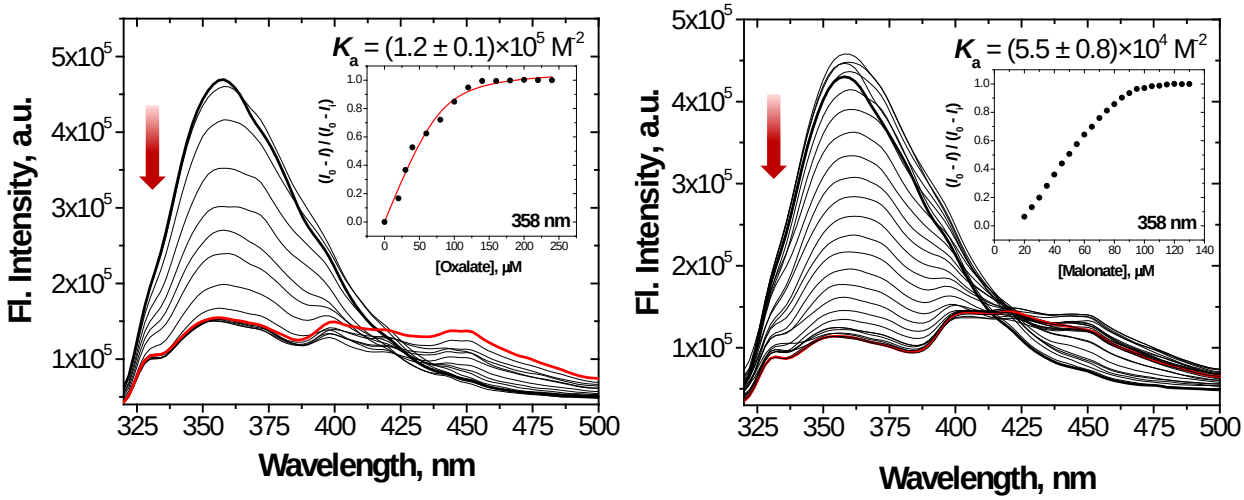

Figure S40. Left: Fluorescence titration spectra (λ_{ex}=305 nm) and isotherm of **S2** (20μM) upon addition of Oxalate anion in DMSO:$CHCl_3$ (3:7, v/v) with Triton X-100 (0.36mM). **Right:** Fluorescence titration spectra (λ_{ex}=305 nm) and isotherm of **S2** (20μM) upon addition of Malonate anion in DMSO:$CHCl_3$ (3:7, v/v) with Triton X-100 (0.36mM).

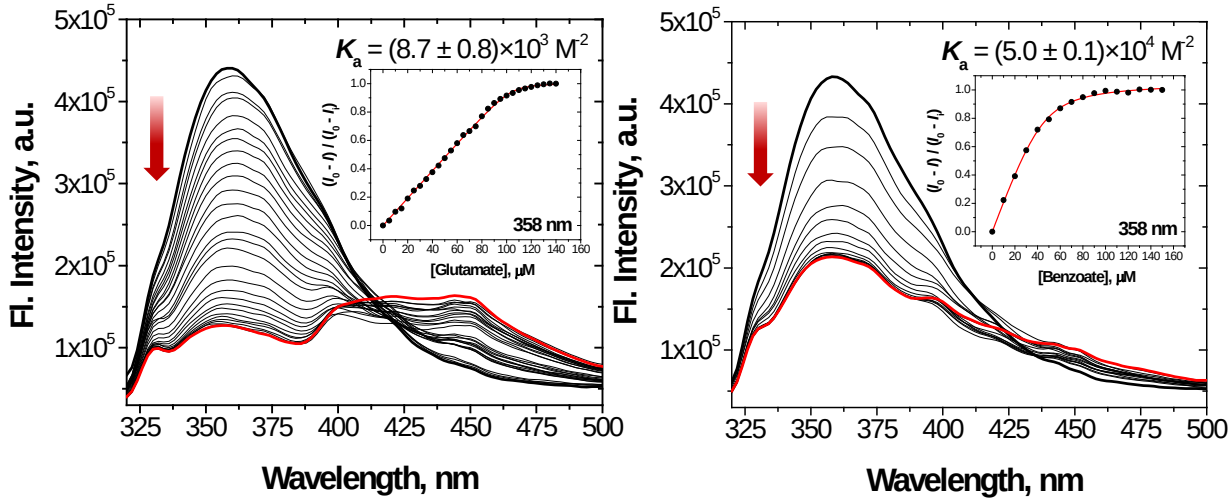

Figure S41. Left: Fluorescence titration spectra (λ_{ex}=305 nm) and isotherm of **S2** (20μM) upon addition of Glutamate anion in DMSO:$CHCl_3$ (3:7, v/v) with Triton X-100 (0.36mM). **Right:** Fluorescence titration spectra (λ_{ex}=305 nm) and isotherm of **S2** (20μM) upon addition of Benzoate anion in DMSO:$CHCl_3$ (3:7, v/v) with Triton X-100 (0.36mM).

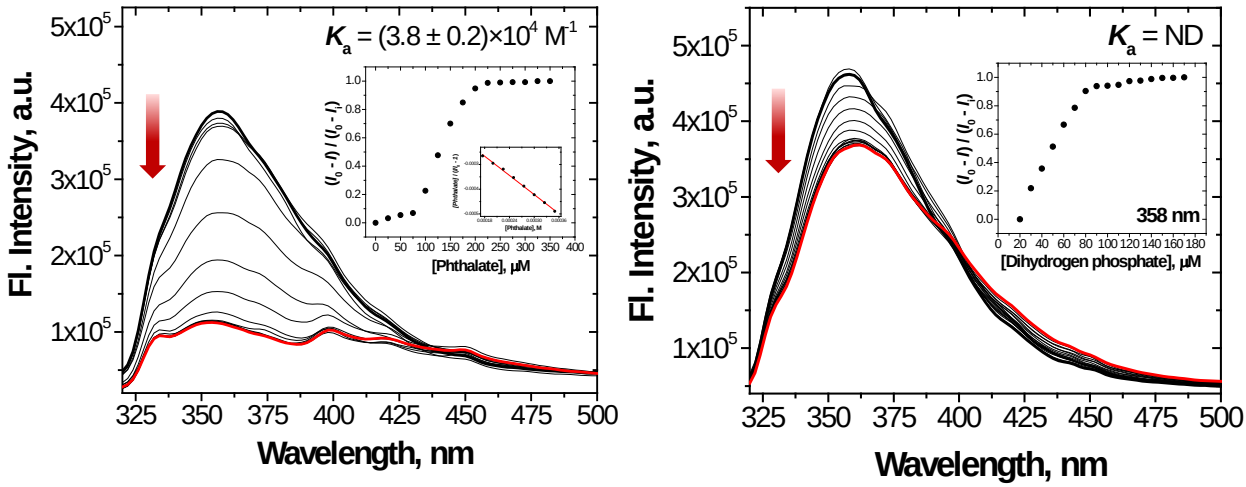

Figure S42. Left: Fluorescence titration spectra (λ_{ex}=305 nm) and isotherm of **S2** (20μM) upon addition of Phthalate anion in DMSO:$CHCl_3$ (3:7, v/v) with Triton X-100 (0.36mM). **Right:** Fluorescence titration spectra (λ_{ex}=305 nm) and isotherm of **S2** (20μM) upon addition of Dihydrogen phosphate anion in DMSO:$CHCl_3$ (3:7, v/v) with Triton X-100 (0.36mM).

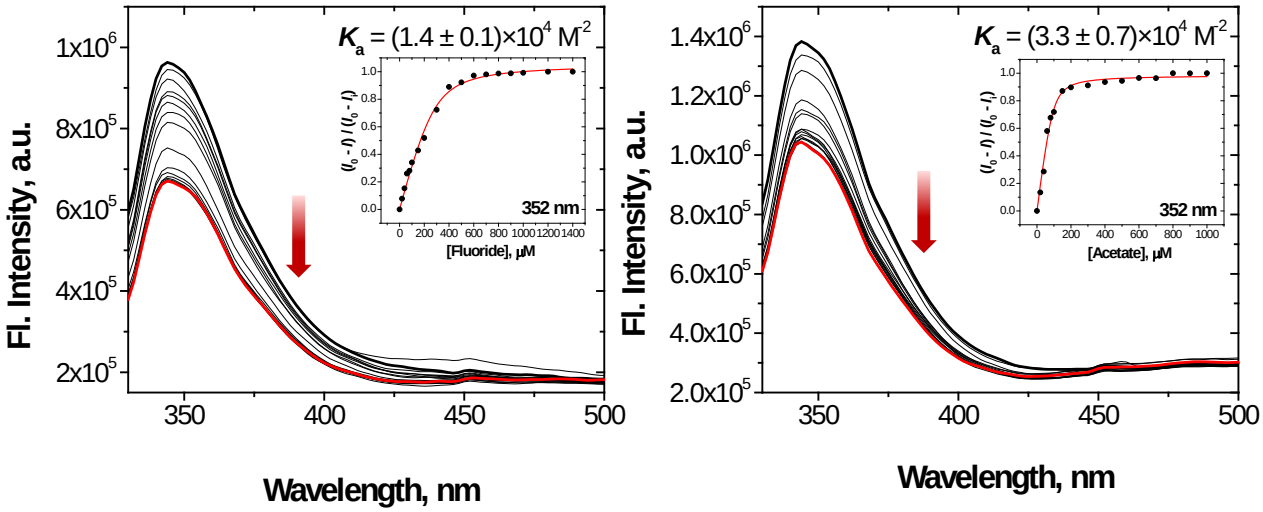

Figure S43. Left: Fluorescence titration spectra (λ_{ex}=315 nm) and isotherm of **S3** (8 μM) upon addition of Fluoride anion in DMSO:$CHCl_3$ (3:7, v/v) with Triton X-100 (0.36mM). **Right:** Fluorescence titration spectra (λ_{ex}=315 nm) and isotherm of **S3** (8 μM) upon addition of Acetate anion in DMSO:$CHCl_3$ (3:7, v/v) with Triton X-100 (0.36mM).

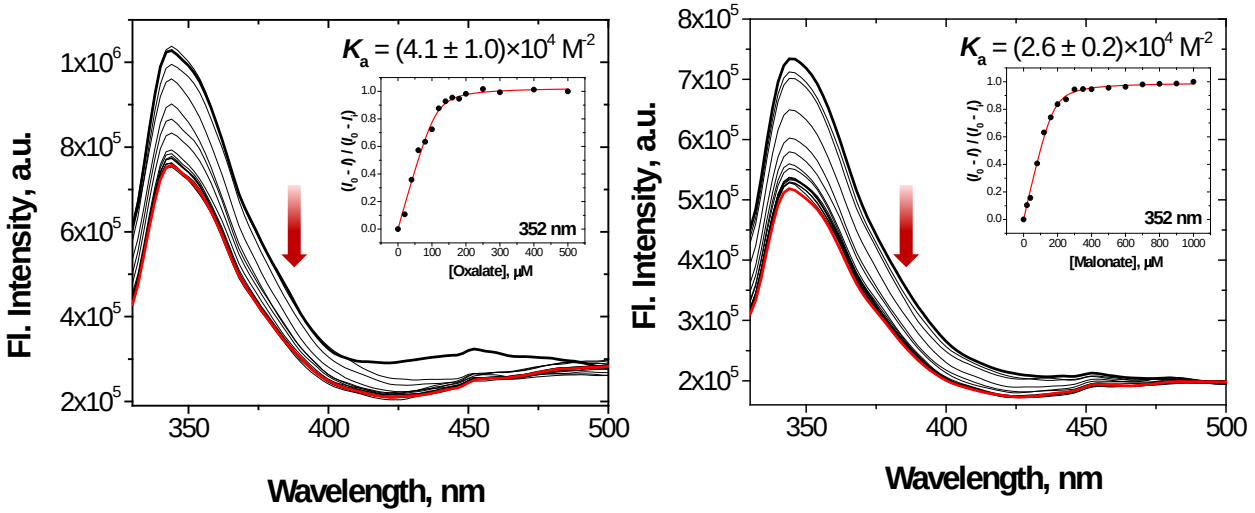

Figure S44. Left: Fluorescence titration spectra (λ_{ex}=315 nm) and isotherm of **S3** (8 μM) upon addition of Oxalate anion in DMSO:$CHCl_3$ (3:7, v/v) with Triton X-100 (0.36mM). **Right:** Fluorescence titration spectra (λ_{ex}=315 nm) and isotherm of **S3** (8 μM) upon addition of Malonate anion in DMSO:$CHCl_3$ (3:7, v/v) with Triton X-100 (0.36mM).

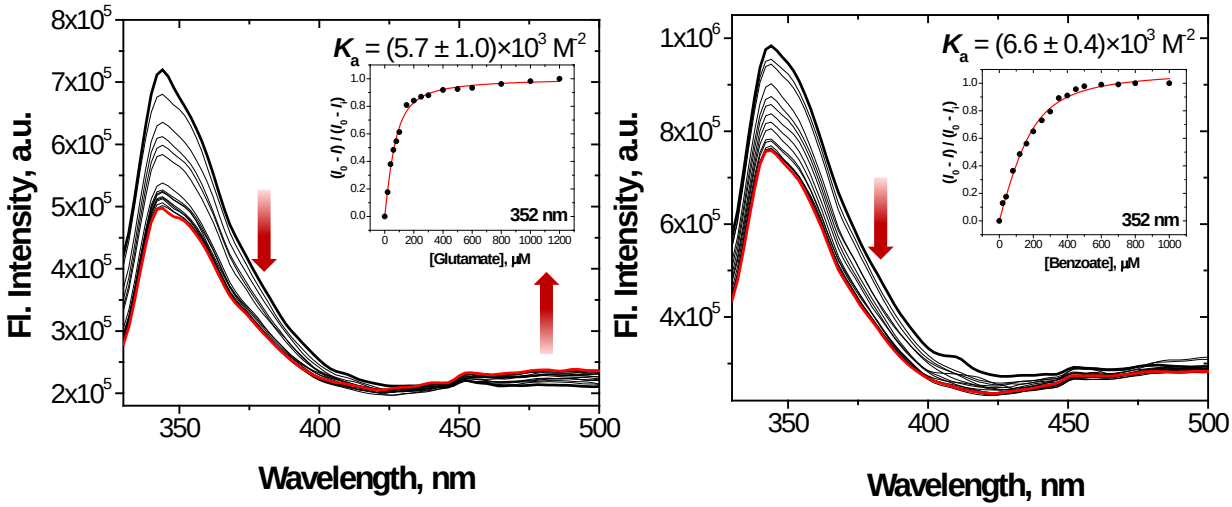

Figure S45. Left: Fluorescence titration spectra (λ_{ex}=315 nm) and isotherm of **S3** (8 μM) upon addition of Glutamate anion in DMSO:$CHCl_3$ (3:7, v/v) with Triton X-100 (0.36mM). **Right:** Fluorescence titration spectra (λ_{ex}=315 nm) and isotherm of **S3** (8 μM) upon addition of Benzoate anion in DMSO:$CHCl_3$ (3:7, v/v) with Triton X-100 (0.36mM).

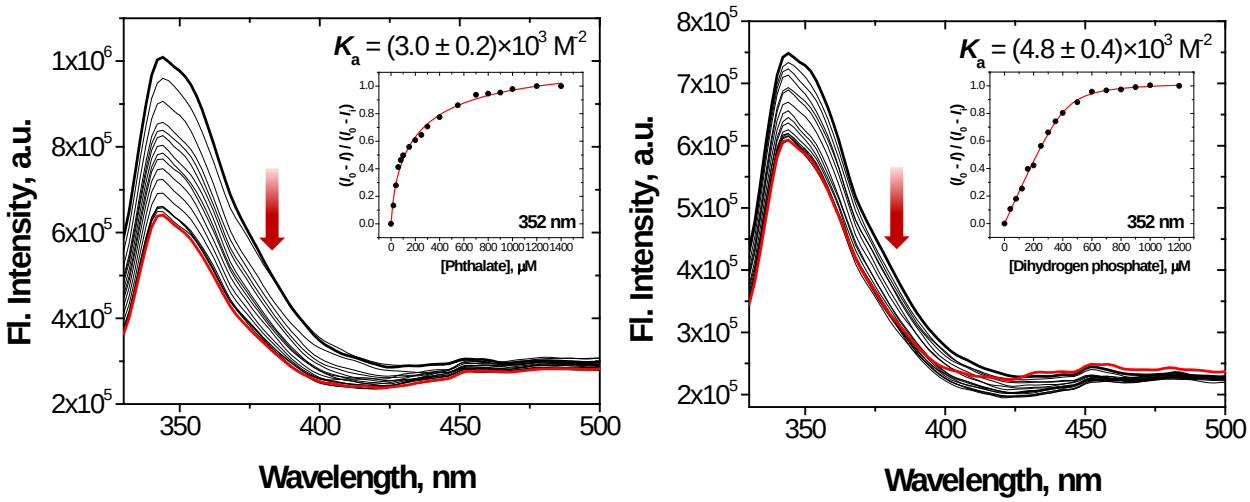

Figure S46. Left: Fluorescence titration spectra (λ_{ex}=315 nm) and isotherm of **S3** (8 μM) upon addition of Phthalate anion in DMSO:$CHCl_3$ (3:7, v/v) with Triton X-100 (0.36mM). **Right:** Fluorescence titration spectra (λ_{ex}=315 nm) and isotherm of **S3** (8 μM) upon addition of Dihydrogen phosphate anion in DMSO:$CHCl_3$ (3:7, v/v) with Triton X-100 (0.36mM).

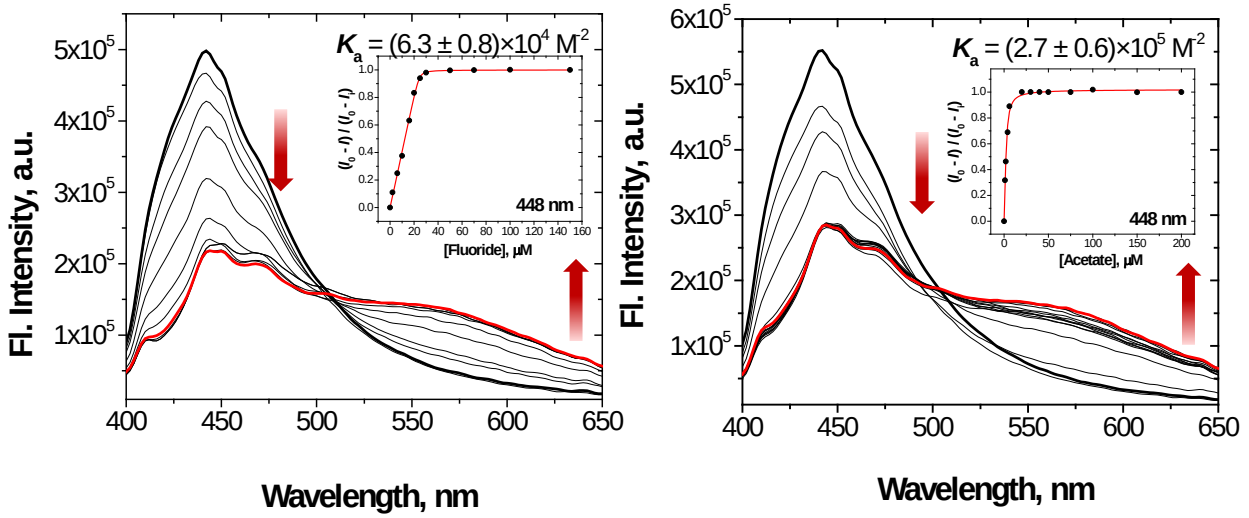

Figure S47. Left: Fluorescence titration spectra (λ_{ex}=375 nm) and isotherm of **S4** (0.2 μM) upon addition of Fluoride anion in DMSO:$CHCl_3$ (3:7, v/v) with Triton X-100 (0.36mM). **Right:** Fluorescence titration spectra (λ_{ex}=375 nm) and isotherm of **S4** (0.2 μM) upon addition of Acetate anion in DMSO:$CHCl_3$ (3:7, v/v) with Triton X-100 (0.36mM).

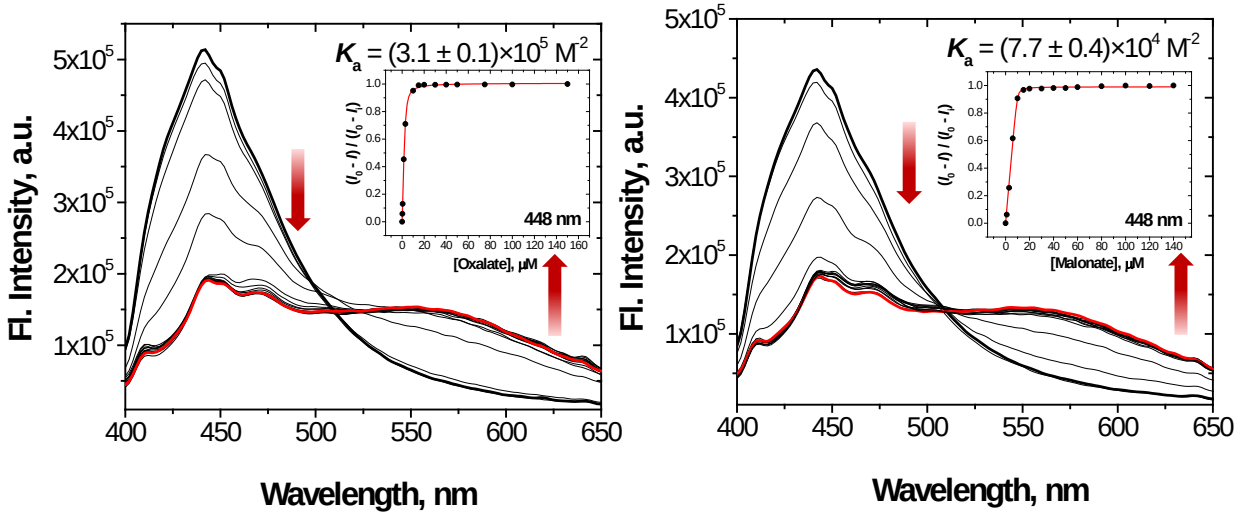

Figure S48. Left: Fluorescence titration spectra (λ_{ex}=375 nm) and isotherm of **S4** (0.2 μM) upon addition of Oxalate anion in DMSO:$CHCl_3$ (3:7, v/v) with Triton X-100 (0.36mM). **Right:** Fluorescence titration spectra (λ_{ex}=375 nm) and isotherm of **S4** (0.2 μM) upon addition of Malonate anion in DMSO:$CHCl_3$ (3:7, v/v) with Triton X-100 (0.36mM).

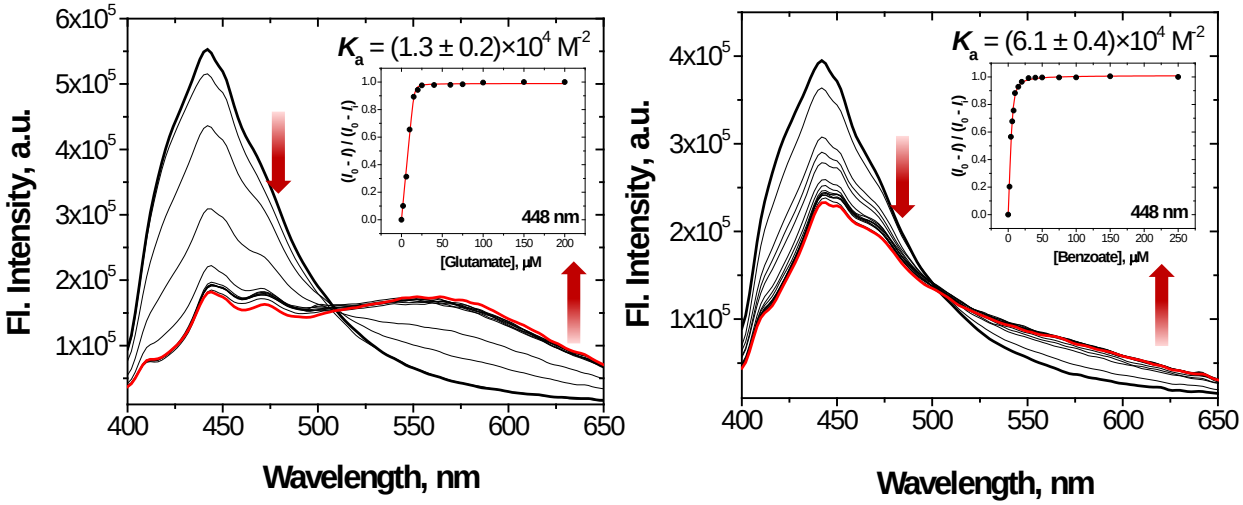

Figure S49. Left: Fluorescence titration spectra (λ_{ex}=375 nm) and isotherm of **S4** (0.2 μM) upon addition of Glutamate anion in DMSO:$CHCl_3$ (3:7, v/v) with Triton X-100 (0.36mM). **Right:** Fluorescence titration spectra (λ_{ex}=375 nm) and isotherm of **S4** (0.2 μM) upon addition of Benzoate anion in DMSO:$CHCl_3$ (3:7, v/v) with Triton X-100 (0.36mM).

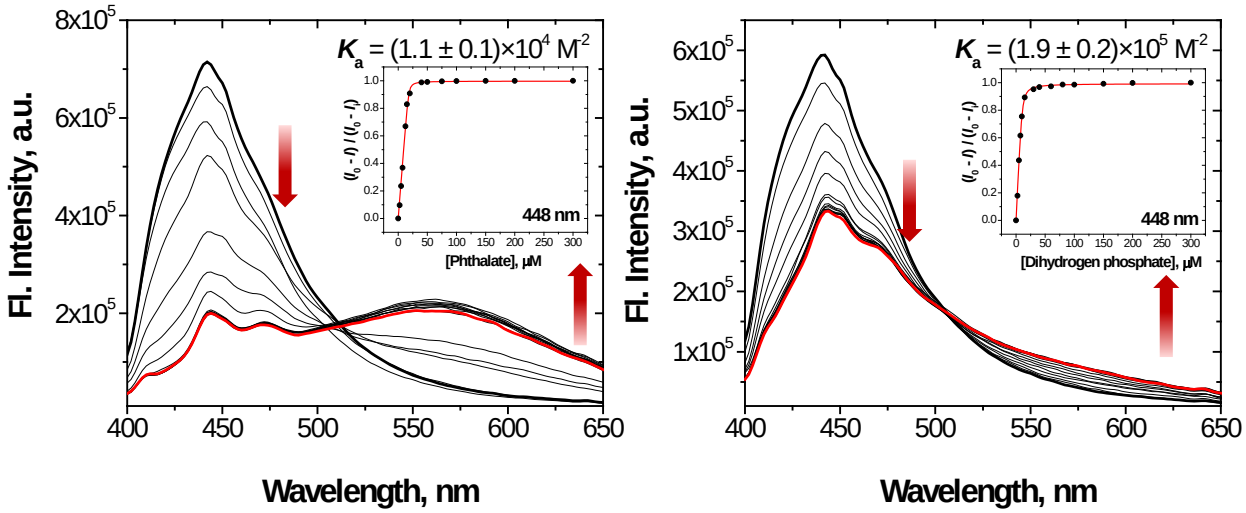

Figure S50. Left: Fluorescence titration spectra (λ_{ex}=375 nm) and isotherm of **S4** (0.2 μM) upon addition of Phthalate anion in DMSO:$CHCl_3$ (3:7, v/v) with Triton X-100 (0.36mM). **Right:** Fluorescence titration spectra (λ_{ex}=375 nm) and isotherm of **S4** (0.2 μM) upon addition of Dihydrogen phosphate anion in DMSO:$CHCl_3$ (3:7, v/v) with Triton X-100 (0.36mM).

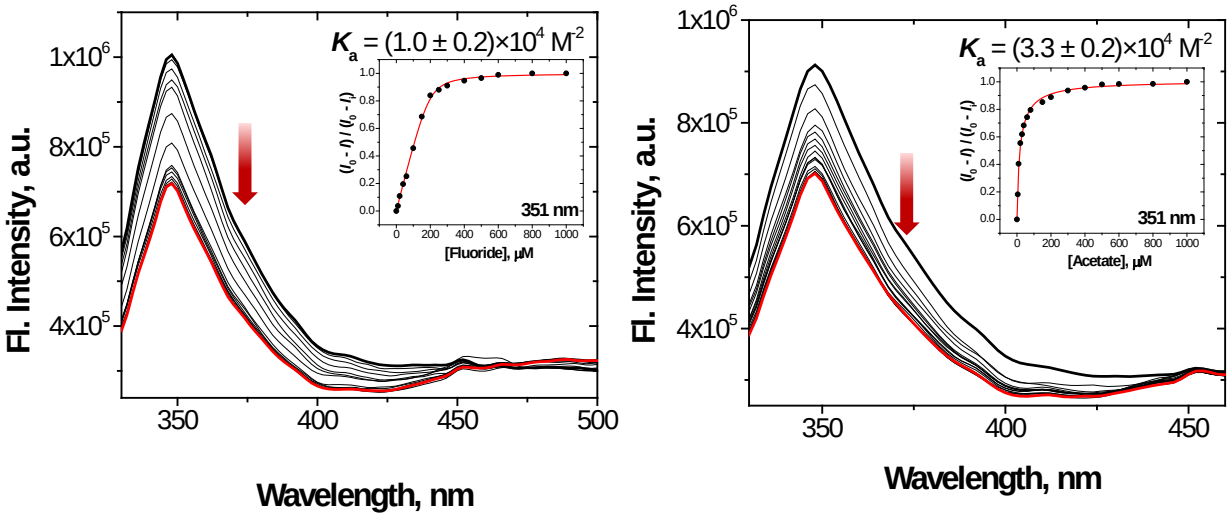

Figure S51. Left: Fluorescence titration spectra (λ_{ex}=315 nm) and isotherm of **S6** (8 μM) upon addition of Fluoride anion in DMSO:$CHCl_3$ (3:7, v/v) with Triton X-100 (0.36mM). **Right:** Fluorescence titration spectra (λ_{ex}=315 nm) and isotherm of **S6** (8 μM) upon addition of Acetate anion in DMSO:$CHCl_3$ (3:7, v/v) with Triton X-100 (0.36mM).

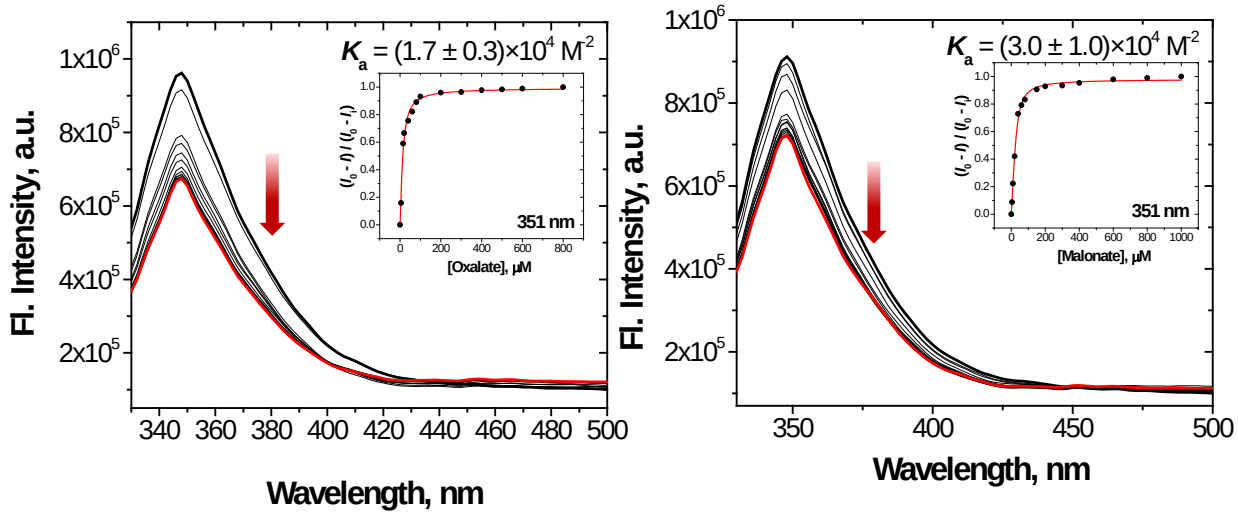

Figure S52. Left: Fluorescence titration spectra (λ_{ex}=315 nm) and isotherm of **S6** (8 μM) upon addition of Oxalate anion in DMSO:$CHCl_3$ (3:7, v/v) with Triton X-100 (0.36mM). **Right:** Fluorescence titration spectra (λ_{ex}=315 nm) and isotherm of **S6** (8 μM) upon addition of Malonate anion in DMSO:$CHCl_3$ (3:7, v/v) with Triton X-100 (0.36mM).

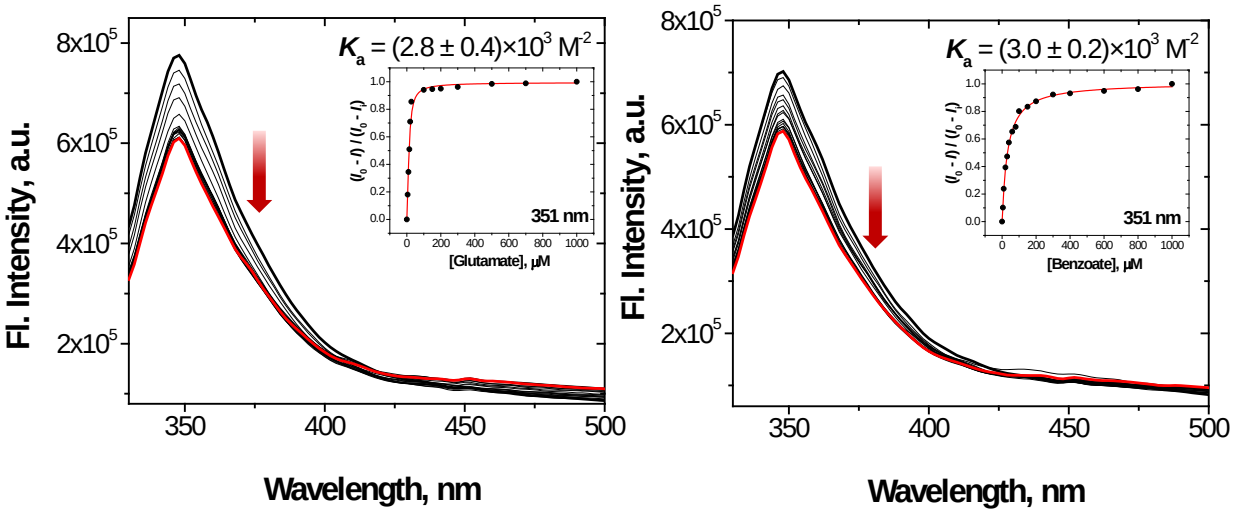

Figure S53. Left: Fluorescence titration spectra (λ_{ex}=315 nm) and isotherm of **S6** (8 μM) upon addition of Glutamate anion in DMSO:$CHCl_3$ (3:7, v/v) with Triton X-100 (0.36mM). **Right:** Fluorescence titration spectra (λ_{ex}=315 nm) and isotherm of **S6** (8 μM) upon addition of Benzoate anion in DMSO:$CHCl_3$ (3:7, v/v) with Triton X-100 (0.36mM).

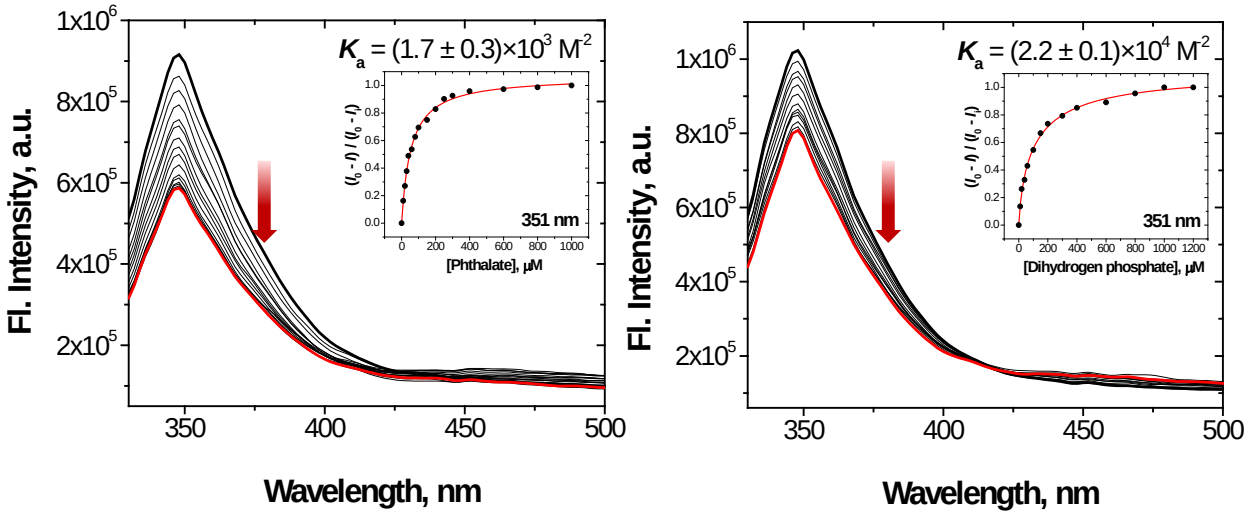

Figure S54. Left: Fluorescence titration spectra (λ_{ex}=315 nm) and isotherm of **S6** (8 µM) upon addition of Phthalate anion in DMSO:$CHCl_3$ (3:7, v/v) with Triton X-100 (0.36mM). **Right:** Fluorescence titration spectra (λ_{ex}=315 nm) and isotherm of **S6** (8 µM) upon addition of Dihydrogen phosphate anion in DMSO:$CHCl_3$ (3:7, v/v) with Triton X-100 (0.36mM).

6 Proton NMR titrations

The anion binding properties of **S1**-**S6** in DMSO solution were studied with ^{1}H NMR titration method. ^{1}H NMR spectra were recorded on a Bruker Avance III (500 MHz) spectrometer at 348 K in DMSO-d_6.

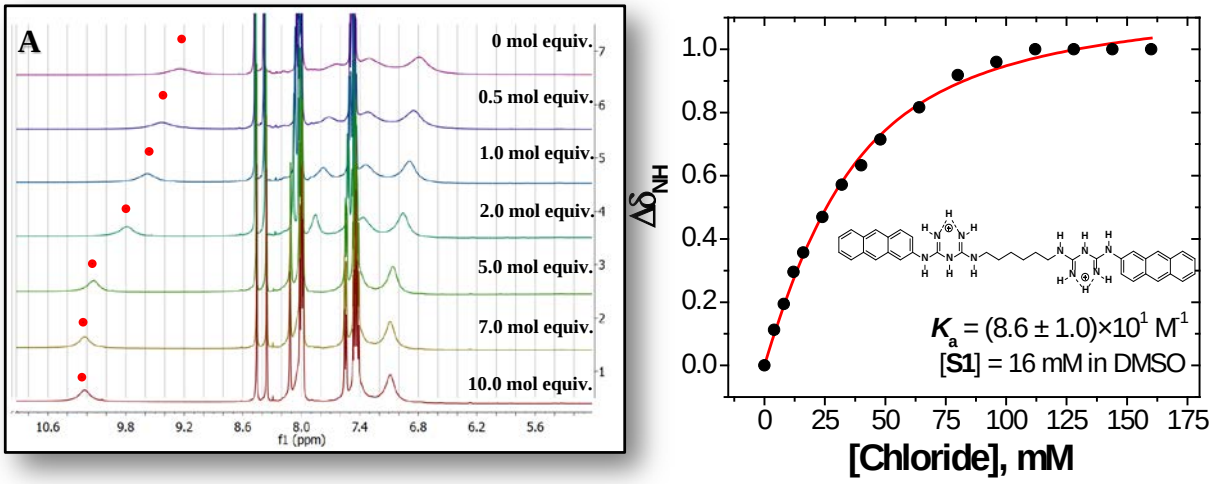

Figure S55. Panel A: ^{1}H NMR titration (selected region) of a solution of **S1** (16 mM) with tetrabutylammonium chloride (0-10.0 mol. eq.) in DMSO (500 MHz) at 348K. **Panel B**: ^{1}H NMR titration isotherm for selected N*H* signal (●).

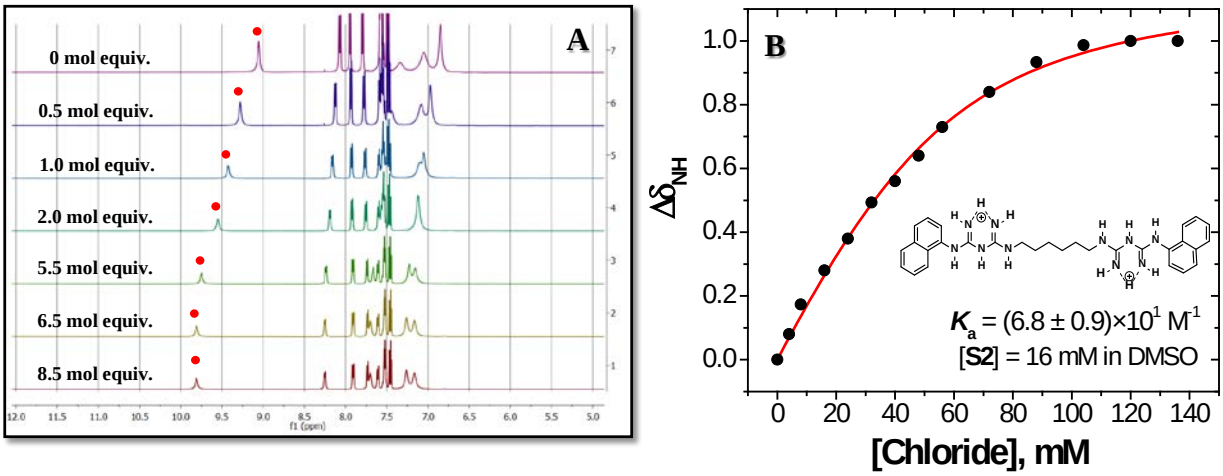

Figure S56. Panel A: ^{1}H NMR titration (selected region) of a solution of **S2** (16 mM) with tetrabutylammonium chloride (0-8.5 mol. eq.) in DMSO (500 MHz) at 348K. **Panel B**: ^{1}H NMR titration isotherm for selected N*H* signal (●).

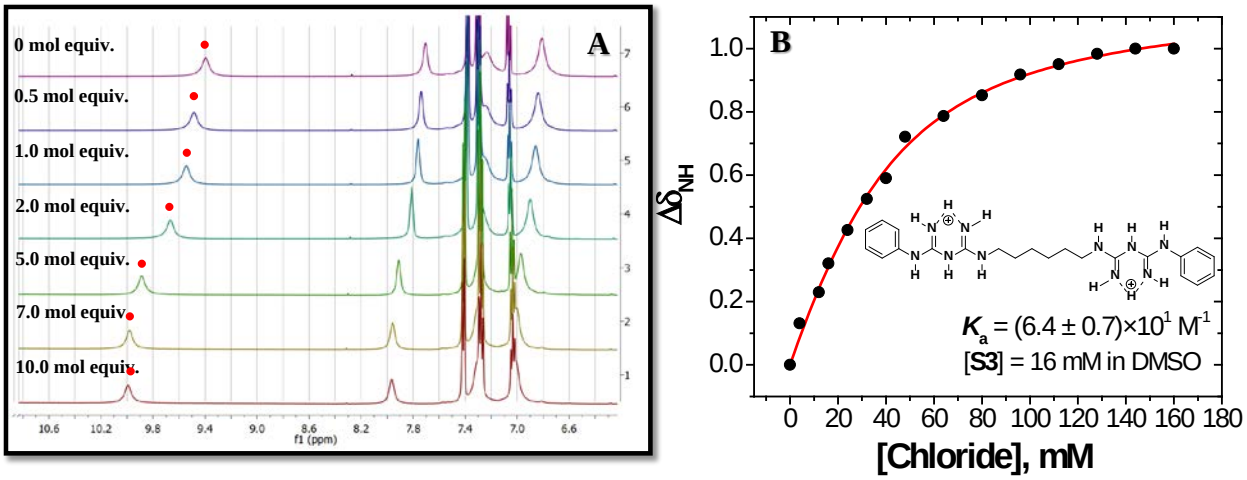

Figure S57. Panel A: ^{1}H NMR titration (selected region) of a solution of **S3** (16 mM) with tetrabutylammonium chloride (0-10.0 mol. eq.) in DMSO (500 MHz) at 348K. **Panel B**: ^{1}H NMR titration isotherm for selected N*H* signal (●).

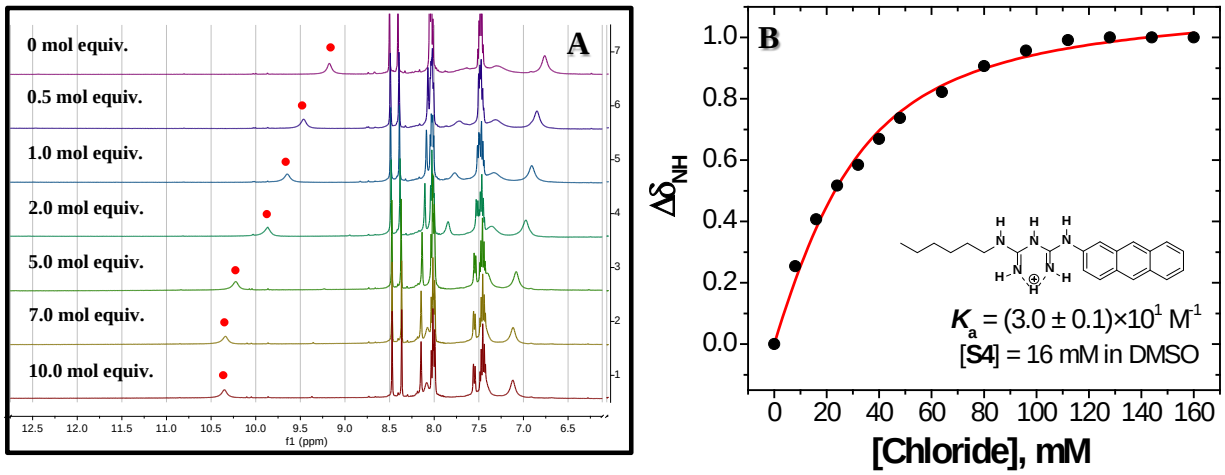

Figure S58. Panel A: ^{1}H NMR titration (selected region) of a solution of **S4** (12 mM) with tetrabutylammonium chloride (0-10.0 mol. eq.) in DMSO (500 MHz) at 348K. **Panel B**: ^{1}H NMR titration isotherm for selected N*H* signal (●).

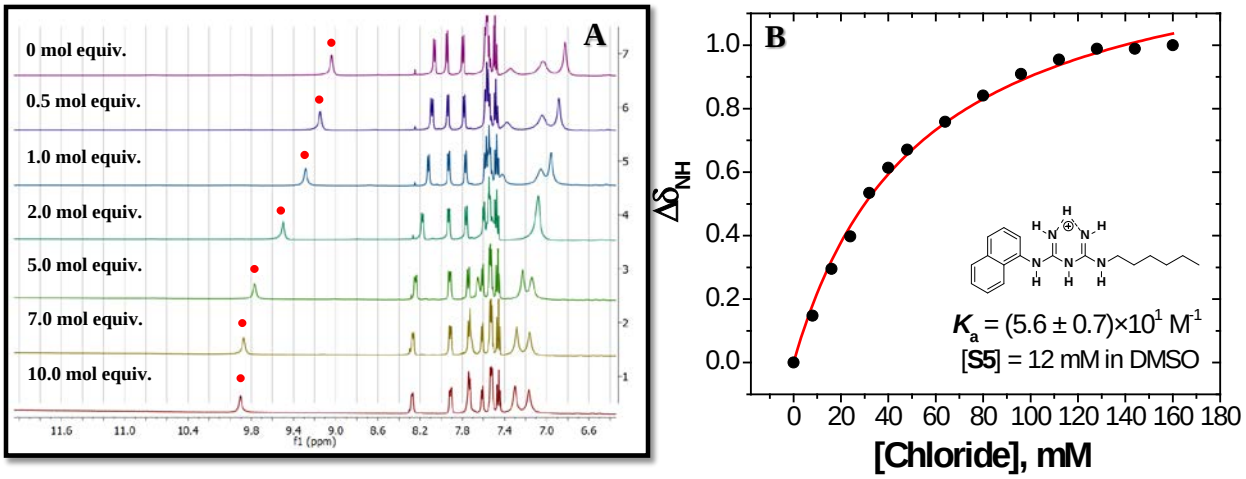

Figure S59. Panel A: ^{1}H NMR titration (selected region) of a solution of **S5** (12 mM) with tetrabutylammonium chloride (0-10.0 mol. eq.) in DMSO (500 MHz) at 348K. **Panel B**: ^{1}H NMR titration isotherm for selected N*H* signal (●).

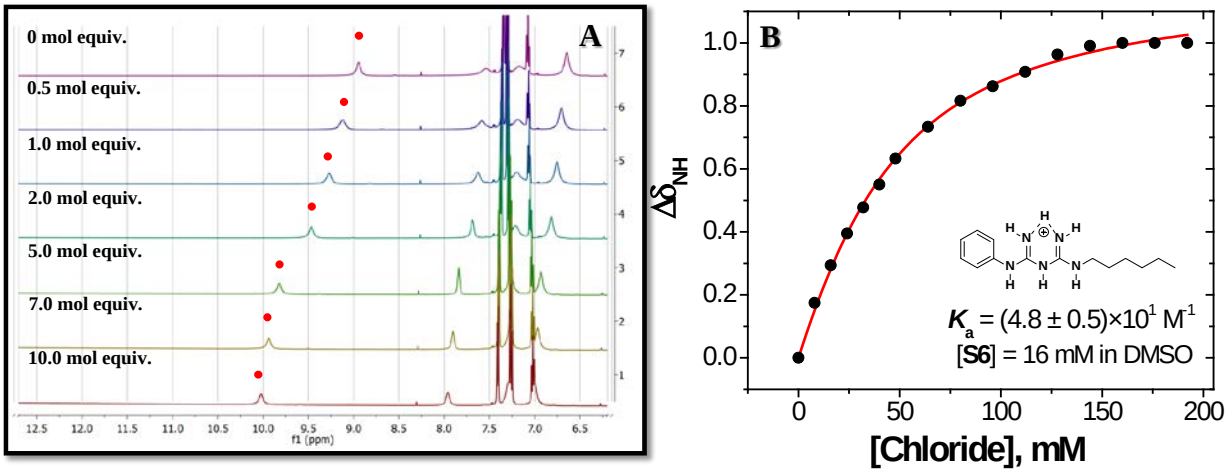

Figure S60. Panel A: ^{1}H NMR titration (selected region) of a solution of **S6** (16 mM) with tetrabutylammonium chloride (0-10.0 mol. eq.) in DMSO (500 MHz) at 348K. **Panel B**: ^{1}H NMR titration isotherm for selected N*H* signal (●).

7 Stoichiometry determination: Job's plot

The anion binding properties, namely the ratio between sensors **S1**-**S6** and an anion, were studied with Job's plot fluorescence method, using tetrabutylammonium fluoride and tetrabutylammonium acetate as the anion sources in mix DMSO:$CHCl_3$ (3:7) with addition of surfactant Triton X-100. The obtained results show 1:2 ratio for all complexes of fluoride and acetate anions.

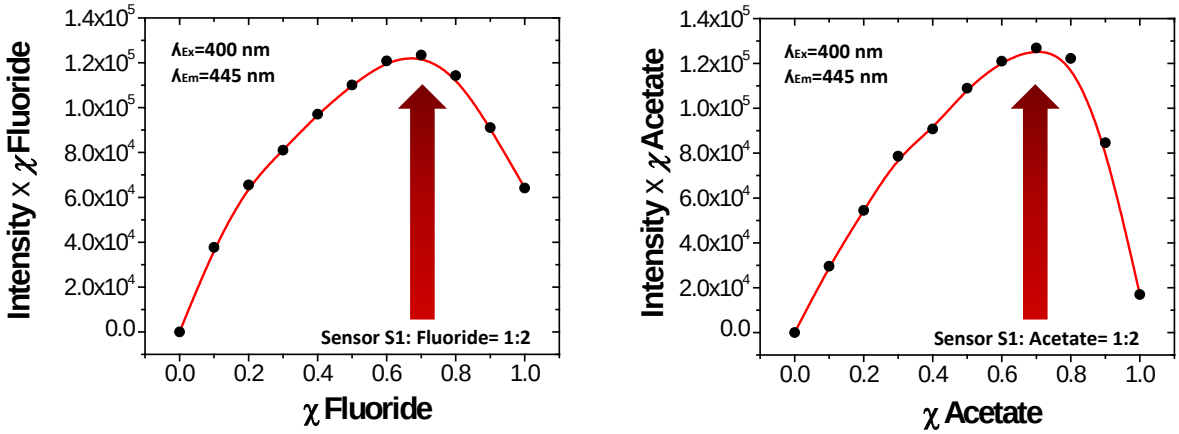

Figure S61. Left: Job's plot for the determination of the stoichiometry of **S1** and F^- in the complex in DMSO:$CHCl_3$ (3:7) with addition of surfactant Triton X-100 (0.36mM). **Right:** Job's plot for the determination of the stoichiometry of **S1** and OAc^- in the complex in DMSO:$CHCl_3$ (3:7) with addition of surfactant Triton X-100 (0.36mM).

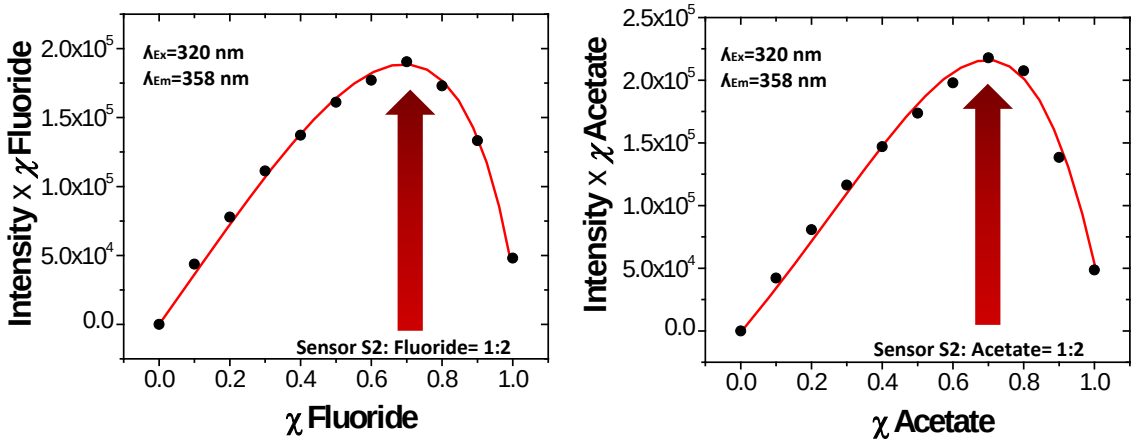

Figure S62. Left: Job's plot for the determination of the stoichiometry of **S2** and F^- in the complex in DMSO:$CHCl_3$ (3:7) with addition of surfactant Triton X-100 (0.36mM). **Right:** Job's plot for the determination of the stoichiometry of **S2** and OAc^- in the complex in DMSO:$CHCl_3$ (3:7) with addition of surfactant Triton X-100 (0.36mM).

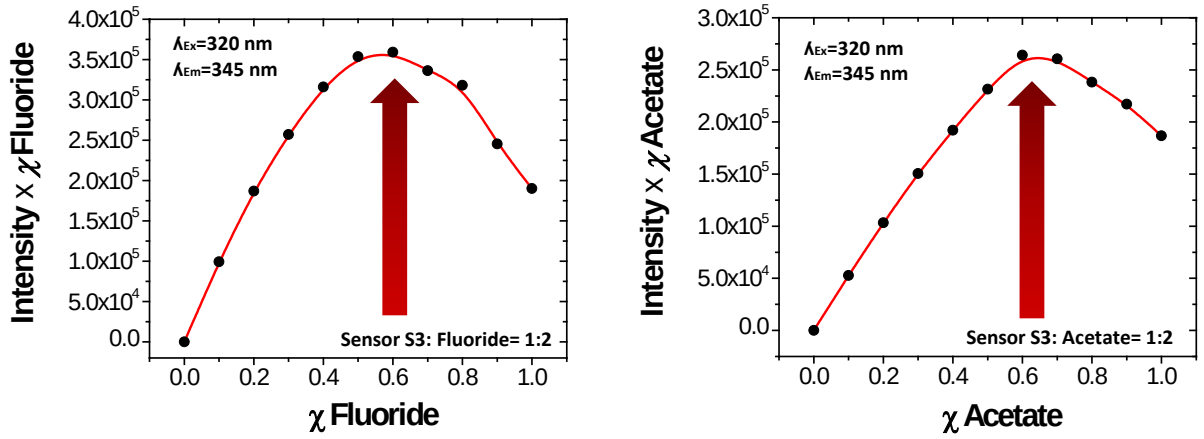

Figure S63. Left: Job's plot for the determination of the stoichiometry of **S3** and F^- in the complex in DMSO:$CHCl_3$ (3:7) with addition of surfactant Triton X-100 (0.36mM). **Right:** Job's plot for the determination of the stoichiometry of **S3** and OAc^- in the complex in DMSO:$CHCl_3$ (3:7) with addition of surfactant Triton X-100 (0.36mM).

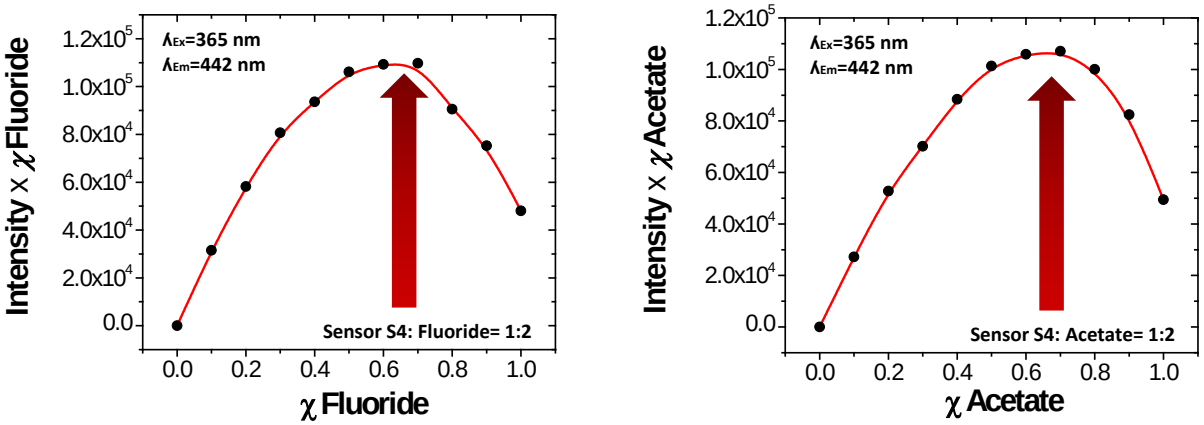

Figure S64. Left: Job's plot for the determination of the stoichiometry of **S4** and F^- in the complex in DMSO:$CHCl_3$ (3:7) with addition of surfactant Triton X-100 (0.36mM). **Right:** Job's plot for the determination of the stoichiometry of **S4** and OAc^- in the complex in DMSO:$CHCl_3$ (3:7) with addition of surfactant Triton X-100 (0.36mM).

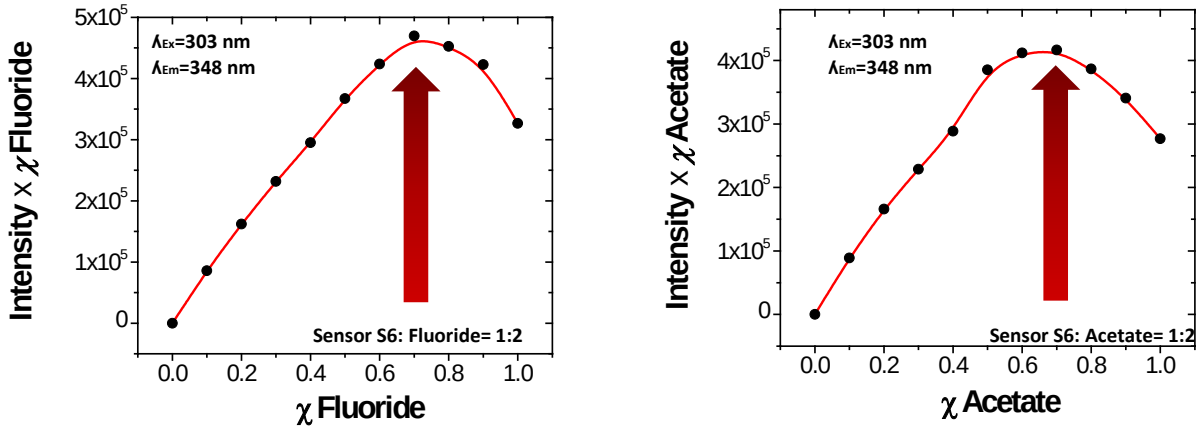

Figure S65. Left: Job's plot for the determination of the stoichiometry of **S6** and F^- in the complex in DMSO:$CHCl_3$ (3:7) with addition of surfactant Triton X-100 (0.36mM). **Right:** Job's plot for the determination of the stoichiometry of **S6** and OAc^- in the complex in DMSO:$CHCl_3$ (3:7) with addition of surfactant Triton X-100 (0.36mM).

8 Paper microzone plates study

The plates were printed on chromatography paper (Whatman) with a Xerox ColorQube model 8570 wax printer. After printing, it was baked in an oven for 4 minutes at 110 ^{o}C allowing for the penetration of wax into the paper. These plates were used for qualitative classification of analytes and quantitative analysis of various anions in water. Qualitative analysis was made by reacting 5 mM solution of sensors **S1**-**S6** (1 µL) in DMSO with 5 mM solution of different analytes (1 µL) in water. The responses were recorded by Kodak Image Station 440CF and Kodak Image Station 4000MM. Fluorescence intensities were classified by using Linear Discriminant Analysis (LDA). In quantitative analysis the responses from sensor arrays were evaluated by LDA classification for semi-quantitative analysis and Support Vector Machine (SVM) regression. Cross-validation results confirms 100% classification.

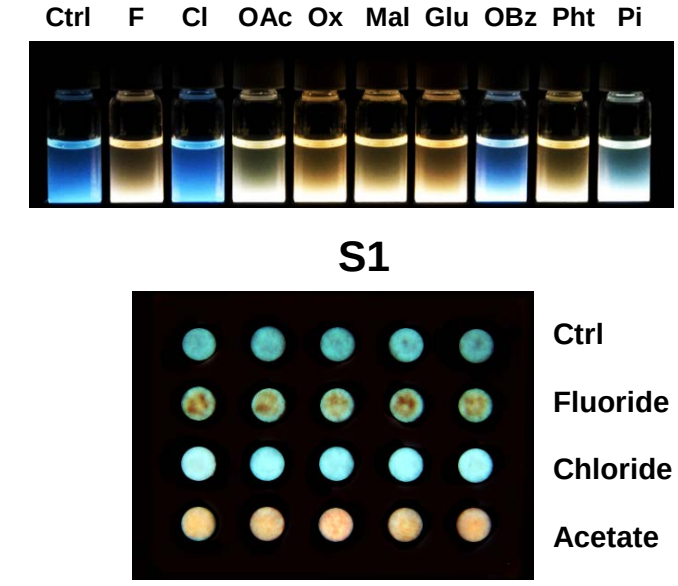

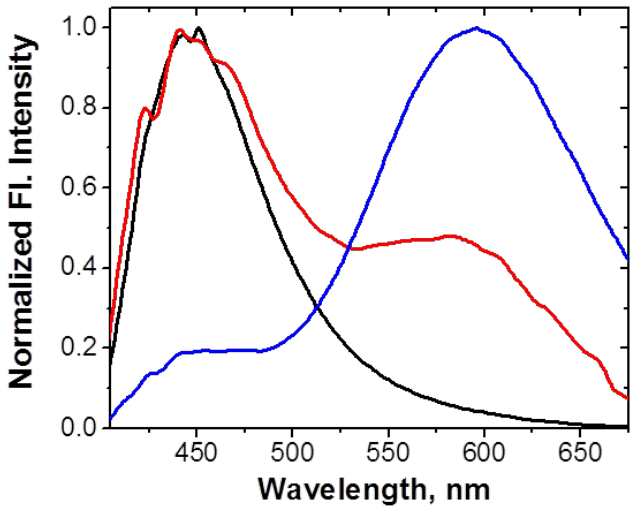

Figure S66. Top: Fluorescence photograph of sensor **S1** (0.4mM) with different anions (2.5mM) in DMSO:$CHCl_3$ (3:7). **Middle:** Fluorescence image from the paper microzone array of sensor **S1** (5mM) with four analytes (10mM), obtained as a sum of the RGB channels collected in the measurements. **Bottom:** Fluorescence spectrum of S1 (0.2 µM) (DMSO:CHCl3, 3:7, v/v) (black). Fluorescence spectrum of S1 (0.2 µM) in a presence of Dihydrogen phosphate anion (DMSO:CHCl3, 3:7, v/v) (red). Fluorescence spectrum of S1 (0.2 µM) in a presence of Fluoride anion (DMSO:CHCl3, 3:7, v/v) (blue)

Qualitative Assay for S1-S6 with different analytes

Table S4. Table of cumulative proportion of total dispersion for the qualitative assay of **S1**-**S6** (5mM) with various anions (5mM) in water (and one control).

F1	F2	F3	F4	F5	F6	F7	F8	F9	F10	F11	F12
0.799	0.912	0.957	0.976	0.989	0.995	0.998	0.999	0.999	1	1	1

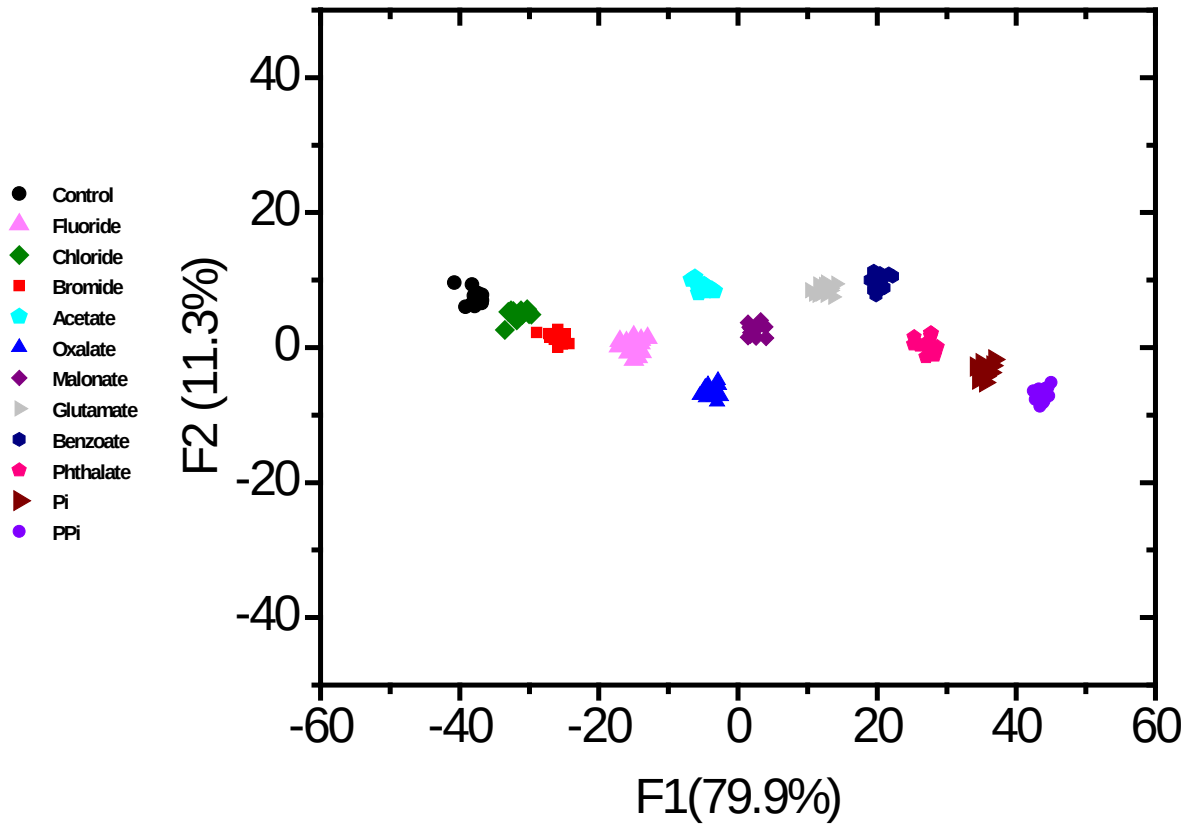

Figure S67. Graphical output of the qualitative LDA for a competitive assay of **S1**-**S6** (5mM) with various anions (5mM) in water. Achieved with 10 excitation/emission channels for each sensor, 13 repetitions, 100 % correct classification.

Semi-Quantitative Paper-Based Assay

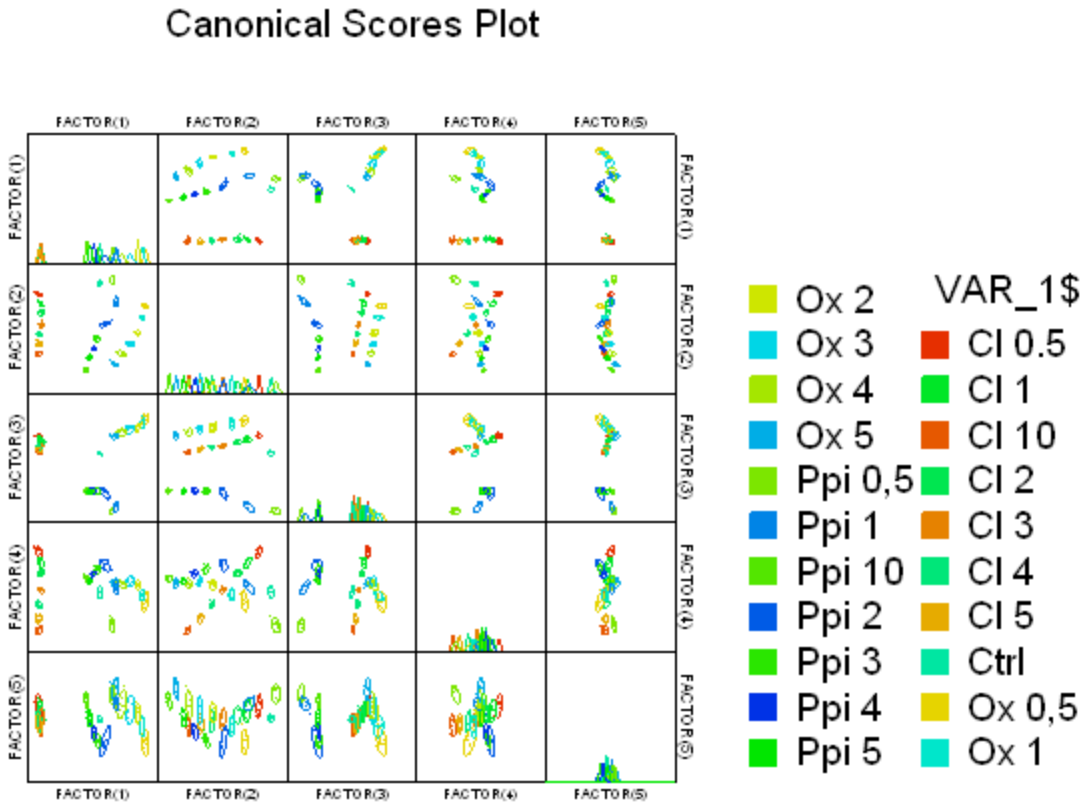

Figure S68. Canonical scores plot for LDA for the semi-quantitative assay for **S1**-**S6** and Oxalate, Chloride and Hydrogen pyrophosphate anions and a control.

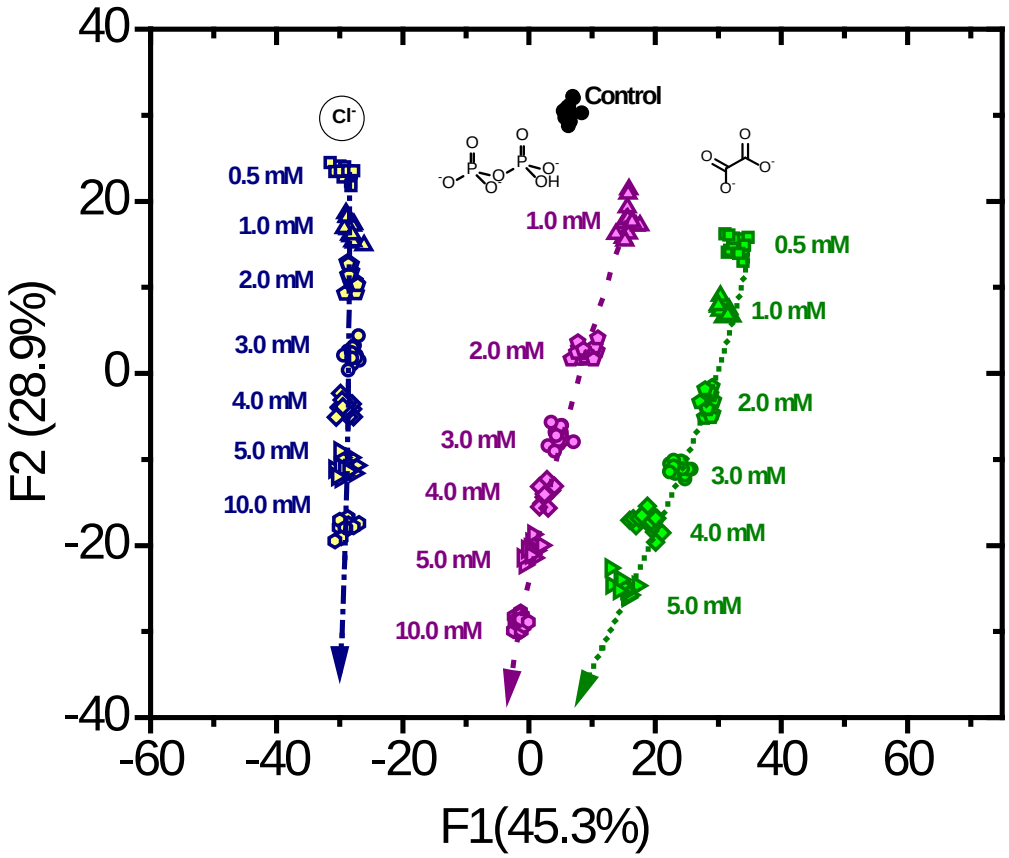

Figure S69. 2 D graphical output of Linear Discriminant Analysis for paper-based assay for sensors **S1**-**S6** (5mM) with chloride, hydrogen pyrophosphate and oxalate anions. Achieved with 6 excitation/emission channels for each sensor, 15 repetitions, 100 % correct classification.

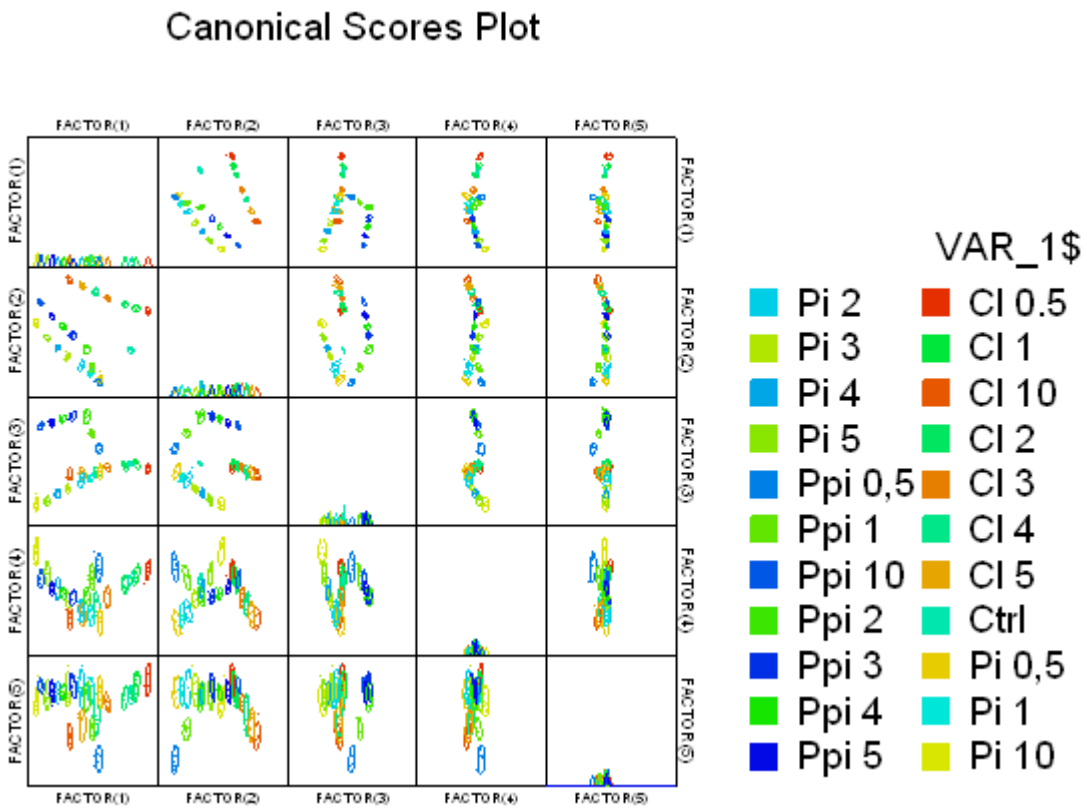

Figure S70. Canonical scores plot for LDA for the semi-quantitative assay for **S1**-**S6** Chloride, Dihydrogen phosphate and Hydrogen pyrophosphate anions and a control.

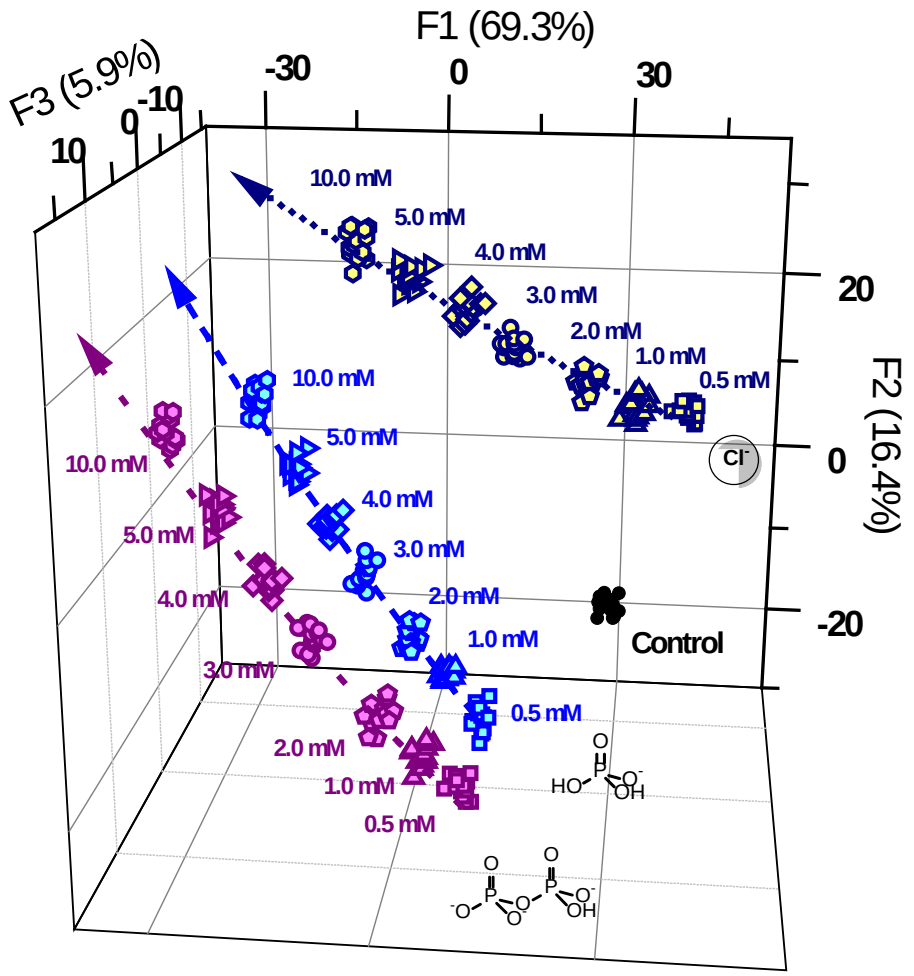

Figure S71. 3 D graphical output of Linear Discriminant Analysis for paper-based assay for sensors **S1** - **S6** (5mM) with chloride, hydrogen pyrophosphate and dihydrogen phosphate anions. Achieved with 6 excitation/emission channels for each sensor, 15 repetitions, 100 % correct classification.

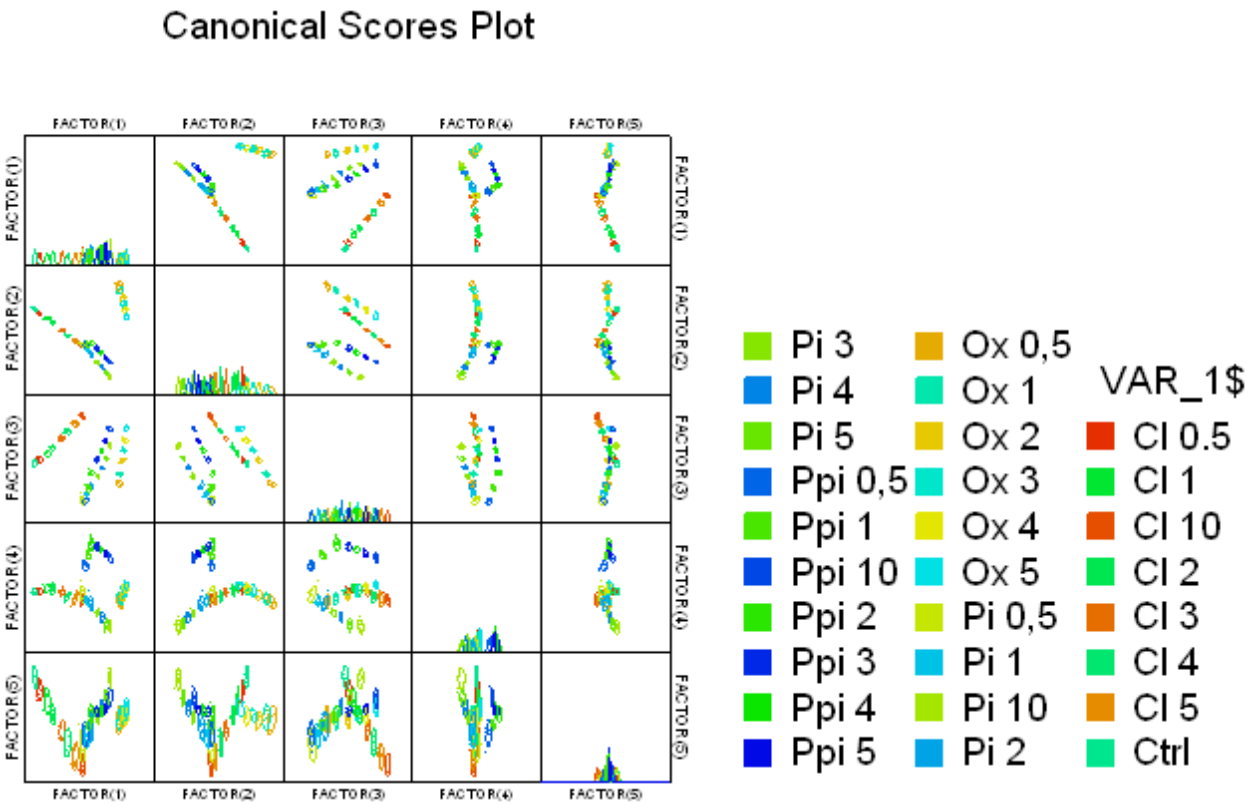

Figure S72. Canonical scores plot for LDA for the semi-quantitative assay for **S1**-**S6** Chloride, Oxalate, Dihydrogen phosphate and Hydrogen pyrophosphate anions and a control.

Table S5. Table of cumulative proportion of total dispersion for the qualitative assay of **S1**-**S6** (5mM) with Chloride, Oxalate, Dihydrogen phosphate and Hydrogen pyrophosphate anions (5mM) in water (and one control).

F1	F2	F3	F4	F5	F6	F7	F8	F9	F10	F11	F12	F13	F14
0.359	0.695	0.957	0.925	0.980	0.991	0.995	0.998	0.998	0.999	0.999	0.999	0.999	1

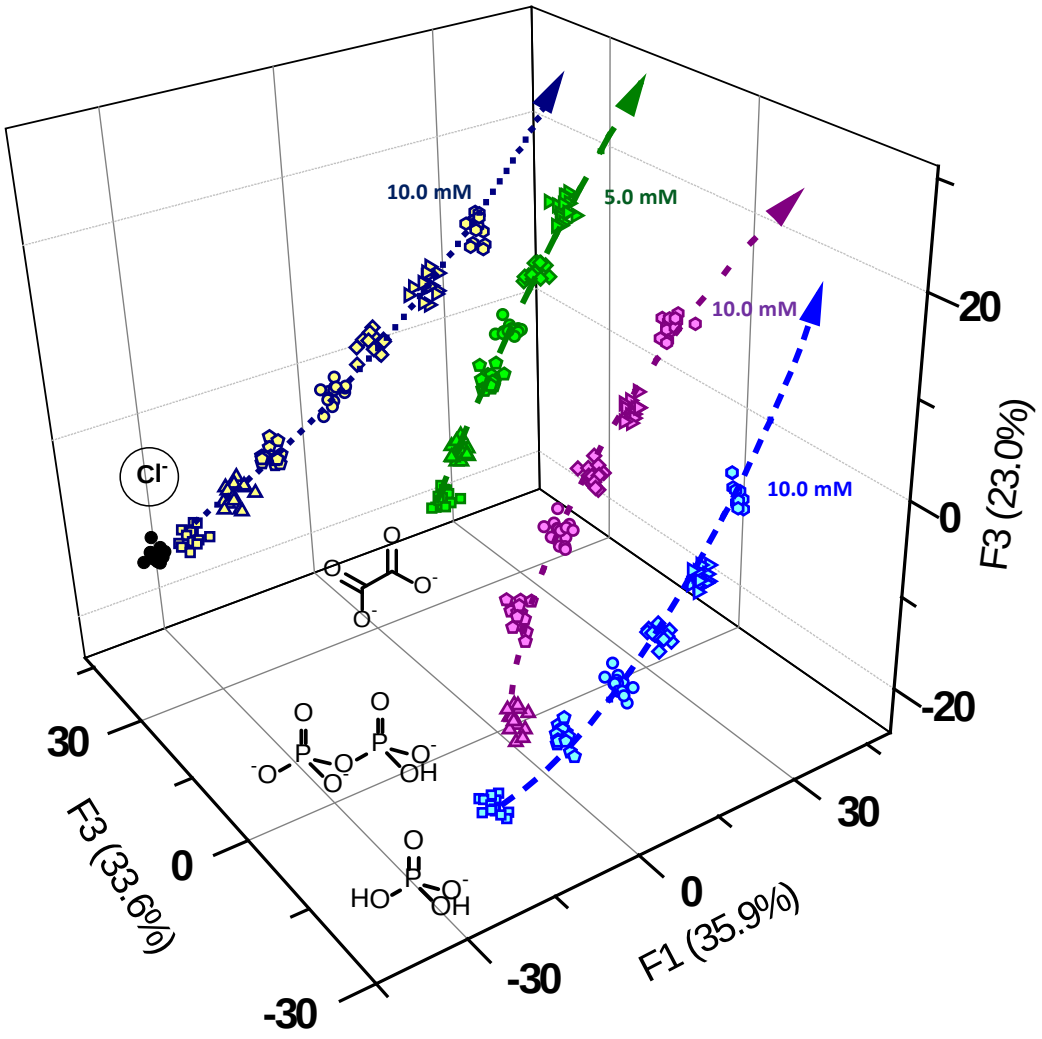

Figure S73. 3 D graphical output of Linear Discriminant Analysis for paper-based assay for sensors **S1**-**S6** (5mM) with Chloride, Hydrogen pyrophosphate, Dihydrogen phosphate and Oxalate anions and a control. Achieved with 6 excitation/emission channels for each sensor, 15 repetitions, 100 % correct classification.

Quantitative Assays

The plot of the actual *vs.* predicted concentration shows high accuracy of prediction for multiple Chloride concentration values. The root-mean-square errors (RMSE) of calibration (RMSEC), cross-validation (RMSECV), and prediction (RMSEP) attest to the quality of the model and prediction. Two unknown samples (red circle ●) were simultaneously correctly analyzed for Chloride (1mM and 4mM).

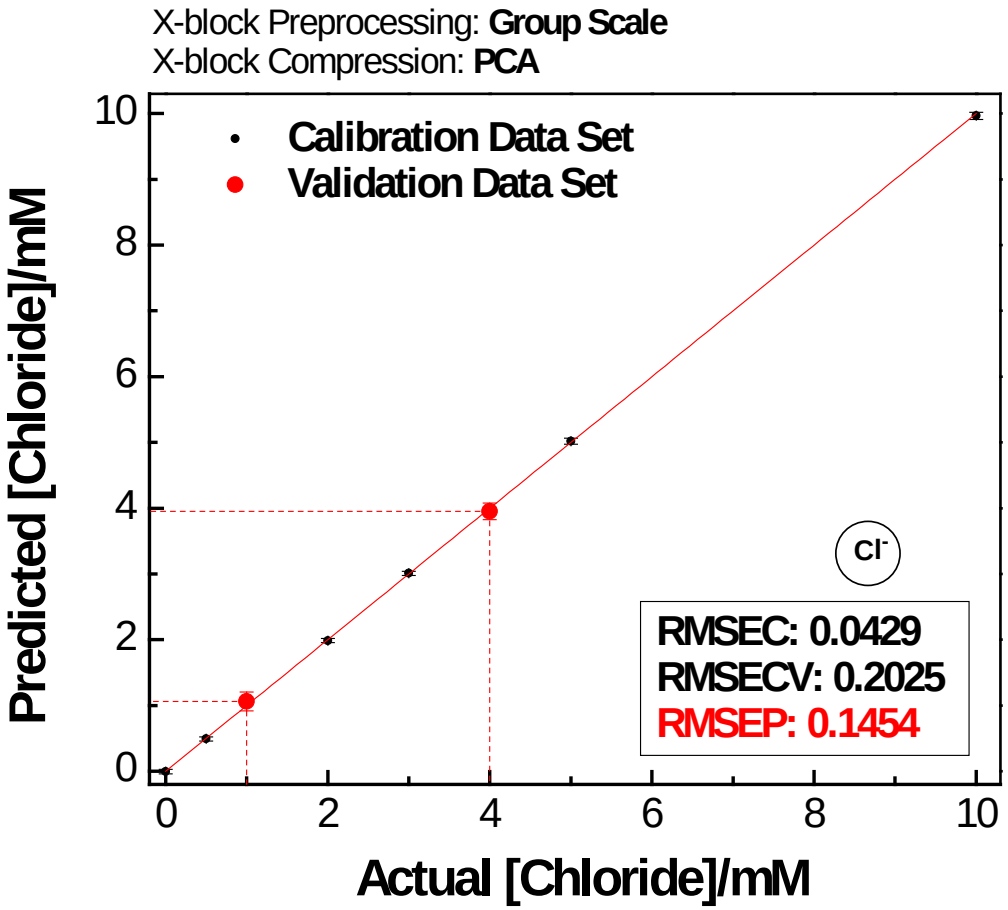

Figure S74. Results of linear regression by Support Vector Machine (SVM) for Chloride anion. Red circles (●) represent two unknown samples (1.0mM and 4.0mM), which were correctly analyzed using the model.

The plot of the actual *vs.* predicted concentration shows high accuracy of prediction for multiple Oxalate concentration values. The root-mean-square errors (RMSE) of calibration (RMSEC), cross-validation (RMSECV), and prediction (RMSEP) attest to the quality of the model and prediction. Two unknown samples (red circle ●) were simultaneously correctly analyzed for Oxalate (0.5mM and 3mM).

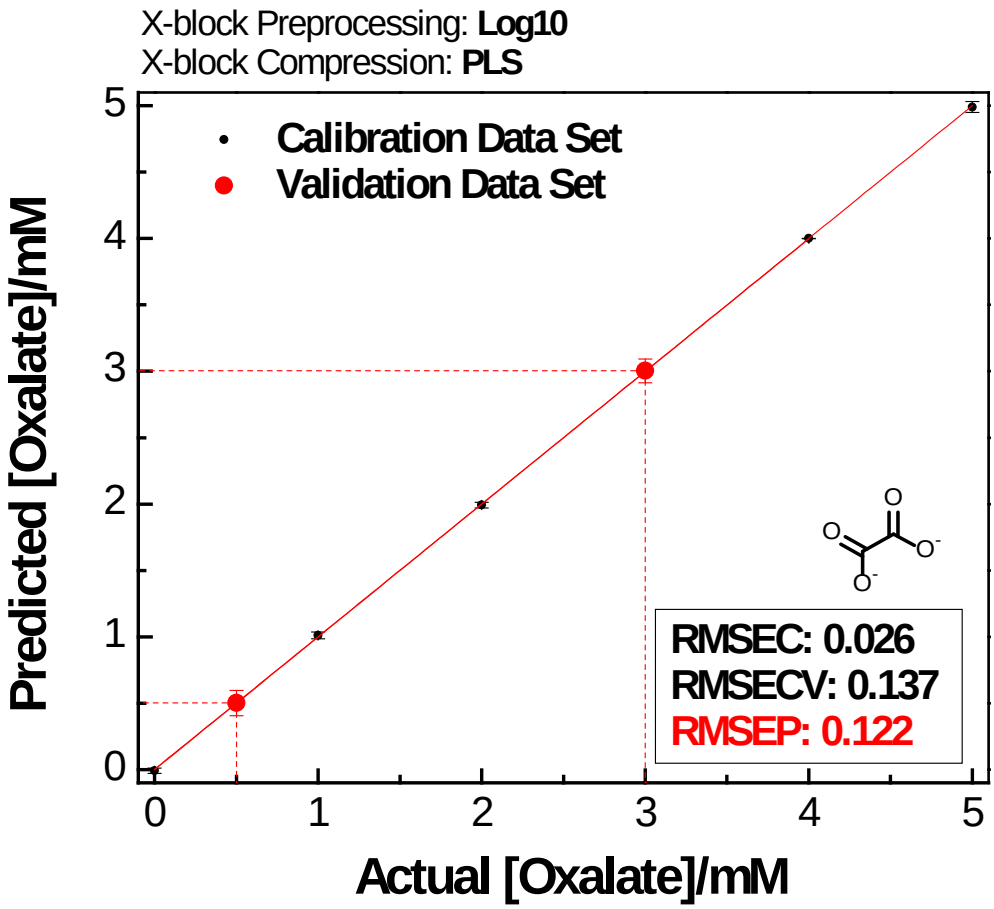

Figure S75. Results of linear regression by Support Vector Machine (SVM) for Oxalate anion. Red circles (●) represent two unknown samples (0.5mM and 3.0mM), which were correctly analyzed using the model.

The plot of the actual *vs.* predicted concentration shows high accuracy of prediction for multiple Hydrogen pyrophosphate concentration values. The root-mean-square errors (RMSE) of calibration (RMSEC), cross-validation (RMSECV), and prediction (RMSEP) attest to the quality of the model and prediction. Two unknown samples (red circle ●) were simultaneously correctly analyzed for Hydrogen pyrophosphate (1mM and 4mM).

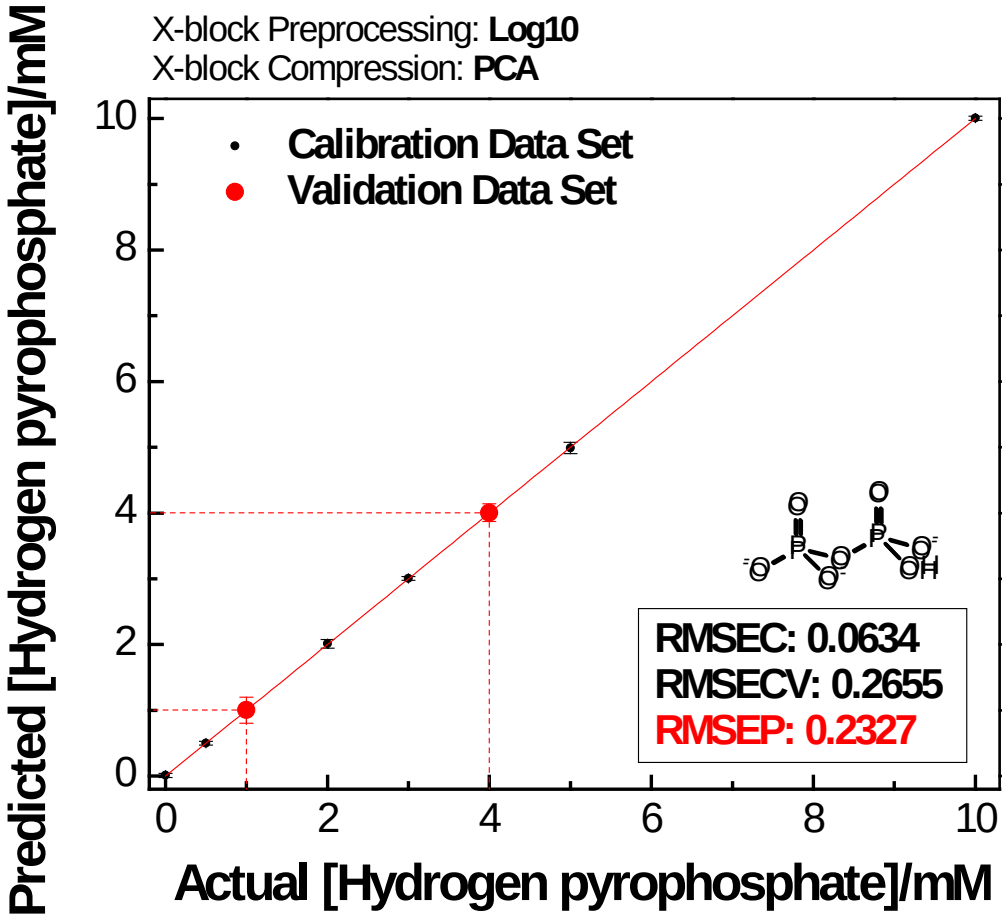

Figure S76. Results of linear regression by Support Vector Machine (SVM) for Hydrogen pyrophosphate anion. Red circles (●) represent two unknown samples (1.0mM and 4.0mM), which were correctly analyzed using the model.

The plot of the actual *vs.* predicted concentration shows high accuracy of prediction for multiple Dihydrogen phosphate concentration values. The root-mean-square errors (RMSE) of calibration (RMSEC), cross-validation (RMSECV), and prediction (RMSEP) attest to the quality of the model and prediction. Two unknown samples (red circle ●) were simultaneously correctly analyzed for Dihydrogen phosphate (1mM and 4mM).

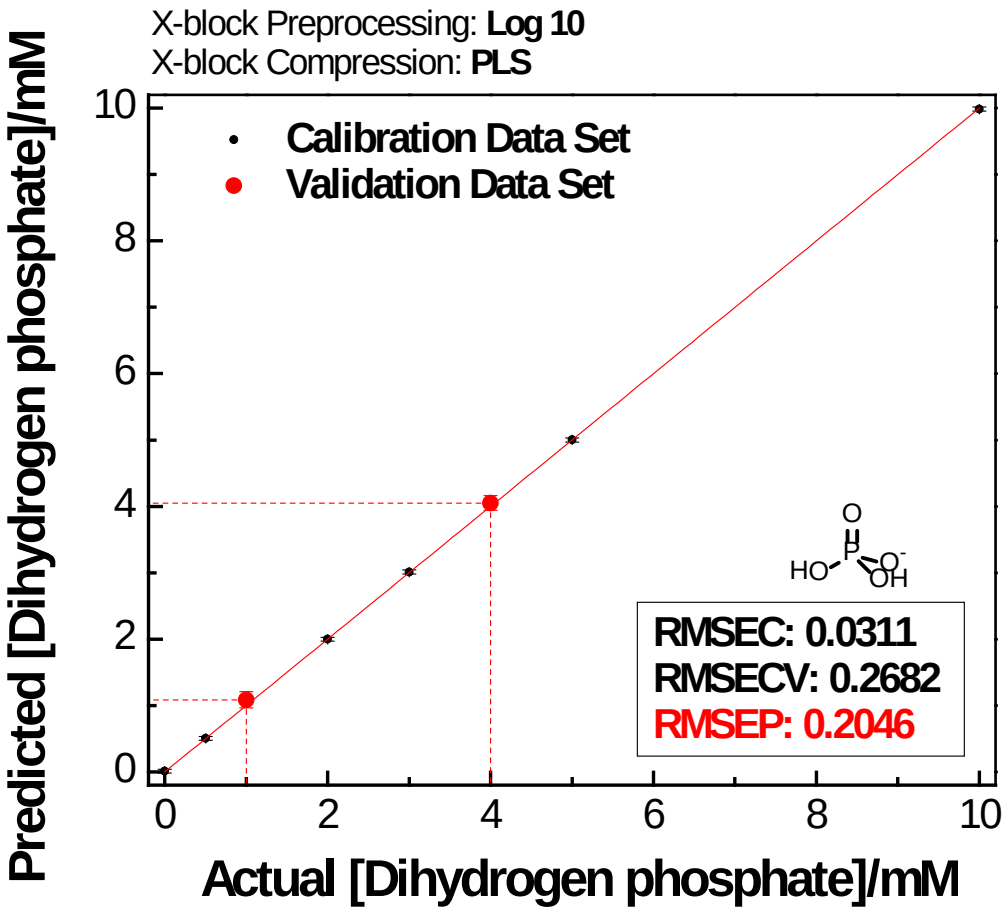

Figure S77. Results of linear regression by Support Vector Machine (SVM) for Dihydrogen phosphate anion. Red circles (●) represent two unknown samples (1.0mM and 4.0mM), which were correctly analyzed using the model.

9 Competitive titrations of acetate anion in chloride rich solutions

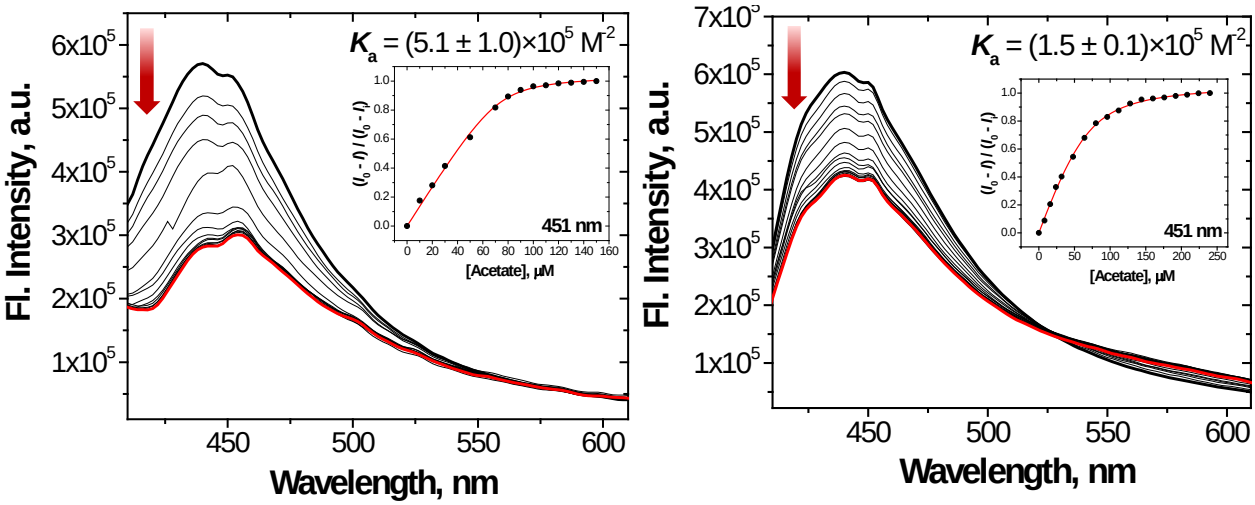

Figure S78. Left: Fluorescence titration spectra and isotherm of **S1** (0.2 μM) upon addition of acetate anion. **Right:** Fluorescence titration spectra and isotherm of **S1** (0.2 μM) upon addition of acetate anion in a presence of chloride anion (500 μM). Both titrations were acquired in DMSO:$CHCl_3$ (3:7, v/v).

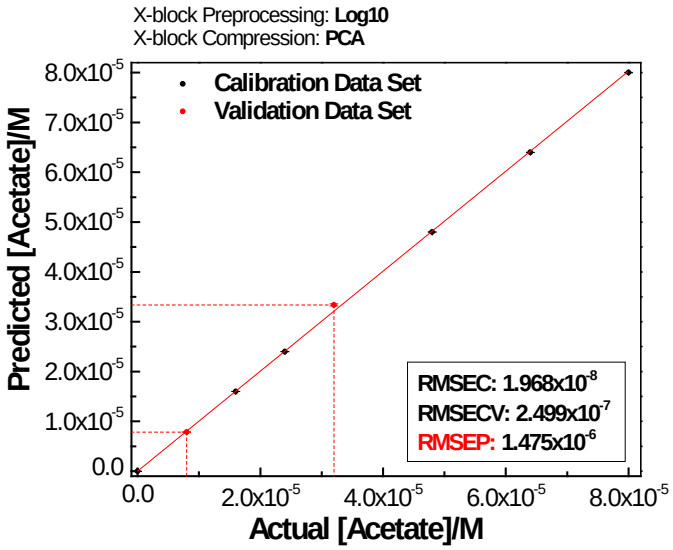

Figure S79. Results of linear regression by Support Vector Machine (SVM) based on fluorescence titrations for Acetate anion in a presence of Chloride anion (500μM). Red circles (●) represent two unknown samples (8.0μM and 32μM), which were correctly analyzed using the model.

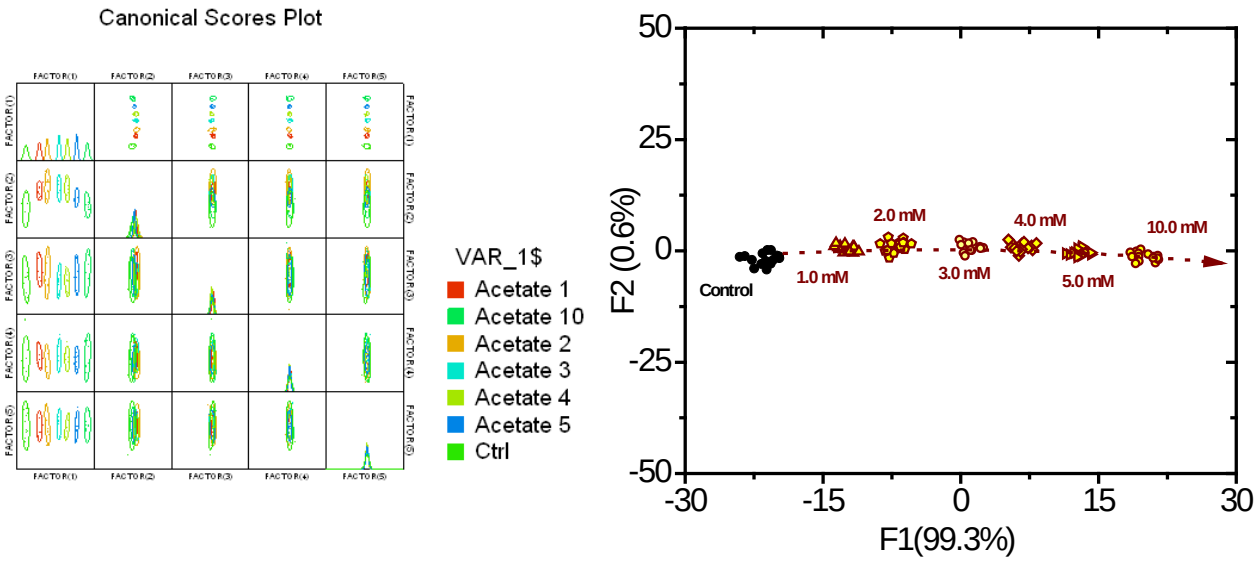

Figure S80. Left: Canonical scores plot for LDA for the semi-quantitative assay for **S1** and Acetate and a control in a presence of Chloride anion (10mM). **Right:** 2 D graphical output of Linear Discriminant Analysis for paper-based assay for sensors **S1** (5mM) with acetate anion in a presence of chloride anion (10mM). Achieved with 9 excitation/emission channels, 15 repetitions, 100 % correct classification.

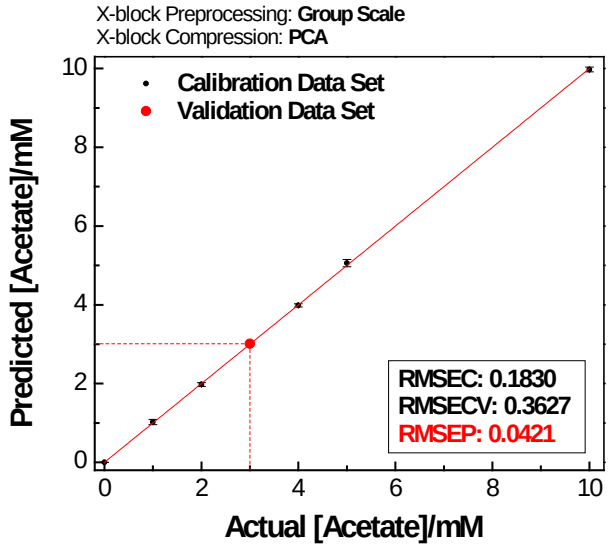

Figure S81. Results of linear regression by Support Vector Machine (SVM) for Acetate anion in a presence of Chloride anion (10mM). Red circle (●) represents one unknown sample (3mM), which was correctly analyzed using the model.

Supplemental References

[1] A. K. Connors. *Binding Constants: the Measurement of Molecular Complex Stability*; Wiley: New York, **1987**.
[2] Rose, F.L.; Swain, G. *J. Chem. Soc*. **1956**, 4422–4425.